ABSTRACT

COMPARATIVE ANALYSIS OF TWO HUMAN CANCER CELL LINES FOLLOWING EXPOSURE TO LOW DOSE RADIATION

by Gladys N. Nangami

December 2011

Director: Roberta M. Johnke, PhD

DEPARTMENT OF PHYSICS

Over the past two decades, studies on the cellular response to very low dose radiation have been revolutionizing historically-held paradigms of cellular radioresponse. Indeed, a host of seemingly contradictory events have recently been reported to occur within this dose range of radiation exposure which make extrapolation of data derived from high dose studies to these low dose ranges no longer a feasible alternative. In this study, we investigate the radioresponse of two human tumor cell lines, A375 human melanoma cells and PC3 human prostate cancer cells, which appear to behave quite differently in the very low dose radiation range. More specifically, we (a) characterize the cell survival response following low dose radiation in the A375 human melanoma cells and PC3 human prostate cancer cell lines; (b) investigate the kinetics and magnitude of cell cycle arrest that occurs following low dose radiation exposure in these cell lines; and (c) ascertain whether signaling through the MAPK and NF-κB proliferative pathways is being stimulated following exposure to low doses of radiation. The results of these studies demonstrate that two different and contradictory survival responses are seen following exposure to very low dose irradiation (hyper-radioresistance in A375 cells vs. hyper-radiosensitivity in PC3 cells). Furthermore, the data indicate that differential regulation of G2/M cell cycle arrest may be involved in the contradictory survival responses observed.

COMPARATIVE ANALYSIS OF TWO HUMAN CANCER CELL LINES FOLLOWING EXPOSURE TO LOW DOSE RADIATION

A Dissertation

Presented to

The Faculty of the Department of Physics

East Carolina University

In Partial Fulfillment

Of the Requirements for the Degree

Doctor of Philosophy in Biomedical Physics

by

Gladys N. Nangami

December 2011

COMPARATIVE ANALYSIS OF TWO HUMAN CANCER CELL LINES FOLLOWING EXPOSURE TO LOW DOSE RADIATION

By

Gladys N. Nangami

APPROVED BY:

DISSERTATION ADVISOR_____
Roberta M. Johnke, Ph.D.

COMMITTEE MEMBER_____
Michael Dingfelder, Ph.D.

COMMITTEE MEMBER_____
Jean Luc Scemama, Ph.D.

COMMITTEE MEMBER_____
Jefferson L. Shinpaugh, Ph.D.

COMMITTEE MEMBER_____
Orville Day, Ph.D.

CHAIR OF THE DEPARTMENT OF PHYSICS_____
John C. Sutherland, Ph.D.

DEAN OF THE GRADUATE SCHOOL_____
Paul J. Gemperline, Ph.D.

DEDICATION

In Memory of my daughter, Joy
To my dear Mother Florence Khwaka and my children Brenda, Maureen, Faith and Paul

ACKNOWLEDGEMENTS

First, I would like to thank my dissertation advisor, Dr. Roberta Johnke, for giving me an opportunity to work in her laboratory and for believing in my abilities to do meaningful research under her supervision. I greatly appreciate her devotion to my success, the many hours she was available to offer insightful advice and to teach me how to be a successful researcher. I would also like to thank the members of my dissertation committee, Dr. Michael Dingfelder, Dr. Jean Luc Scemama, Dr. Orville Day, and Dr. Jefferson Shinpaugh, for offering their time and suggestions to improve and complete these studies. Finally, a special thanks goes to Dr. Douglas Weidner for his assistance with the flow cytometry studies presented in this dissertation.

I want to thank the fellow graduate students who were colleagues in the laboratory with me. Their friendship and assistance were invaluable. I am especially grateful to Jenny Sattler, MS for her computer expertise and help in the laboratory. Also, I want to thank Nick Bakken, MS for his help with molecular protocols and quality control of the x-ray machine. A special thanks also goes to the Departments of Physics and Radiation Oncology as a whole for providing the support and resources needed to make these studies possible.

I feel especially indebted to the members of Temple Free Will Baptist Church, Greenville, NC, for their love, support and, above all, their prayers. I would never have made it without the moral and spiritual support that they provided my family and me. I am especially grateful to the families of Ms. Tammy Cone, Ms. Sherry Churchill, Ms. Angie Umphlett and Mr. Ti Barnhill for helping to watch over my children and assisting them in every way possible, so that I might have the time to complete the work described in this dissertation.

I want to thank my children, Brenda, Maureen, Faith and Paul. I am so grateful for the unconditional love and patience they have shown. They have truly been my inspiration, and

have always provided me with a reason to press on, especially during the difficult times. Also, I want to especially thank my dear friend, James Hyman, for his moral support, encouragement and unconditional love for me and my children during the last two years of preparing this manuscript.

Above all, I thank my heavenly Father for giving me wisdom and knowledge and for answering my many silent prayers.

TABLE OF CONTENTS

LIST OF FIGURES

LIST OF ABBREVIATIONS

53BP	P53 binding protein 1
ADP	Adenosine diphosphate
Apaf-1	Apoptotic protease activating factor 1
ATM	Ataxia telangiectasia mutated
ATP	Adenosine triphosphate
ATR	Ataxia telangiectasia rad3-related
ATRIP	ATR- interacting protein
ATTC	American Type Tissue Culture
Bcl	B-cell leukemia lymphoma protein
BRCA	Breast cancer susceptibility
BSA	Bovine serum albumin
Cdc	Cell dependent cyclins
CDK	Cyclin dependent kinase
Chk	Checkpoint
DISC	Death-inducing signal complex
DNA-PK	DNA-dependent protein kinase
DNA-PKcs	DNA-PK catalytic subunit
DSB	Double-strand break
ELISA	Enzyme linked immunosorbent assays
ERCC1	Excision repair cross complementing rodent repair deficiency complementation group 1
ERK	Extracellular signal regulated.

FANC	Franconi anemia subtype
GJIC	Gap junctional intercellular communication
H2AX	H2A histone member family, member X
HR	Homology directed recombination
IAPs	Inhibitor of apoptosis proteins
ICC	Immunocytochemistry
IL-1	Interleukin 1
IκB	Inhibitor of NF-κB
IKK	IκB kinase
IMDM	Iscove's modified Dulbecco's medium
IMRT	Intensity modulated radiation therapy
IR	Ionizing radiation
IGRT	Image guided radiation therapy
JNK	c-JUN NH_2.terminal kinase
LET	Linear energy transfer
Lig4	Ligase IV
MAPK	Mitogen activated protein kinase
MDC1	Mediator of mammalian damage checkpoint 1
Mre11	Meiotic recombination 11
MRM	Mre11, Rad50, Nbs1 complex
Nbs1	Nijmegen breakage syndrome 1 gene
NF-κB	Nuclear factor kappa B
NHEJ	Non-homologous end joining

NIK	NF-κB inducing kinase
NO	Nitric oxide
PBS	Phosphate buffered saline
PCNA	Proliferating cell nuclear antigen
PI	Propidium iodide
RAD	RADiation sensitivity abnormal yeast RAD related
Rb	Retinoblastoma protein
ROS	Reactive oxygen species
RPA	Replication protein A
SMAC	Second mitochondrial derived activator of caspases
TNF	Tumor necrosis factor
XPF	Xeroderma pigmentosum, complementation group F

CHAPTER 1: INTRODUCTION

1.1 THE PROBLEM - INCREASING EXPOSURE OF THE WORLD POPULATION TO LOW DOSE RADIATION

Since the discovery of x-rays and radioactivity by Wilhelm Roentgen and Marie Curie at the end of the nineteenth century, the use of ionizing radiation (IR) in the medical, as well as non-medical fields has been on the rise (1, 2). Many reports have been written on the biological effects of radiation, especially at high doses (3-9), but the effects of low dose radiation (defined as 1 Gy or less), and especially very low dose radiation (defined as 20 cGy or less), still remain largely unclear. Nevertheless, exposure to low doses of radiation has exponentially increased in the past two decades. For example, with carbon-based energy sources of the world depleting rapidly, many governments have turned to nuclear power as a source of energy (10). If this trend continues, an increase in human populations exposed to low doses of ionizing radiation from nuclear industrial waste and accidents is a realistic expectation.

Additionally, the exposure to low doses of radiation in the form of x-ray procedures for diagnostic imaging is reaching more and more individuals throughout the world and with greater frequency. Furthermore, ionizing radiation has emerged as a primary treatment for many carcinomas, either alone or in combination with other treatment modalities (e.g. chemotherapy and surgery). Whereas methods of radiation delivery such as intensity modulated radiation therapy (IMRT) and image guided radiation therapy (IGRT) have emerged with a record of more targeted delivery of radiation to the tumor site, these protocols also expose larger sections of normal tissues to low doses of ionizing radiation (1, 11).

Finally, the threat posed by the use of nuclear terrorism within the United States and in many parts of the world has grown significantly in recent years. Indeed, one of the unique problems of the twenty first century is the emergence of terrorist groups. A nuclear terrorism

attack can expose a large number of people to low doses of ionizing radiation, as well as the more lethal higher doses often publicized by the media. Certainly, therefore, biological effects at low doses of ionizing radiation have become increasingly important in the present era.

1.2 THE CHALLENGE - PARADIGM SHIFTS IN OUR UNDERSTANDING OF LOW DOSE RADIORESPONSE

Because of the central role played by the DNA in cellular function, radiobiologists have traditionally modeled the response of cells to ionizing radiation on DNA damage and repair. To model the observable effects, ionizing radiation (especially photon irradiations such as x-rays and gamma rays) was assumed to cause two types of breaks in the DNA. The first of these was the single strand break that was easily repaired, and the second was the double strand break that was much harder to repair (12). It was assumed that low doses resulted mostly in single strand breaks that were quickly repaired while higher doses were dominated by double strand breaks that were much harder to repair. In brief, proponents of this theory assumed that a threshold of double strand breaks was required to inactivate a cell, leading to reproductive death. Ultimately, a linear quadratic equation [$\ln S = -(\alpha D + \beta D^2)$] formed the basis of much of cellular radioresponse (in the above equation, S is the survival fraction after a dose D and α and β are constants). Effects of radiation at low doses were simply extrapolated back from the high dose data.

Currently, however, many radiobiologists believe that the DNA centric modeling of radiobiological effects may not be completely valid. In fact, several reports now indicate that low doses of ionizing radiation may have profound, and perhaps lasting, effects on cellular metabolism and cell-cell communication - not only on cells that have been directly hit by

radiation, but also on cells that have no direct contact with the incoming photons. Specifically, reports on low dose ionizing radiation have documented that radiation in this dose range can stimulate signaling pathways that are not reliant on direct DNA damage. Indeed, scientists are documenting a host of previously unexpected and oftentimes contradictory responses. For example, following low dose radiation exposure, observations of bystander effects (13-15), adaptive responses (16), hyper-radiosensitivity (17), genomic instability (18), and hyper-radioresistance (19-21) of cells have increasingly been reported in the literature. However, mechanisms by which cells translate the radiation signal to affect cell metabolism, proliferation and even survival still remain incompletely understood, and much debate has centered around the fact that these above-mentioned responses to low dose radiation appear to be highly cell type specific. The following sections will first briefly discuss some of the cellular responses known to be induced by exposure of cells to ionizing radiation, and, subsequently, will present a summary of the newly emerging observations and evidence that are rapidly changing historically-held tenets regarding the cellular effects of low dose radiation exposures.

1.3 MOLECULAR MECHANISMS OF RADIATION-INDUCED CELL RESPONSE

Cells have evolved complex mechanisms to cope with damaging agents such as ionizing radiation. These include the ability to: (1) halt progression of the cell cycle (cell cycle arrest or "block") to repair DNA damage prior to entering mitosis and cell division; (2) trigger programmed cell death (apoptosis) in cells so badly damaged that genetic stability may be compromised; and (3) to upregulate growth factors which stimulate proliferation to replenish lost cells (12, 22-25). In the sections that follow, a summary of these responses will be presented.

1.3.1 Cell Cycle Changes Following Exposure to Radiation

Dividing cells go through a cell cycle consisting of four distinct phases: G1, G2, S, and M. Quiescent cells not undergoing cell cycle progression are designated to be in G0. A schematic of this process is presented below. Briefly, in G1, the cell increases in size and synthesizes extra RNA and proteins; in S phase, the DNA is replicated; in G2, the cell makes proteins necessary for cell division; and, finally, in M phase, the cells go through mitosis.

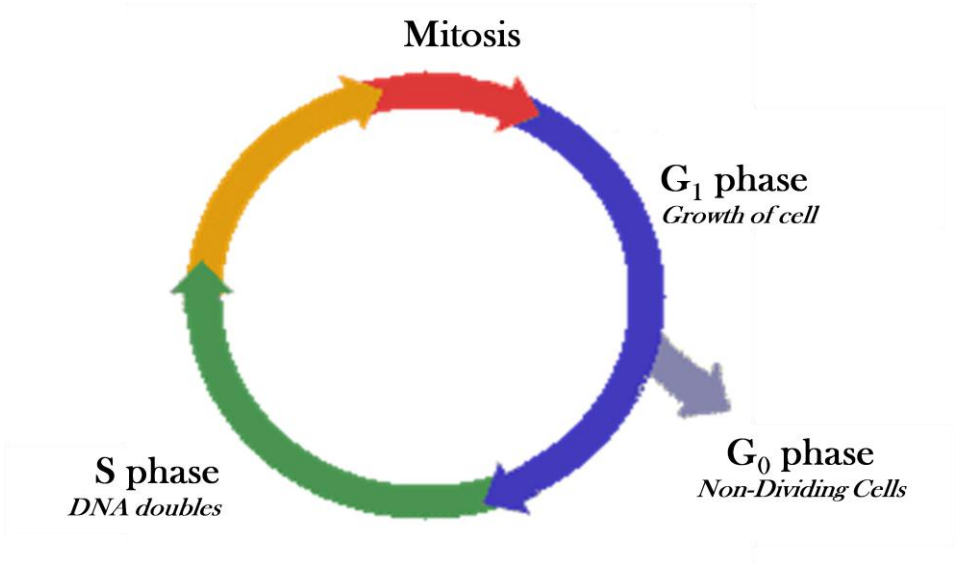

Figure 1.1: The Cell Cycle

Progression through the cell cycle in normal cells is regulated at various checkpoints by a group of proteins known as cyclins and their corresponding cyclin dependent kinases (CDK's). Cycin kinase inhibitors (CKI; e.g. p21/WAF-1) are also involved (24, 26-29). While the levels of CDK's stay relatively constant throughout the cell cycle, the concentrations of the cyclins fluctuate greatly from one cell cycle phase to another as demonstrated in Figure 1.2 below.

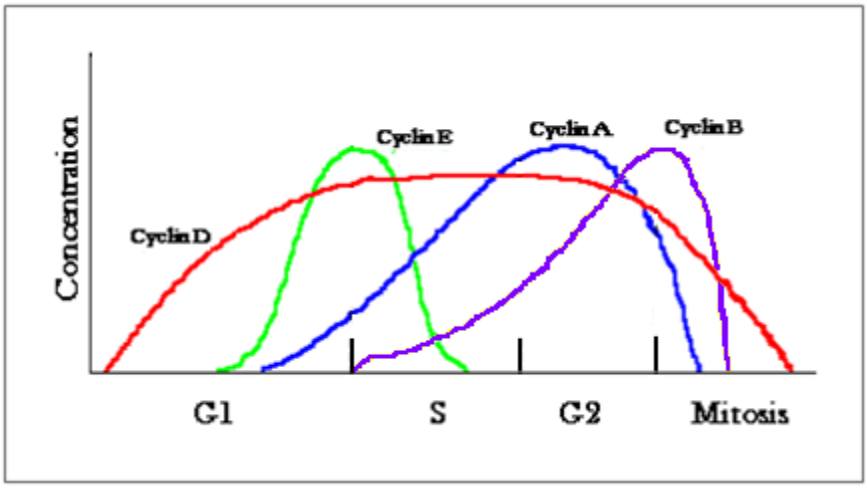

Figure 1.2: Cyclin Levels as a Function of Cell Cycle Phase

Cyclins must bind with their corresponding CDKs to activate them as demonstrated below. Once formed, the activated cyclin/CDK complexes phosphorylate particular proteins involved in the progression of the cell cycle from one phase to another.

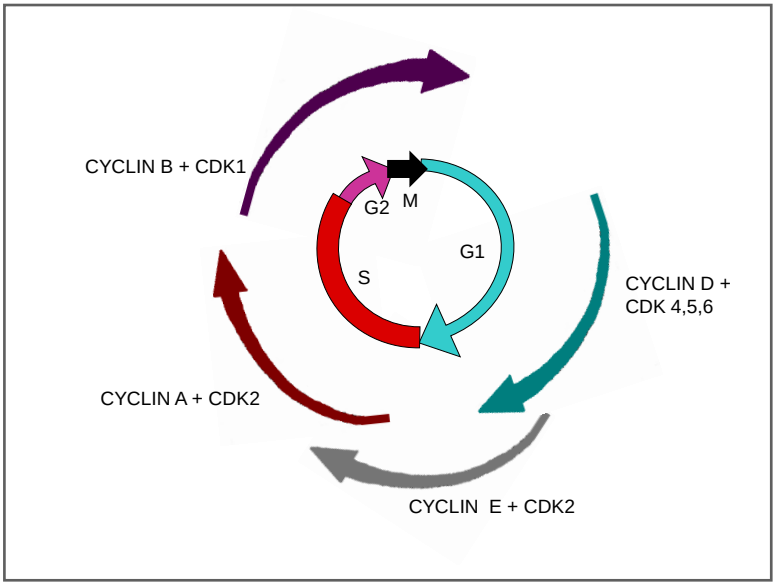

Figure 1.3: Cyclin/CDK Complexes Throughout the Cell Cycle

Cells respond to DNA damaging agents, such as ionizing radiation by activating cell

cycle checkpoints. Halting progression of the cell cycle at these checkpoints allows the cell time to repair damaged DNA before proceeding to the next phase, thereby decreasing the potential for genetic mutations (27, 30). Numerous reports have demonstrated the existence of ionizing radiation-induced arrests in the G1, G2 and S phases of the cell cycle [reviewed in 24]. For example, irradiation with high doses in HeLa cells, a human adenocarcinoma cell line, induced delays in the S phase, while moderately low doses caused a G2 phase arrest (31, 32).

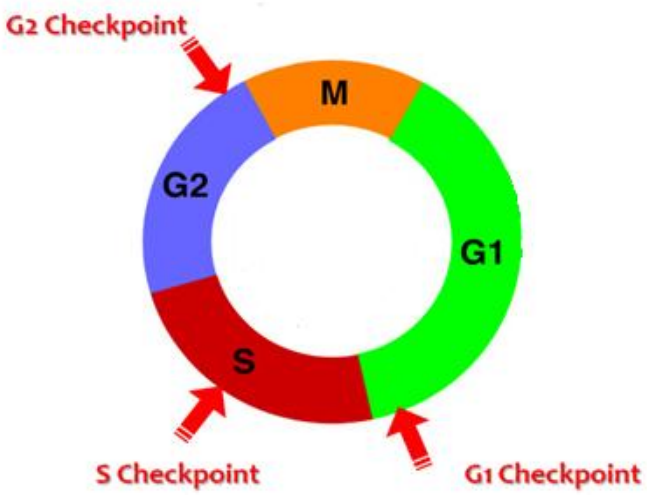

Figure 1.4: Cell Cycle Checkpoints

G1 Checkpoint - Cells in the G1 phase at the time of irradiation are deterred from entering the DNA replication phase (S phase) by the G1 (also called the G1/S) checkpoint (12, 22, 27, 29). In the absence of DNA damage, normal progression of cells from G1 to S phase is controlled by the cyclin E/CDK2 complex (23, 24, 27, 29). To enable the G1/S transition, the cyclin E/CDK2 complex must be activated by Cdc25A, which if inactivated as a result of radiation induced DNA-damage events, prevents the cell from making the G1/S transition. Following radiation induced DNA damage, the sequence of events described below are believed

to lead to the activation of the G1 checkpoint, ultimately preventing the cell from proceeding to the S phase.

The first step in the activation of the G1 checkpoint starts with detection of DNA damage. Currently, many reports attribute the recognition of DNA double strand breaks (DSB) resulting from ionizing radiation to the ATM molecule (26, 29, 33, 34). Bakkenist and Kastan have provided a model for DNA double strand break damage recognition by the ATM molecule (33). They have demonstrated that, following ionizing radiation-induced DSB, changes in chromatin structure activates ATM, which exists in the nucleus in homodimeric form, causing it to dissociate from its homodimeric form to monomeric form by homodimer autophosphorylation on ser-1981 (33). Each of the monomers then phosphorylate many downstream proteins involved in the cell cycle checkpoint activation such as Chk2 and p53 (reviewed in (29). The activated ATM molecule then activates many downstream targets, that lead to two simultaneous pathways of events resulting in G1/S checkpoint arrest and maintenance (27, 29). In one pathway, the DNA damage-activated ATM is thought to activate Chk2 by phosphorylation of Thr68 (35). Activated Chk2 then phosphorylates Cdc25A phosphatase. Phosphorylated Cdc25A is removed from the nucleus by ubiquitin-mediated proteolytic degradation (26, 29). Decreased levels of Cdc25A in the nucleus lead to increased levels of phosphorylated cyclin E/CDK2 complex. Phosphorylated cyclin E/CDK2 is inactive and unable to phosphorylate Cdc45, which is necessary to set off DNA synthesis (26, 29). Immediately following the first pathway for G1/S checkpoint activation, is a second pathway for its maintenance (29). While the first pathway is believed to be p53 independent, the second pathway is thought to be heavily dependent on the status of the p53 protein in the cell, because mutant cells lacking functional p53 have been found to have a defective G1/S checkpoint (36). Like the first pathway, the ATM has been associated

with initial recognition of radiation-induced DNA damage (37). Upon recognition of the damage, the phosphorylated ATM activates Chk1 which, in turn, activates p53 by sequential phosphorylation (38). Phosphorylation of p53 stabilizes it, thereby inhibiting it from nuclear export and degradation (27, 29). Consequently, active p53 accumulates in the nucleus and activates its target genes p21 (26-29). Activated p21 binds to the Cdk2/cyclin E complex, thus preventing the S phase transition and maintaining the G1/S arrest (26, 27, 29).

S Checkpoint - The G1 checkpoint prevents the cells irradiated in the G1 phase from entering the S phase with damaged DNA, but does not benefit the cells present in the S phase at the time of irradiation. Evidence of the existence of the S phase checkpoint (also called intra-S checkpoint) came from observations that irradiated cells did not integrate radioactive precursors into newly synthesized DNA (39, 40). Of the three checkpoints (G1, G2, and S), mechanisms involved in the activation of the S checkpoint following irradiation are least understood. Like the G1/S checkpoint, the S checkpoint also consists of two pathways (29) and is very similar to the first G1/S pathway described above, that is, the ATM-Chk2-Cdc25A-Cdk2 signaling cascade (27, 29). Degradation of Cdc25A ultimately leads to inactivation of Cdk2/cyclin A/cyclin E complexes and a delay in DNA synthesis and replication (22, 41, 42). The second pathway is less known and involves such molecular regulators as NBS1, Mre11, Rad50, and BRAC1 (43-46). Currently, the role of p53 and p21 proteins in S phase checkpoint is not fully elucidated and it is not clear if p53 is activated upon exposure to ionizing radiation (47, 48).

G2 Checkpoint - Cells entering the G2 phase with damaged DNA or those that are irradiated in the G2 phase are kept from entering the M phase with damaged DNA by the G2 (also called the G2/M) checkpoint. Currently, numerous reports have attributed a long G2 delay in cells with radioresistance to cell kill (49-51). Conversely, defects in the G2 checkpoint have

been linked to elevated radiation sensitivity (49-51). By utilizing several human cell lines, there is mounting evidence suggesting the existence of two molecularly distinct G2/M checkpoints (33, 52). The first is the traditional checkpoint that has been known for many years for cells irradiated at doses higher than 1 Gy, and is associated with accumulation of cells in G2 that were irradiated in the G1 and S phases (25, 53). The second checkpoint appears to be activated in cells that are irradiated when they are already in the G2 phase of the cell cycle (52). For higher doses (>1 Gy), activation of the classical G2/M check point has been demonstrated to be dependent on dose, while the second G2/M checkpoint is independent of dose. Studies at low doses of irradiation, albeit few, have demonstrated that cells irradiated with low doses exhibit activation of an early ATM dependent G2 checkpoint for cells irradiated in the G2 phase, while for cells irradiated in the S and G1 phases, reports suggest the activation of a late ATM-independent G2/M checkpoint (54, 55). Irrespective of the phase at which the cells are irradiated, numerous studies have attributed the trigger of both types of G2 checkpoints to the recognition of DNA damage by the ATM protein (26-29, 33, 41, 55, 56). Similar to the G1 an S checkpoints, the G2/M checkpoint also consists of two pathways, one for initiation and the other for maintenance of the checkpoint arrest. Following DNA damage with ionizing radiation, the rapid ATM-Chk2-Cdc25A pathway is activated (22, 26, 34). Once phosphorylated, Cdc25A phosphatase binds to 14-3-3 proteins, and it is extruded from the nucleus and sequestered in the cytoplasm where it is degraded by the ubiquitin proteosome pathway (29). Inactive Cdc25A phosphatase inhibits the activation of cyclin B/CDK1 complex, leading to G2/M block (29, 34). The maintenance of the G2/M checkpoint is accomplished by the p53/p21 pathway in a sequence similar to G1/S checkpoint maintenance (23, 29). As mentioned earlier, the function of these cell cycle checkpoints is to delay the progression through the cell cycle to allow for more time for

DNA to be repaired or to redirect unrepairable cells through a programmed cell death called apoptosis (27, 30, 51).

1.3.2 Radiation-Induced Cell Death - Apoptosis and Necrosis

Irradiation of cells may not only activate DNA repair and cell cycle arrest, but can also lead to cell death through two principal mechanisms - necrosis and apoptosis. The decision about shunting the cell towards apoptosis or directing it along a DNA repair pathway is dependent on both cell type and the scale of the DNA damage (57). Necrosis is a passive cell death, often linked to damage so extensive that the metabolic machinery of the cell can no longer function well enough to undergo either repair or programmed death. Cells undergoing necrotic death show early loss of membrane permeability, dilation of cytoplasmic vesicles, swelling, lysis and elicitation of an inflammatory response that can potentially damage surrounding tissue (58). On the other hand, apoptosis, commonly described as a programmed cell death, is a highly regulated program initiated by the cell. It is characterized by morphological changes such as chromatin condensation, cell shrinkage, nuclear and cytoplasmic blebbing and formation of membrane bound apoptotic bodies, and it requires energy in the form of ATP. In apoptotic cells, degradation of the DNA has been observed to come before loss of membrane integrity (58).

Radiation-induced cell death via necrosis is well documented, and, currently, there is mounting evidence that suggests exposure of cells to ionizing radiation generates reactive oxygen species (ROS) that can initiate oxidation of membrane lipids, thereby setting off apoptosis (59, 60). γ-irradiation of normal human lymphoblasts with 20 Gy was found to increase apoptosis significantly above those of unirradiated controls (60), while x-irradiated U937 human monoblastic leukemia cells generated 80% increase in ceramide (a marker of

apoptosis) levels (61). Rat-1 Myc-ER fibroblastic cells exposed to 10 Gy also had 80% more ceramide levels compared to the control (62).

1.3.3 MAPK Signal Transduction Pathways Activated by Radiation

Several reports written in the last decade indicate that exposure to ionizing radiation not only leads to the classically held paradigm of DNA damage and subsequent cell cycle arrest and/or death, but also can stimulate pathways that trigger cell proliferation (3, 63-66). For example, studies have demonstrated that exposure of cells to ionizing radiation can activate cytokine receptors such as epidermal growth factor receptors (EGFR) and tumor necrosis factor receptors (TNFR) on the cell membrane, and can set off the mitogen activated protein kinase pathways (MAPKs) similar to those activated by growth factors and other external cellular stresses (3, 63-66). In human cells, there are three families of fairly understood MAPK pathways. These include (1) the ras-MAPK (also known as the extracellular signal-regulated kinase 1 and 2 or ERK1/2) signal transduction pathway which transmits extracellular signals from the receptor tyrosine kinase and the heterotrimeric G-protein linked receptor which induce cell proliferation and differentiation, (2) the c-jun NH_2-terminal kinase (JNK) pathway that is also activated by extracellular stresses like heat, high osmolarity, UV irradiation, and pro-inflammatory cytokines, and (3) the p38 MAPK pathway that is traditionally activated by osmotic stress, heat shock, tumor necrosis factor α (TNFα) and interleukin 1(IL-1) (66, 67). All three of these pathways are, in general, organized at three levels consisting of a MAPK, a MAPK kinase activator (MAPK kinase, MEK or MKK), and a MAPK kinase kinase (MEK kinase or MAPKKK). Signals are transmitted by phosphorylation from upstream MAPKKKs to downstream MAPKs.

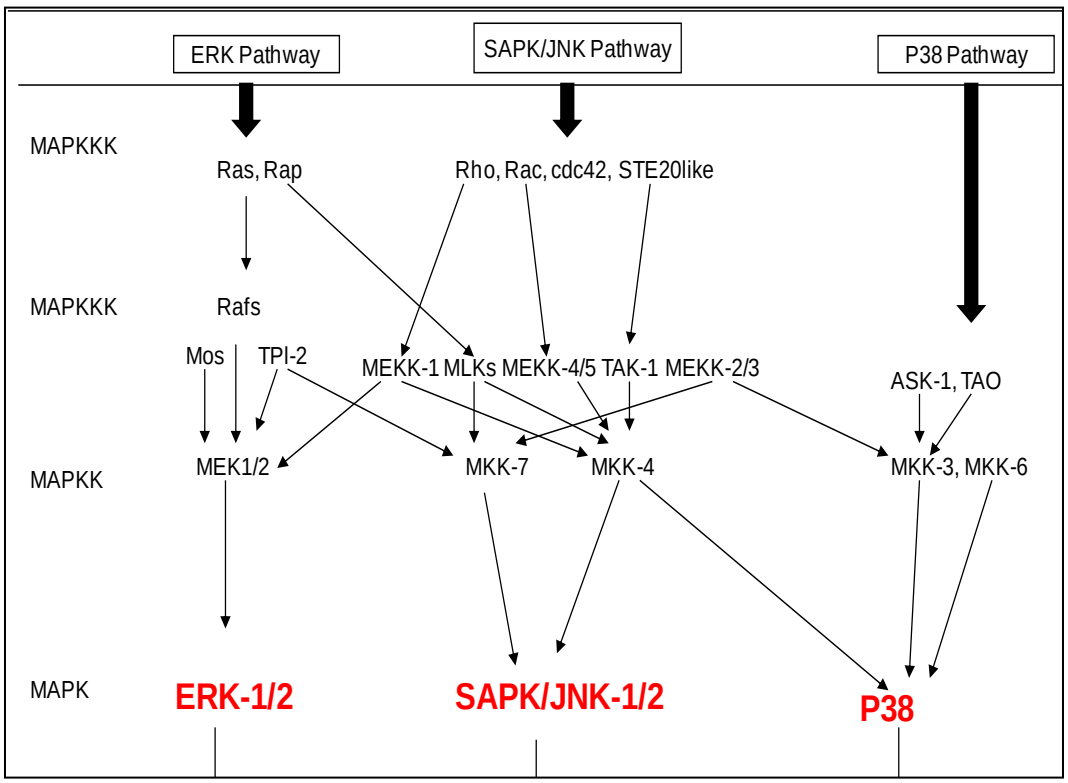

Figure 1.5: Organization of MAPK Pathways

The Ras/ERK1/2 signal transduction pathway - It is now fairly understood that one of the defense mechanisms cells utilize to cope with radiation insult is to enhance proliferation in the surviving fraction of cells (68) by triggering signal transduction pathways such as the Ras/ERK1/2 that lead to activation of genes involved in cellular proliferation and prevention of apoptosis. Indeed, studies indicate that exposure of cells to ionizing radiation can activate the epidermal growth factors receptor (EGFR, also called ERBB1 and HER1) in several normal and carcinoma cells, leading to increased proliferation (3, 69, 70). For instance, activation of the epidermal growth factor in MCF-7, A431 and MDA-MB-231 cancer cells was observed at a dose of about 0.5 Gy (3, 71), and some scientists have argued that the reason we sometimes have poor

prognosis in treating cancers *in vivo* with a radiotherapeutic protocol is because the ionizing radiation may be activating the epidermal growth factor receptors that cause increased tumor growth.

The MAPK, ERK1 protein was described for the first time in 1986 as a 42-kDa protein that was stimulated after insulin exposure (72). Soon after its discovery, another closely related protein of 44-kDa was also revealed and demonstrated to share the same function as the 42-kDa protein discovered earlier. These two proteins are closely related in function, and they are designated as ERK1/2. Many growth factors and mitogens have been demonstrated to activate ERK1/2, and, for this reason, this protein has popularly been referred to as mitogen-activated protein kinase or MAPK. Studies have shown that the MAPKs are regulated by another protein kinase MKK1/2 (also designated MAPKK, or MEK1/2) (67, 73). The MKK1/2 are, in turn, activated by the kinase activity of a family of serine-threonine protein kinases Raf1 (73, 74). Additionally, it has been suggested that the Raf1 proto-oncogenes can inhibit apoptosis signaling kinase 1 (ASK1). Briefly, the mechanism by which ionizing radiation appears to be acting is through the initiation of a phosphorylation cascade that starts with activation of plasma membrane growth factor receptors , subsequent activation of Ras (through the exchange of GDP for GTP) which leads to Raf1-MKK1/2-ERK1/2 activation as presented in Figure 1.6 below. Phosphorylated ERK1/2 then translocates to the nucleus where it activates several substrates such as c-myc, c-fos, c-jun, Rsk, SOS, Elk-1,and STATS (75). C-fos, c-myc and c-jun proteins and mRNA are stabilized by activated ERK1/2, which, in turn, play a key role in cell proliferation, differentiation, and oncogenic transformation (76).

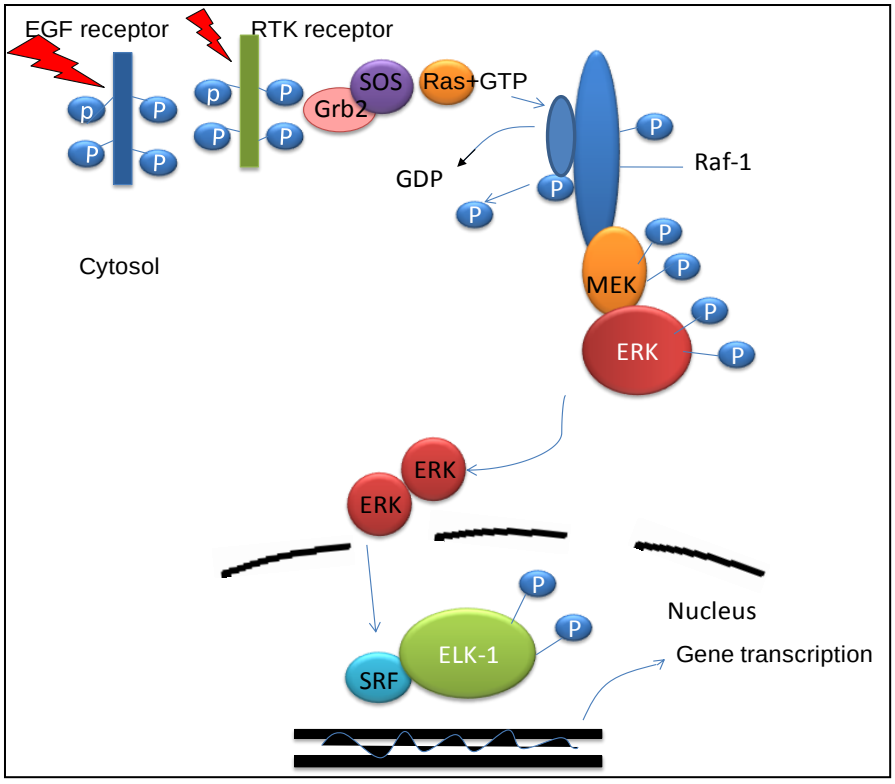

Figure 1.6: The ERK Signal Transduction Pathway

At doses of radiation greater than 1 Gy, several reports have demonstrated activation of the ERK pathway by phosphorylation of the EGFR receptors and, subsequently, setting off the whole ERK1/2 signaling transduction pathway (3, 77, 78). Carter *et al* showed that 1 Gy of radiation can cause more *activation* of ERK1/2 than 6 Gy of radiation (79). Several studies by Schmidt-Ullrich *et al* have shown that activation of the EGF receptors in A431 squamous carcinoma cells and MDA-MB-231 differ for low and high radiation doses (3, 78). Currently, studies on activation of the ERK1/2 pathway at low doses of radiation are very limited. Suzuki *et al* demonstrated that doses between 2 cGy and 5 cGy enhanced proliferation in normal human diploid cells and phosphorylated ERK1/2 as efficiently as 6 Gy of dose (19). Kim *et at* demonstrated that a dose of 5 cGy stimulated proliferation through activation of transient

ERK1/2 (20). However, the mechanism of low dose radiation-induced proliferation is currently not well understood, and more studies are needed to elucidate this phenomenon.

The c-JUN NH_2-terminal kinase pathway (JNK) - Another MAPK pathway that can be activated when cells are exposed to ionizing radiation is the c-JUN NH_2-terminal kinase. The c-JUN NH_2-terminal kinase pathway was discovered in the 1990s (80) and was initially thought to be initiated only by environmental stress. For this reason, it is also called stress activated protein kinase (SAPK) (81). However, it is now known that the c-JUN NH_2-terminal kinase pathway can also be activated by UV radiation, ionizing radiation, cytotoxic drugs, and reactive oxygen species such as H_2O_2 (82). Unfortunately, at present, it is not clearly known how ionizing radiation initiates the c-JUN NH_2-terminal kinase phosphorelay cascade. However, there are two proposals on the mechanism of activation. The first implicates the Ras proto- oncogene, while the second proposes activation through either the P13K or the protein kinase C or both (80, 83)

Activation of the JNK pathway follows a parallel route only slightly different from the Ras-MAPK pathway (see Figure 1.7 below). However, in the JNK pathway, the GTP- binding Rho families of proteins play a role similar to the Ras to trigger the JNK pathway. Examples of Rho family proteins involved are the Rac1 and cdc42 (84). The MAPKKK of the SAPK/JNK signal pathway consist of the kinases MKKK1-4, TAK-1 and Tpl-2. Activated MKKKs activate the MKKs which, in turn, activate the MAPKs JNK1 and JNK2. Protein kinases that serve as MKKs in the SAPK/JNK pathway include the MKK-7 and the MKK-4.

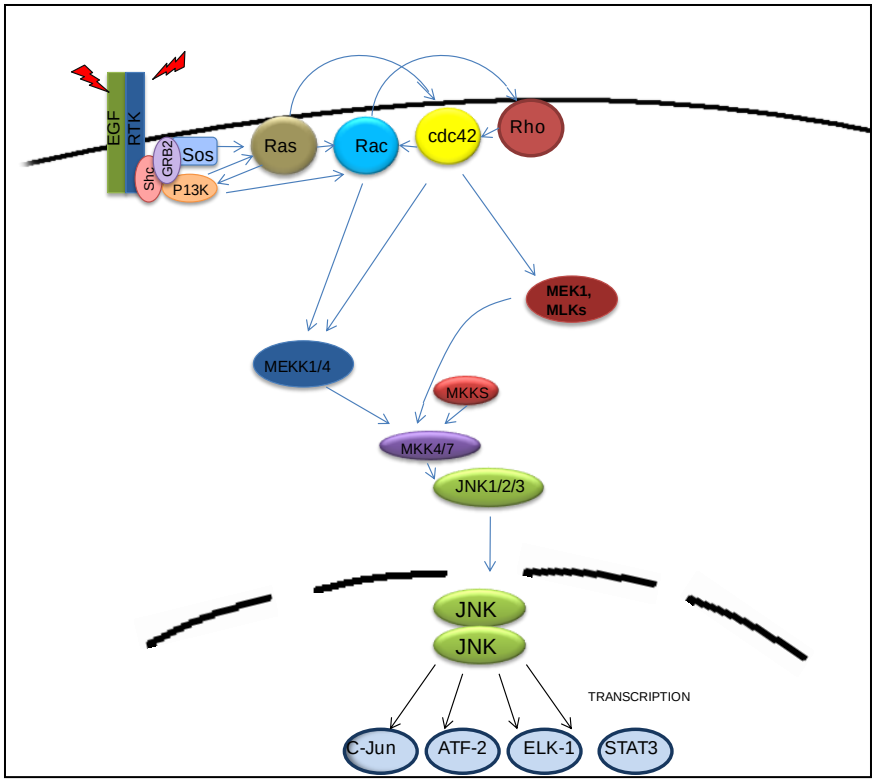

Figure 1.7: The JNK Signal Transduction Pathway

JNK1/4 has been demonstrated to play a central regulatory role in apoptosis (85) . Studies have shown that the binding of p53 protein to JNK leads to ubiquitin-mediated degradation of p53 (85-87). The JNK1/2 are capable of phosphorylating the NH_2-terminal sites in c-Jun and c-Myc, and, ultimately, inducing cell apoptosis (61, 88). Phosphorylated JNK has been shown to target both pro-and anti-apoptotic members of the Bcl-2 familly. Several studies have demonstrated inhibition of anti-apoptotic proteins Bcl-2 and Bcl-xl by phosphorylated JNK (89), while other studies have shown JNK is involved in the degradation of caspase 8 inhibitor (90).

Currently, most studies that link the activation of the JNK pathway to radiation have been performed at very high doses, in a region with an obvious expectation of high cell death. Studies

exploring JNK pathway activation following low dose radiation are far fewer in number. However, recent studies in several cell lines have shown that low doses of radiation can cause disproportionately higher cell death than would have been predicted by extrapolation back from the reports using exposure of cells to high doses of radiation (17, 55, 56, 91-96), and there is speculation that this observed radio-hypersensitivity in the low dose region may be linked, at least in part, to apoptosis (96, 97).

The p38 MAPK pathway - Signalling through the p38 pathway has been shown to be similar to both JNK and Ras pathways (see Figure 1.8 below). The p38 MAPK pathway is activated through Rho families of GTPases, which are activated by phosphorylated receptors following irradiation. Activation of p38 by ionizing radiation at high doses has yielded unpredictable results, ranging from strong (98) to weak (99) to no activation (100) of the pathway. p38 has been shown to be activated by other factors as well such as environmental stress, inflammatory cytokines, insulin and growth factors (101, 102). The PAK family of kinases plays the role of the MAPKKK (103), while the MAPKK kinases consist of the MKK3 and the MKK6 (104). The four p38 MAPK so far known are p38α, p38β, p38γ and p38δ (105). P38 has been shown to phosphorylate and, subsequently, activate various substrates including ATF (activating transcription factors), GADD (growth arrest DNA damage 153), CREB, and SRF (106, 107). Kim et al demonstrated that 5 cGy of ionizing radiation enhanced proliferation through the activation of ERK1/2 and p38 in normal human lung fibroblasts (20). Of interest, the p38 MAPK pathway has been demonstrated to promote both cell death as well as cell survival (108, 109), but, currently, the mechanisms of low dose radiation hyper-radiosensitivity/hyper-proliferation still remain unclear.

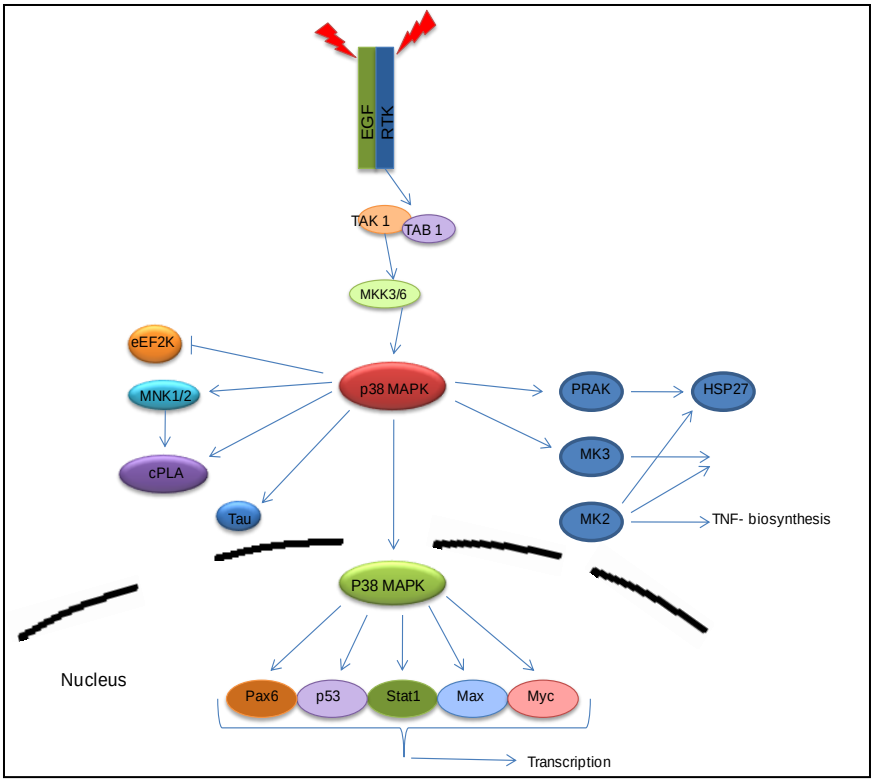

Figure 1.8: The p38 Signal Transduction Pathway

1.3.4 NF-κB Transduction Pathways Activated by Radiation

NF-κB is a major transcription factor involved in the regulation of genes that are involved in response to cellular stress (110-114). In unstimulated cells, NF-κB resides in the cytoplasm complexed to its inhibitory protein IκB (Inhibitor of κB) (114, 115). When activated by either internal or external stress (i.e. radiation), NF-κB is released from its inhibitor IκB, translocates to the nucleus where it binds to DNA and upregulates transcription of stress response genes (116). Several studies have demonstrated the potential of radiation to activate NF-κB (113, 117), with three main mechanisms of action being described (see Figure 1.9). First is activation through the protein kinases ATM and DNA-PK that are involved in sensing damaged DNA (117-119). On recognizing the DNA radiation damage, the ATM activates several downstream targets that lead

to phosphorylation of the IκB proteins, thereby permitting release of the NF-κB from its inhibitor and subsequent translocation to the nucleus. A second mechanism being reported is that radiation-induced ROS directly stimulate the IKK (IκB kinase) complex that, in turn, phosphorylates IκB, releasing the NF-κB from its tether in the cytoplasm and allowing it to translocate to the nucleus (120). Finally, it has been demonstrated that radiation-induced ROS can activate the TNFR (tumor necrosis factor receptors) family of membrane receptors. Once activated, the TNFR engage the NF-κB inducing kinase (121) to phosphorylate the IKK, initiating the cascade that results in NF-κB relocating to the nucleus.

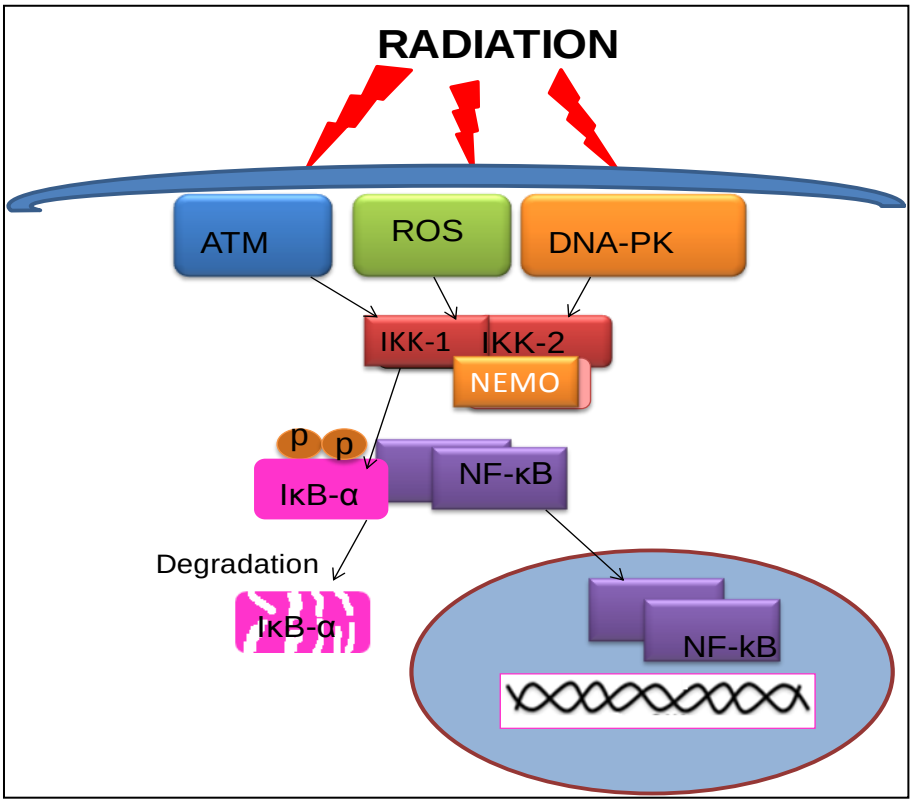

Figure 1.9: NF-kB Activation by Ionizing Radiation

Several studies have reported radiation-induced NF-κB activation, but results vary greatly. In most of these studies, doses required for maximal activation of NF-κB are dependent

on cell type and experimental conditions. For example, U1-Mel human melanoma cells exposed to IR displayed a steady increase in activation of NF-κB from 0 to 4.5 Gy, after which activation fell gradually with increasing dose (122). However, in the KG-human myeloid cell line, NF-κB was increasingly activated by ionizing radiation from 2 Gy upward, peaking at doses between 5 to 20 Gy (123). Finally, in human EBV-transformed 244B human lymphoblastoid cells, activation of NF-κB was observed between 0.25 -2 Gy with a maximum at 0.5 Gy (124).

1.4 LOW DOSE RADIATION PHENOMENA

As stated previously, scientists are documenting a host of unexpected and seemingly contradictory responses following exposure to low doses of radiation. For example, observations of bystander effects (13-15), low dose hyper-radiosensensitivity (17, 125, 126) and even hyper-proliferation (19-21) have increasingly been reported in the literature. In the sections that follow, some of these responses will be discussed.

1.4.1 Low Dose Hyper-Radiosensensitivity

In the last decade, several *in vitro* studies have demonstrated that cell survival curves at low doses (below 1 Gy) deviate from the standard linear quadratic cell survival curve extrapolated from high doses (17, 54, 92, 93, 126). For many cell lines, this deviation is evidenced as increased hyper-radiosensitivity (greater than predicted cell death) in the dose range below 50 cGy. The exact mechanisms and pathways responsible for the hyper-radiosensensitivity are not completely understood, although several explanations have been proposed to explain the shape of the curve. One currently popular explanation given for the hyper-radiosensensitivity curve is that cells need to accumulate some minimum damage before DNA repair mechanisms

are turned on (56). If DNA damage is below this minimum amount, there is no upregulation of repair pathways and the damage remains within the cell and may lead to eventual mitotic failure and death. In support of this damage threshold theory, it was observed that cells pre-treated with very low concentrations of hydrogen peroxide before irradiation did not display the hyper-radiosensensitivity seen in irradiated-only cells (127), because the DNA damage from hydrogen peroxide added on to the DNA damage from the radiation surpassed the damage threshold required for the activation of DNA repair pathways. Furthermore, hyper-radiosensensitivity was not observed in V79 Chinese hamster cells that were pre-irradiated with 20 cGy of x-rays (127). Nevertheless, not all researchers currently support the DNA damage threshold concept. Some have argued that most DNA repair data from low dose radiation studies have been based on indirect estimates of DNA damage (measuring γ-H2AX foci) and not direct measurement of DNA double strand breaks (128).

It is also not clear at present how radiation-induced cell cycle arrest is related to the hyper-radiosensitivity responses observed. However, several researchers have shown that those cells in the G2 phase of the cell cycle at the time of irradiation contribute significantly to hyper-radiosensitivity (54, 55, 125, 129). For example, Kruegar and colleagues have shown that cells in the G2 phase play an important role in the hyper-radiosensensitivity phenomenon, because enrichment of V79 Chinese hamster with G_1 and S phases did not display a hyper-radiosensensitivity phenomenon (55), but a G_2 phase-enriched cell population showed a significant hyper-radiosensitivity phenomenon (125).

1.4.2 Low Dose Radiation-Induced Hyper-Proliferation

Despite the prevalence of low dose hyper-radiosensensitivity in many cell types, other studies have shown that there exist cell lines that display low dose hyper-proliferation (19, 20, 130). The mechanism underlying low dose hyper-proliferation is yet to be completely elucidated, but is believed to involve activation of growth factors. Specifically, in addition to DNA damage, radiation-induced membrane-associated changes include activation of major growth regulators such as epidermal growth factor receptors (EGFR), tumor necrosis factor receptors (TNFR) and tyrosine kinase receptors (3, 61, 69, 78). For example, activation of the EGFR in the plasma membrane has been associated with stimulation of the MAPK pathways (78, 79) which, as described previously, are important mediators of enhanced cell proliferation/survival. Studies are still somewhat limited, but hyper-proliferation of γ-irradiated Chinese hamster fibroblasts and Raji lymphoma cells has been reported to be enhanced at doses between 2 and 10 cGy (130). Additionally, irradiation at doses between 2 and 5 cGy has been documented to cause hyper-proliferation in normal human HE49 cells (19). Finally, exposure to 50 cGy has been reported to stimulate induction of cell proliferation in mouse hematopoietic cells (21), and irradiation at 5 cGy has been shown to enhance cell proliferation via transient ERK1/2 and p38 activation in normal human lung fibroblasts (20).

1.5 HYPOTHESIS AND SPECIFIC AIMS

The biological effects of radiation are governed by many factors, including the cell type being irradiated. Previously, within our laboratory, it was observed that the human melanoma A375 cell line appeared to demonstrate an interval of increased radioresistance following very low doses of radiation. This was in sharp contrast to much of the reported literature which

suggests the majority of cell lines irradiated at these very low doses demonstrate a hyper-radiosensensitivity response, among which is the human prostate carcinoma PC3 line. It is the hypothesis of this proposal that the contradictory responses of the A375 and PC3 cell lines following very low dose radiation exposures is due to differential regulation of mediators controlling two critical signaling pathways within the cell – the pathways involved in cell cycle progression and cellular proliferation (mitogen activated protein kinase or MAPK pathway and the nuclear factor kappa B or NF-κB pathway). The principal objective of this research is to better characterize the cellular response to low dose radiation in these two cell lines and to ascertain the role these molecular pathways play in bringing about this cellular response. To accomplish this, the following specific aims were developed:

1.5.1 Specific Aim 1

To compare cell survival responses in A375 human melanoma cells and PC3 human prostate cancer cells at doses of radiation ranging from 0 to 100 cGy.

1.5.2 Specific Aim 2

The second aim of these studies was to investigate the temporal kinetics and magnitude of cell cycle arrest that occurs following low dose radiation exposure in the A375 and PC3 cell lines over a series of doses ranging from 0 to100 cGy.

1.5.3 Specific Aim 3

The third aim of these studies was to investigate the effect of low doses of radiation on the expression of cell cycle regulator proteins in an effort to correlate the temporal changes in

cell cycle distribution observed in Specific Aim 2 with the downregulation of specific cyclin levels within the cell.

1.5.4 Specific Aim 4

The fourth aim of these studies was to ascertain whether signaling through the MAPK, and NF-κB proliferative pathways is being altered as a function of cellular exposure to low dose radiation (0-100 cGy).

CHAPTER 2: EXPERIMENTAL DESIGN AND METHODS

2.1 EXPERIMENTAL MODEL

The principal objective of this research was to better characterize the molecular pathways involved in the cellular responses to very low doses of ionizing radiation. To accomplish this, we have chose two cell models – the A375 human melanoma cell line and the PC3 prostate carcinoma cell line. The reason these models were chosen is three fold. First, these cell lines were selected because they represent the opposite ends of the spectrum with regard to radiation sensitivity. For example, in classical dose-response survival studies (1 Gy and greater), the A375 cells have been shown to be moderately resistant to radiation, while the PC3 cells have been shown to be relatively sensitive to radiation.

Secondly, as stated above (Hypothesis and Specific Aims), preliminary studies within our laboratory observed that the human melanoma A375 cell line appeared to demonstrate an interval of hyper-radioresistance following very low doses of radiation which was in sharp contrast to reported literature that argued that PC3 cells display very low dose hyper-radiosensensitivity (129, 131).

Finally, because numerous other studies have used these two cell lines, a strong data base exists on these cell lines upon which we can obtain relevant information pertaining to cellular response, experimental design and maintenance. Specifically, A375 cells are characterized by having a wild type p53 and a mutated tumor suppressor gene BRCA1. They also have been shown to possess aberrant caspase 3 activity and a strong tendency for ATM phosphorylation after irradiation, by the association of the ATM with the RAD50/MRE11/Nibrin complex involved in double-strand break repair through both homologous recombination and nonhomologous end-joining (132). On the other hand, the radiosensitive PC3 prostate

carcinoma cells possess a mutated p53, have strong metastatic ability and exhibit some caspase 3 activity.

2.2 EXPERIMENTAL DESIGN

2.2.1 Experimental Design for Specific Aim 1: *Comparison of cell survival responses in A375 human melanoma cells and PC3 human prostate cancer cells at low doses of radiation*.

One of the goals of these studies was to characterize the survival response following low dose radiation in two experimental cell lines – the A375 human melanoma cell line and the PC3 prostate carcinoma cell line. Cell survival was assessed using a standard clonogenic assay over a series of low dose radiation exposures (0, 2, 5, 10, 25, 50 and 100 cGy). Briefly, the clonogenic assay or colony formation assay is an *in vitro* cell survival assay based on the ability of a single cell to grow into a colony (defined to consist of at least 50 cells), and essentially tests for a cell's reproductive integrity (ability to undergo "unlimited" division). The clonogenic assay has been chosen for these studies, because it has long been accepted as the "gold standard" for determining actual cell survival following irradiation. It has been argued that many of the more rapid cell viability assays provide an incomplete assessment of cell killing, since they may not be able to distinguish growth inhibition with actual death, and they may assess only events that have occurred up to the time of the assay.

2.2.2 Experimental Design for Specific Aim 2*: Investigation of the effect of low dose radiation exposure on cell cycle progression in A375 human melanoma cells and PC3 human prostate cancer cells.*

The importance of ionizing radiation as a disruptor of cell cycle progression is well documented, and, for this reason alone, the cell cycle pathway must be considered in any investigation that includes radiation. Indeed, it has long been held that one of the cell's major defenses against radiation damage is to halt progression through the cell cycle (25) for a sufficient amount of time to affect repair of DNA damage, and, in both asynchronous and synchronous cell populations, a G2/M cell cycle arrest has been observed in a large spectrum of cell types over a broad range of radiation doses (50). Several of these studies have reported that radioresistant cells tend to have a more marked G2/M arrest than radiosensitive cell lines have (133), and Marples *et al* have postulated that failure to arrest in G2 phase following low dose radiation may be responsible for the low dose hyper-radiosensensitivity observed in some cell lines (125). The second aim of this proposal, therefore, is to investigate the kinetics and magnitude of cell cycle arrest that occurs following low dose radiation exposures (0, 2, 5, 10, 25, 50 and 100 cGy) in the A375 and PC3 cell lines using flow cytometric analysis of cell cycle distributions over a 24 hour interval following irradiation.

Briefly, the principle underlying the flow cytometric technique is as follows. The nuclear DNA content of a cell can be quantitatively measured by flow cytometry using a procedure that involves binding a fluorescent dye to the DNA of a suspension of permeabilized single cells. The assumption is that the stained cellular material has incorporated an amount of dye proportional to the amount of DNA present. The stained material is then measured in the flow cytometer, and the emitted fluorescent signal yields an electronic pulse with a height

proportional to the total fluorescence emission from the sample. Thereafter, such fluorescence data are considered a measurement of the cellular DNA content, and distribution of cells in the into G0/G1, S and G2/M cell cycle phases can be obtained on the basis of their differing DNA content using software analysis programs such as ModFit (see schematic below from our laboratory experiments).

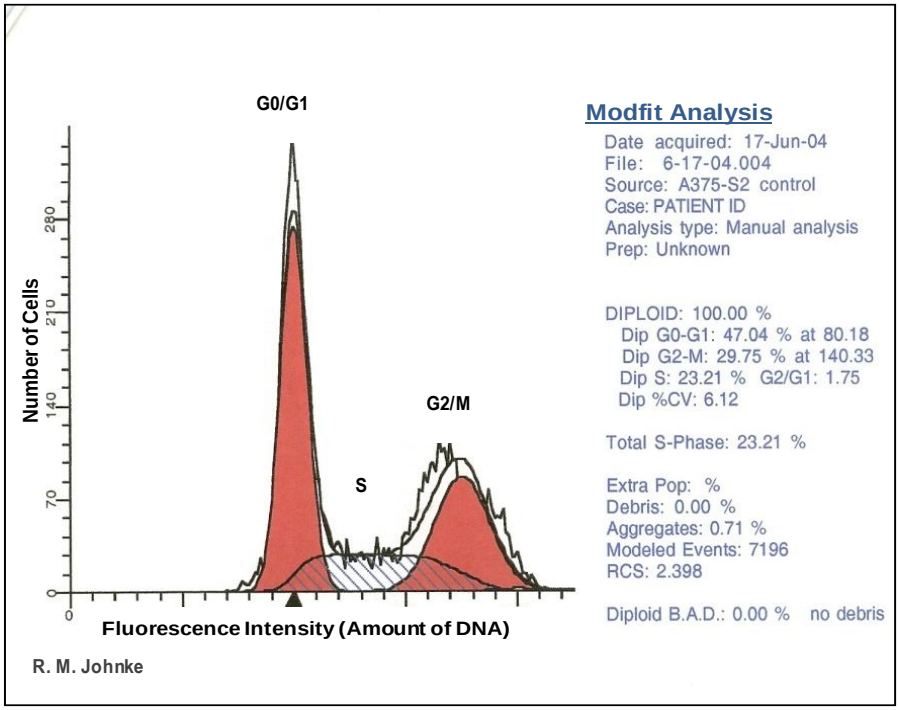

Figure 2.1. Flow Cytometric Histogram of A375 Cell Cycle Distribution with ModFit Analysis Data Included

2.2.3 Experimental Design for Specific Aim 3: *Investigation of the effect of low dose radiation exposure on the expression of cell cycle regulator proteins in A375 human melanoma cells and PC3 human prostate cancer cells*

The third aim of this proposal is to investigate the effect of low doses of radiation on the expression of cell cycle regulator proteins. In normal cells, progression through the cell cycle is regulated at various checkpoints by a group of proteins known as cyclins, their corresponding

cyclin dependent kinases (CDKs), and their cyclin kinase inhibitors (CKIs). Reductions in the levels of cyclins or CDKs, or increases in the levels of CKIs, therefore, will effectively decrease the probability of transiting through these checkpoints, and cell cycle arrest will occur. For example, because progression through the G2 phase is moderated by cyclin B/CDK1, a complex that induces mitosis by phosphorylating and activating enzymes regulating chromatin condensation, nuclear membrane break down and microtubule reorganization, decreases in the levels of cyclin B can reduce the concentration of this complex, increasing the likelihood of cell cycle arrest in G2/M. Hence, in an effort to correlate the temporal changes in cell cycle distribution observed in Specific Aim 2 with the alterations of specific cyclin levels within the cell, this aim proposes to monitor the expression of cyclins involved in cell cycle phases observed to demonstrate an arrest as analyzed by the flow cytometric studies performed in Specific Aim 2. Expression levels will be assessed using Western blot analysis of cell lysates derived from cells exposed to 0, 2, 5, 10, 25, 50, and 100 cGy over a 24 hour interval following irradiation. Briefly, the Western blot procedure is a widely used analytical technique which is used to detect specific proteins within a cellular extract or tissue homogenate. It uses gel electrophoresis to separate denatured proteins according to their polypeptide length. The proteins are then transferred to a PVDF membrane where they are detected by probing with antibodies specific to the target protein.

2.2.4 Experimental Design for Specific Aim 4: *Analysis of the phosphorylation status of the members of the MAPK kinases and Nf-κB pathways following low dose radiation in the A375 human melanoma and PC3 human prostate carcinoma cell lines*.

Ionizing radiation can activate growth factor receptors on the cell membrane, which, in turn, can trigger upregulation of proliferative pathways such as the MAPK and NF-κB pathways. The fourth aim of this proposal is to ascertain whether signaling through these proliferative pathways is being upregulated as a function of cellular exposure to low doses of radiation (0, 2, 5, 10, 25, 50 and 100 cGy). These studies were accomplished by measuring the levels of phosphorylated ERK1/2, JNK1/2, p38 and NF-κB within these pathways. The rationale for selecting these proteins is that they represent key indices of their respective pathways. Expression of these molecules will be determined for cell populations exposed to 0, 2, 5, 10, 25, 50, and 100 cGy over a 24 hour interval following irradiation using enzyme linked immunosorbent assays (ELISA). Briefly, the principle underlying this assay is as follows. Enzyme-linked immunosorbent assay (ELISA) is a biochemical technique used to detect the presence of an antibody or an antigen in a sample. In simple terms, an unknown amount of antigen is affixed to a surface, and then a specific antibody is applied over the surface so that it can bind to the antigen. This antibody is linked to an enzyme, and, in the final step, a substance containing the enzyme's substrate is added. The ensuing reaction produces a detectable color change in the substrate which can be analyzed spectrophotometrically to measure how much antigen is present.

Ionizing radiation can activate growth factor receptors on the cell membrane, which, in turn, can trigger upregulation of proliferative pathways such as the MAPK and NF-κB pathways. The fourth aim of this proposal is to ascertain whether signaling through these proliferative

pathways is being upregulated as a function of cellular exposure to low doses of radiation (0, 2, 5, 10, 25, 50 and 100 cGy). These studies were accomplished by measuring the levels of phosphorylated ERK1/2, JNK1/2, p38 and NF-κB within these pathways.

2.3 MATERIALS AND METHODS

2.3.1 Antibodies and Reagents

Phospho-ERK1/2, phospho-JNK1/2, phospho-p38, phospho-NF-κB and cyclin B1 antibodies were purchased from Cell Signaling Technology (Danvers, MA). Fetal calf serum was purchased from HyClone Laboratories (Logan, Utah). Iscove's Modified Dulbecco's Media, penicillin/streptomycin, and Triton X-100 were purchased from Sigma Aldrich (St. Louis, Missouri). All secondary antibodies (anti-rabbit HRP-conjugated and goat anti-rabbit HRP-conjugated, anti.mouse AP-linked) were purchased from Cell Signaling Technology (Danvers, MA). The chromogenic substrate for horseradish peroxidase in ELISA experiments was TMB (3,3´,5,5´-tetramentylbenzidine) with brand name 1-Step™ Ultra TMB-ELISA was purchased from Thermo Scientific (Pierce, Rockford, IL). For Western blots, the chromogenic substrate was nitro blue tetrazolium/5-bromo-4-chloro-3-indolyl-phosphate from Promega (Madison, WI).

2.3.2 Tumor Cell Lines and Culture Conditions

The A375 human melanoma and PC3 human prostate cancer cell lines were purchased from American Type Culture Collection (Bethesda, MD), and were routinely maintained under sterile conditions in Iscove's Modified Dulbecco's Media (Sigma Aldrich, St. Louis Missouri) supplemented with 10% fetal calf serum (HyClone Laboratories, Logan, Utah) by incubating at

37^0C, 5% CO_2/95% air. Cell cultures were passaged weekly by trypsinization and replating at a density of $2x10^3$ and $5x10^3$ cell/cm^2 for A375 and PC3 cells, respectively.

2.3.3 Ionizing Radiation

A375 and PC3 cells were exposed to varying doses of x-rays from 0-100 cGy using a Siemens Stabilipan x-ray generator housed in a lead-lined 7 ft by 14 ft room within the Division of Radiation Biology. The beam of radiation was delivered using 250 kVp x-rays, 15mA and 2mm Cu filtration. X-Ray dose output was calibrated weekly using a Victoreen ionization chamber to insure accuracy of dose delivery. The irradiation setup is presented in Figure 2.2.

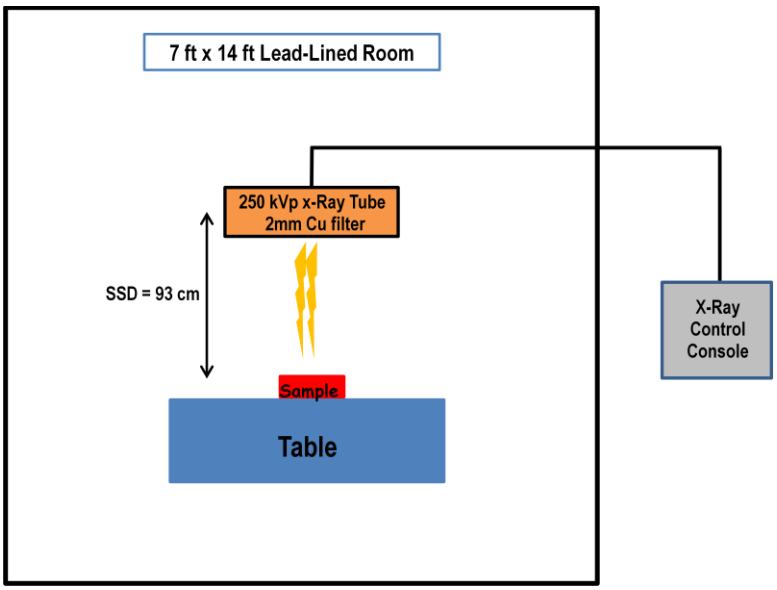

Figure 2.2: Schematic Diagram of Irradiation Setup

2.3.4 Clonogenic Cell Survival Assay

The fraction of cells that survive after irradiation was assessed by the clonogenic survival assay which measures the fraction of cells that continue to reproduce for at least five times after

irradiation. For this assay, cells were grown to 70-80% confluency, and harvested by tripsinization, counted on a hemocytometer and diluted to $1x10^4$ cells/ml of growth media. Cells were then seeded in 35 mm petri dishes with 2 ml of growth medium at appropriate dilutions to yield 40-60 colonies per dish. Quadruplicate dishes were used for each experimental data point. Cells were allowed to settle and attach for 8 hours before being exposed to irradiation at various doses. Dishes were then incubated at 37^oC in 5% CO_2 in a humidified incubator to form colonies for either 9 days (A375) or 14 days (PC3). Colonies were washed with PBS, air dried, stained for 10 minutes with 0.5% crystal violet in methanol, and washed with running tap water to remove nonspecific staining. Colonies (>50 cells) were enumerated under a Fisher Stereomaster II 10X stereoscopic microscope. For each quadruplet set of dishes, the mean, standard deviation and standard error was calculated. The cell survival fraction (SF) was calculated from the formulae:

$$\mathrm{SF} = \frac{\text{Number of colonies per plate}}{\text{Number of cells seeded per plate}}$$

2.3.5 Flow Cytometric Analysis

Cellular DNA content was determined at different intervals (0-24 hours) after exposure of the A375 and PC3 cells to 0-100 cGy of x-ray radiation. To accomplish this, either the A375 or the PC3 cells were grown 70-80% confluency in either 25-cm^2 or 75-cm^2 at a density of $2x10^3$ cells per cm^2 (A375) or $4x10^3$ cells per cm^2 (PC3). On the day of irradiation, fresh pre-warmed growth media was replaced in each flask. The cells were then irradiated in triplicates at doses of 0 2, 5,10, 25, 50 and 100 cGy. For each dose, at various time points (1, 2, 4, 6, 8, 12, and 24 hours) following radiation, the cells were harvested by trypsinization. Harvested cells were centrifuged, and the pellet washed twice in 2ml of PBS, and fixed by resuspending $1x10^6$ cells/ml in ice cold 70% ethanol and stored at -20^0C until the day of flow cytometric analysis.

Prior to analysis, cells were treated with 50µg/ml RNase A (made up in PBS) for 30 minutes at 37^{o}C and, then, incubated with 20µg/ml of propidium iodide (Sigma-Aldrich, St Loius MO) suspended in PBS, 2% FBS and 0.01% NaN_3 for 20 minutes at room temperature. Stained nuclei were analyzed for DNA-PI fluorescence with a FACScan (Becton Dickinson Immunocytometry Systems, San Jose, CA, USA), and resulting DNA distributions were analyzed using ModFit software (ModFit for Mac Version 3, Verity software House Inc, Topsham, USA) to determine the proportion of cells in G0/G1, S, and G2/M. At least $2x10^4$ events were analyzed per sample.

2.3.6 Cell-Based ELISA

Protein levels of phosphorylated ERK1/2, JNK1/2, p38 and NF-κB were determined using 96-well polystyrene microtiter plates. Optimal cell numbers to be seeded per well were determined by plating different cell densities and plotting a calibration curve. It was found that cell densities between $4x10^4$ and $6x10^4$ per well gave the most reliable response at 540nm. Cells were grown to 70-80% confluency, harvested by trypsinization, and, seeded in 96-well plates ($4x10^4$ cells per well). Plates were then returned to the incubator for 16 hours before being x-irradiated with doses ranging from 0-100 cGy. Following irradiation, cells were incubated for 5 hours and, then, fixed in 4% formaldehyde for 20 minutes at room temperature. The cells were washed in PBS containing 0.1% Triton X-100 (Sigma, St. Louis, MO; hereafter referred to as Wash Buffer) and quenched in 100µl of Wash Buffer containing 1% H_2O_2 and 0.1% sodium azide for 20 min at room temperature to inactivate endogenous peroxidase activity. After additional washing steps, cells were blocked in Wash Buffer containing 5% goat serum for 1 hour, and incubated overnight in various dilutions of primary antibody as per the manufacturer's instructions (Cell Signaling, Danvers, MA). Cells were then washed three times in wash buffer,

then incubated with secondary antibody (HRP-conjugated goat anti-rabbit antibody; dilution 1:1000, Cell Signaling, Danvers, MA) in Wash Buffer with 5% bovine serum albumin (BSA) for 1 hour at room temperature, followed by incubation with 100 µl of 1-step ULTRA TMB ELISA (TMB; Pierce, Rockford, IL) for 15-20 minutes at room temperature before addition of 50µl of 2M H_2SO_4. The absorbance at 450nm and 620nm was measured with a microplate reader. After further washing, the cells were dried and stained with 100µl of crystal violet for 30 minutes prior to adding 1% SDS for 1 hr, and taking the absorbance at 540nm. The relative activation of the phosphorylated proteins was calculated by the formula below:

$$\text{Relative absorbance} = \frac{\text{Absorbance at 450nm} - \text{Absorbance at 620nm}}{\text{Absorbance at 540nm}}$$

2.3.7 Western Blotting

To obtain cell lysates for Western blot analysis, A375 and PC3 cells were grown to 60-70% confluency, refed with fresh IMDM growth medium, irradiated at the appropriate dose (0, 2, 5, 10, 25, 50 & 100 cGy) and incubated for various time points ranging from 0-24 hrs prior to harvesting by trypsinization. Harvested cells were then pelleted at 400g for ten minutes, washed and resuspended in ice cold lysis buffer (25mM Tris , 50mM NaCl, 2% IGEPAL, 0.2% SDS and 0.5% deoxycholic acid, 1mM PMSF, 50ug/ml aprotinin, 24ug/ml leupeptin and 0.5mM sodium orthovanadate at a pH of 7.4), and incubated for 30 minutes on ice with vortexing performed every 5 minutes. The cell extracts were then centrifuged (20 minutes, 10,000g, 4^{o}C), supernatants (lysates) aliquoted into multiple tubes and stored at -20^{o}C until analysis. Protein content for the lysates was determined using Bradford analysis. For Western blotting, lysates were mixed 1:1 with 2x sample loading buffer (100mM Tris-HCI pH 6.8, 4% SDS, 0.2%

bromophenol blue, 20% glycerol, 200mM dithiothreitol) and samples (20µg) were resolved on 10% SDS-polyacrylamide gels at 150V constant voltage in standard buffers (25mM Tris with 200mM glycine and 0.1% SDS). Pre-stained molecular weight markers were run on gels to provide a visible QC on protein transfer along with molecular weight standards (Santa Cruz, CA). After electrophoresis, gels were rinsed in ice-cold transfer buffer (24.8 mM Tris base, 192 mM glycine, 10% methanol, pH 8.3) and proteins transferred to prepared polyvinylidene difluoride (PVDF) membranes at 100V constant voltage for 1 hour. The resulting blots were incubated overnight at 4^0C in blocking buffer (0.1% Tween-20 with 5% w/v nonfat dry milk in TBS), then incubated with cyclin B1 primary antibody (Cell Signaling Technology, Danvers, MA*)* diluted in TBST (TBS, 0.1% Tween-20), with 5% BSA for 2.5 hours. The dilution for the cyclin B1 primary antibodies was 1:2000. The membrane was then incubated for 1.5 hrs with biotinylated secondary antibody conjugated with streptavidin-alkaline phosphatase anti-IgG (anti-mouse, Cell signaling technology, Danvers, MA). To visualize the bands, membranes were incubated with 10ml of nitro blue tetrazolium/5-bromo-4-chloro-3-indolyl-phosphate as substrate (Promega, Madison, WI). Resultant blots were scanned and analyzed by ImageJ software.

CHAPTER 3: RESULTS

3.1 EFFECT OF LOW DOSE RADIATION ON CELL SURVIVAL OF A375 AND PC3 CELLS

The goal of these studies was to characterize the survival response following low dose radiation in two cell lines – the A375 human melanoma cell line and the PC3 prostate carcinoma cell line. To achieve this, survival was assessed using the clonogenic assay. As mentioned in the previous chapter, this assay essentially tests for reproductive integrity (the ability of a cell to undergo "unlimited" division) and has long been considered to be the method of choice to determine radiation-induced cell death.

Figure 3.1 shows the survival curve of A375 cells relative to the untreated controls after irradiation with x-ray doses of 0, 2, 5, 10, 25, 50 and 100 cGy. Cells were irradiated during exponential growth phase (~70% confluence) and the percentage of survival was determined using a standard clonogenic assay. Results are means of at least 8 independent experiments with quadruplets for each data point and error bars representing the standard error of the mean (SEM). Data show that, relative to unirradiated controls, survival was significantly increased in the A375 cells following doses of 2 and 5 cGy (p-value ≤ 0.01), suggesting that these cells display hyper-radioresistance in the very low dose range of radiation. Specifically, irradiation with 2 cGy increased survival up to 110% compared to unirradiated controls, while 5 cGy increased survival to approximately 120% of unirradiated controls. In contrast, the survival of A375 cells irradiated with doses above 10 cGy decreased as a function of increasing dose.

Figure 3.2 shows the survival curve of the PC3 cells, also irradiated with doses between 0 and 100 cGy. As with the A375 cells, irradiations were performed during exponential growth phase (~70% confluence) and the percentage of survival was determined using a standard

clonogenic assay. Results are means of at least 6 independent experiments with quadruplets for each data point and error bars representing the standard error of the mean. Results demonstrate that, in contrast to the A375 cells, survival of PC3 cells following irradiation with 2 and 5 cGy was significantly decreased relative to unirradiated controls (p-value $\leq$ 0.01). This hyper-radiosensitivity response was significant with survival being reduced as much as 15 and 20% following 2 and 5 cGy, respectively. Similar to A375 cells, at doses greater than 10 cGy, PC3 cell survival also decreased as a function of increasing dose.

Figure 3.3 is a combined plot of survival curves for A375 and PC3 cells to allow for easy comparison of the differential responses that these two cell lines demonstrate following exposure to doses of radiation in the very low dose range. Additionally, this figure also demonstrates that the PC3 cell line appears to be more radiosensitive than the A375 cell line over the entire range of doses investigated (0 – 100 cGy), thereby confirming the numerous reports demonstrating marked cell type differences in response to radiation.

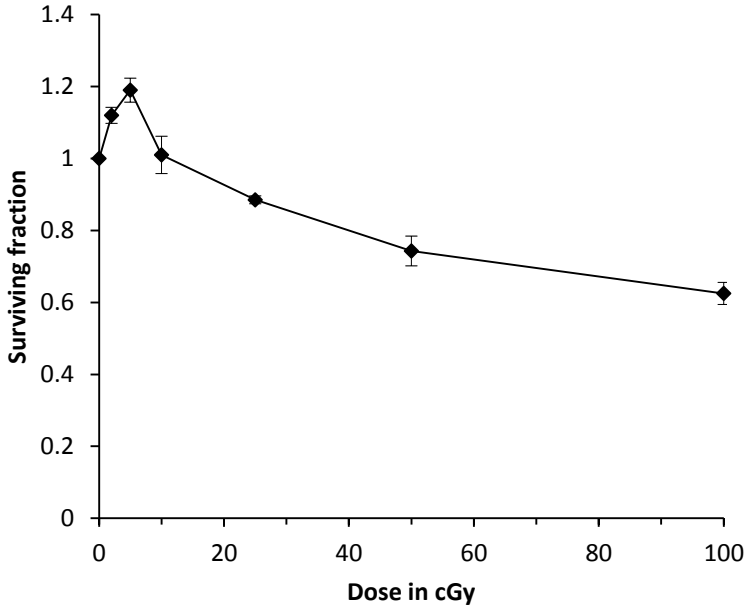

Figure 3.1. Cell survival curve of human melanoma A375 cells over a dose range of 0 and 100 cGy demonstrating hyper-radioresistance in the very low dose range of radiation.

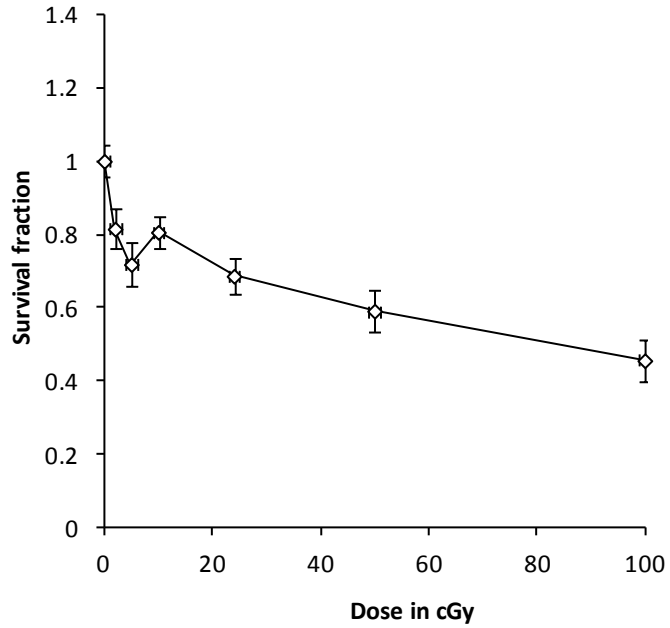

Figure 3.2. Cell survival curve of human prostate cancer PC3 cells over a dose range of 0 and 100 cGy demonstrating hyper-radiosensitivity in the very low dose range of radiation.

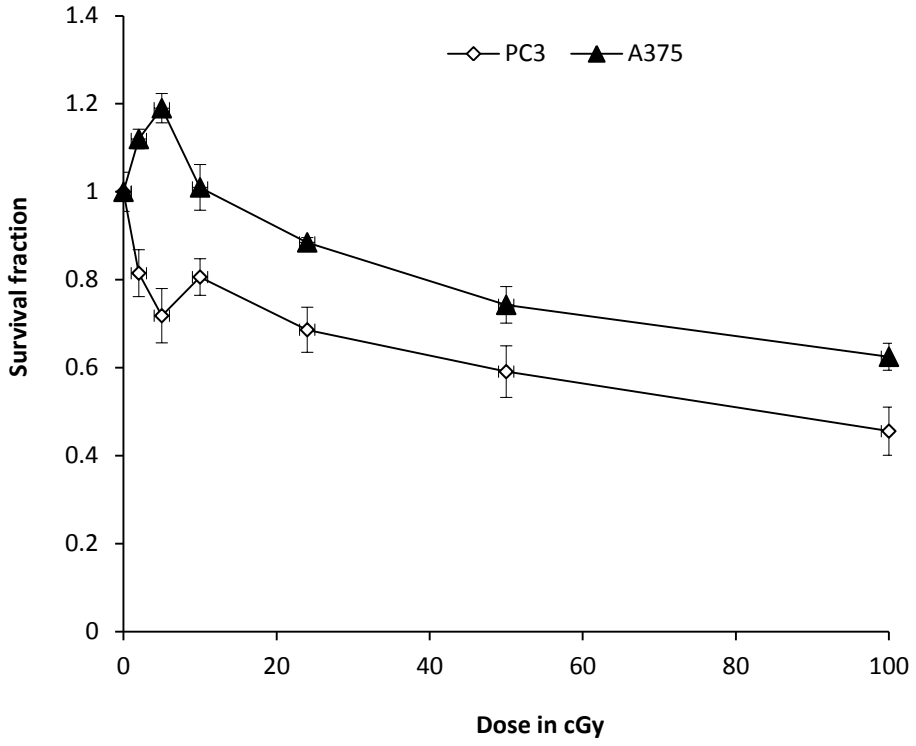

Figure 3.3. Comparison of cell survival curves for human melanoma A375 cells and human prostate cancer PC3 cells over a dose range of 0-100 cGy demonstrating the differential pattern of response for these two cell lines at radiation doses between 0 and 100 cGy.

3.2 TEMPORAL KINETICS OF CELL CYCLE DISTRIBUTION FREQUENCIES FOLLOWING IRRADIATION

To investigate whether cell cycle changes were correlated with the observed hyper-radioresistance in the A375 cells and hyper-radiosensitivity in the PC3 cells, flow cytometric analysis was performed to measure nuclear DNA content of experimental cell populations at various intervals over a 24 hour period following a radiation stress. Following flow cytometric acquisition of data, ModFit software was used to analyze the DNA content of the cell samples and determine the relative distribution of cells in the G0/G1, S, and G2/M phases of the cell cycle. Results are presented in Figures 3.4 and 3.5 with all values being expressed as percentages of unirradiated controls, and all data points representing the mean (±SEM) of three individual studies.

Figure 3.4 shows the relative distribution of irradiated human melanoma A375 cells in G0/G1, S, and G2/M phases of the cell cycle as a function of time up to 24 hours. Results demonstrate that, for cells exposed to 2 cGy (Figure 3.4, panel A), there was a significant accumulation of cells in the G2/M phase between 2 and 12 hours post irradiation, indicating a marked cell cycle block was occurring at this time. Between 12 and 24 hours post irradiation, release of the block and a return to pre-irradiated control levels was observed. In addition, panel A also shows that, between 12 and 24 hours post irradiation, there is a modest increase in cells residing in the G0/G1 phase and a small decrease in cells within S phase. While these changes did not prove to be statistically significant at this dose exposure, they are temporally correlated with the release of the G2/M block, and may represent radiation-induced cell sychronization (synchronization is brought about by the 'piling up' of cells at the G2/M block, so that a large cohort of cells travels into the G0/G1 phase at the same time and transits through the rest of the cell cycle together)(134).

A375 cells irradiated with 5 cGy (Figure 3.4, panel B) followed a similar pattern of cell cycle progression as cells irradiated with 2 cGy, in that a pronounced G2/M block was observed to occur between 2 and 12 hours post irradiation. As with the 2 cGy exposure, release of the block and return to control levels by 24 hours is also observed following this radiation dose. Of interest as well, is the observation that, correlated with the release of the G2/M block, there is a significant increase in cells present in the G0/G1 phase and a reduction of cells present in S phase of the cell cycle between 12 and 24 hours post irradiation. As stated above for the cell response to 2 cGy, these changes in G0/G1 and S phase are most likely a manifestation of the radiation-induced phenomenon of cell sychronization. Further evidence of this can be derived from the observation that increased G0/G1 and decreased S phases are observed from 12 to 24 hours post irradiation following any dose that displays a pattern of increased G2/M accumulation within the first 12 hours post irradiation (Figure 3.4, panels A, B, D, E, F).

The relative distribution of A375 cells following 10 cGy of irradiation as a function of time up to 24 hours is displayed in panel C. In contrast to cells exposed to 2 and 5 cGy, results from these A375 cell studies demonstrate that essentially no changes in the accumulation of cells in any cell cycle phase is observed following 10 cGy, thereby suggesting that radiation-induced cell cycle arrest is not occurring in any of the three phases monitored over the 24 hour interval investigated. Additionally, within the A375 population studied, no cell synchronization event appears to be present following this radiation dose exposure, since no increases in the G0/G1 phase or concomitant decreases in S phase between 12 and 24 hours is observed.

Following a 25 cGy exposure (Figure 4, panel D), small fluctuations in the accumulation of cells in G2/M appear during the first twelve hours following irradiation. However, the changes monitored did not prove to be statistically different from control levels, so it is difficult

to determine whether a slight cell cycle arrest is occurring at this time or not. What is apparent from the data in panel D is that, similar to the 5 cGy irradiation exposure, statistically significant increases of cells in G0/G1 phase and decreases of cells in S phase are present at 24 hours post irradiation, which suggests that a synchronized cohort of cells is traversing through the G0/G1 phase of the cell cycle during this time.

Finally, the relative cell cycle distribution of human melanoma A375 cells following 50 cGy and 100 cGy as a function of time up to 24 hours are presented in panels E and F, respectively. For cells irradiated with these higher doses of radiation, there is a return to the pattern seen following 2 and 5 cGy irradiation in that a significant accumulation of cells in the G2/M phase is observed, suggesting that cell cycle arrest is occurring. Following 50 cGy, the interval of this arrrest occurred between 2 and 12 hours, while after a 100 cGy exposure, the arrest appeared to come on more slowly, but last over a longer period of time (4 – 24 hours). Increases in the level of G0/G1 and decreases in the level of S phase accumulation between 12 and 24 hours post irradiation were also seen at these dose exposures, suggesting that a synchronized cohort of cells is present.

Overall therefore, results displayed in Figure 3.4 suggest there is a marked, biphasic G2/M block in A375 cells following irradiation, with both very low doses (2 and 5 cGy) and higher doses (50 and 100 cGy) demonstrating a pronounce G2/M cell cycle arrest, while doses between these extremes (10 and 25 cGy) exhibit little-to-no block. Results also demonstrate the presence of a radiation-induced synchronization of the cell population may be present in those cells exhibiting a cell cycle block.

Radiation-Induced Temporal Changes in A375 Cell Cycle Distribution

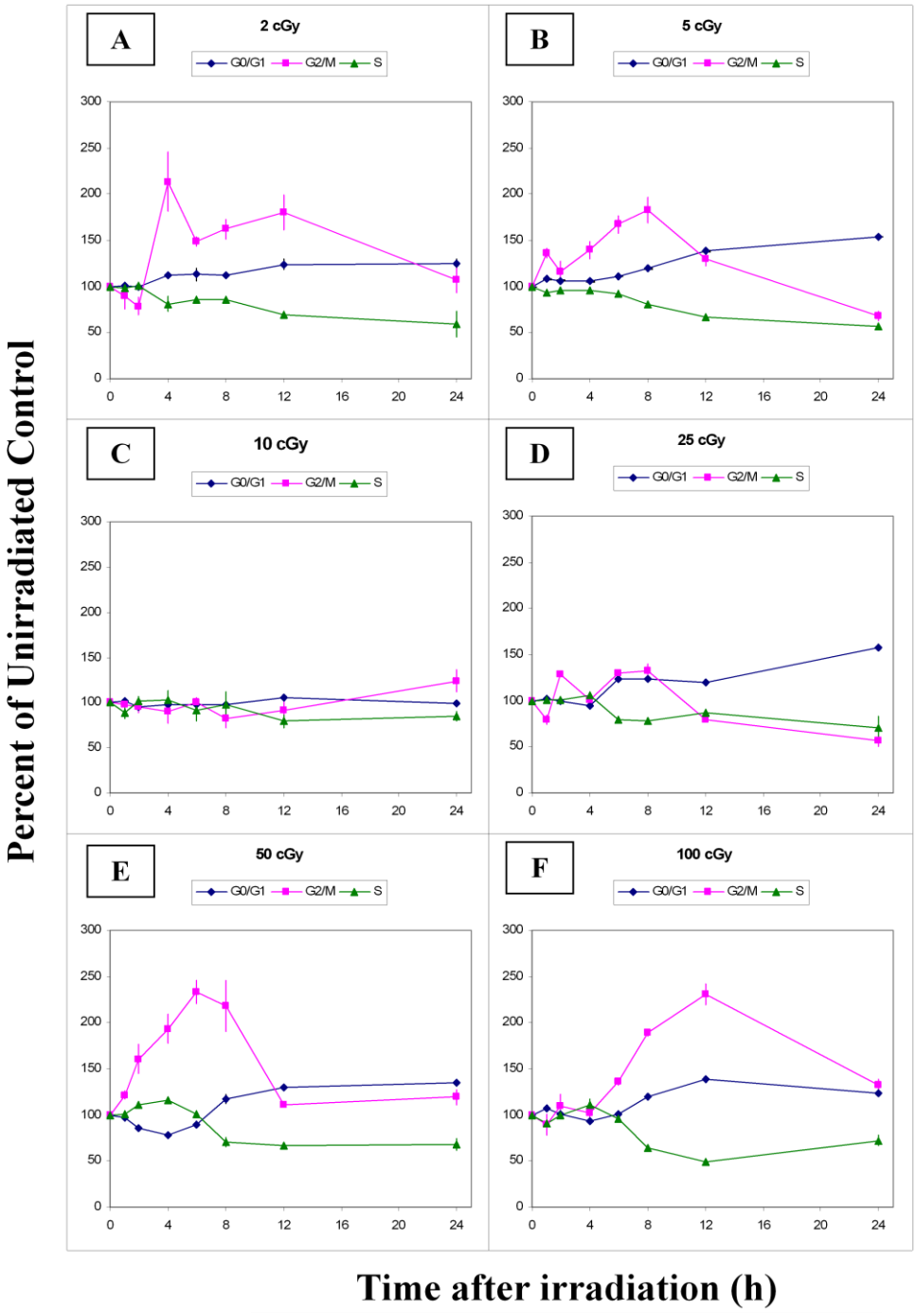

Figure 3.4. Relative distribution of human melanoma A375 cells in G0/G1, S, and G2/M cell cycle phases following irradiation with 2-100 cGy (panels A-F). Data points represent the mean (±SEM) of three individual studies analyzed flow cytometrically over a 24 hour interval post irradiation. Data suggest the presence of a marked biphasic pattern in the frequency of cells undergoing G2/M arrest.

The relative distribution of PC3 cells following irradiation as a function of time up to 24 hours is presented in Figure 3.5, and the marked differences between this cell line's response to radiation and the A375 cell line's radioresponse is readily apparent. Indeed, following 2 cGy and 5 cGy, radiation doses which brought about a strong G2/M block in the A375 cell line between 2 and 12 hours post irradiation, PC3 cells (Figure 3.5, panel A & B) demonstrated no appreciable accumulation of cells in any of the three phases of the cell cycle monitored. Furthermore, similar to the 2 cGy and 5 cGy exposures, the relative distribution of PC3 cells in the various cell cycle phases (panel C) following 10 cGy demonstrated no statistically significant changes in accumulation throughout the 24 hour time period monitored. Finally, over the 24 hour period observed, not only was a lack of cell cycle arrest observed at these very low doses of 10 cGy and below, but the PC3 cells also did not display the pattern of increased cells present in G0/G1 and decreased cells present in S phase that is typical of a radiation-induced cell synchronization event.

However, at doses higher than 10 cGy, small fluctuations in the accumulation of cells in the G2/M phase can be observed between 2 and 12 hours following 25 cGy (Figure 3.5, panel C) and 50 cGy (Figure 3.5, panel E) exposures. The minor increase in accumulation of cells in G2/M following a 25 cGy exposure did not prove to be statistically significant when compared to unirradiated controls, but is, perhaps, indicative of the beginning of a G2/M cell cycle arrest. However, the G2/M accumulation following a 50 cGy exposure was statistically significant at 8 hours post irradiation, suggesting a small G2/M block is present. In addition, an increase in S phase accumulation is also seen following exposure to 50 cGy, but the increase in this cell cycle phase is also not statistically significant. As with the PC3 cell cycle distributions following the lower doses of radiation discussed above, exposure to 25 cGy and 50 cGy doses of radiation did

not result in statistically significant elevations of cells in G0/G1 phase or statistically decreased cells in S phase of the cell cycle between 12 and 24 hours post irradiation, suggesting the lack of a synchronized cohort of cells.

Finally, PC3 cells irradiated with 100 cGy exhibited a G2/M block, with significant accumulation of cells in the G2/M phase occurring between 2 and 12 hours following irradiation. While significant, however, the G2/M accumulation observed for PC3 cells at this dose was not as pronounced as any of the G2/M blocks observed following irradiation of the A375 cell line (Figure 3.4, panels A, B, E, F). However, similar to the A375 cell studies, the release of this block is temporally correlated with a small, but significant increase of cells in G0/G1 phase and a decrease of cells found in the S phase, suggesting some synchronization of the population has occurred.

Radiation-Induced Temporal Changes in PC3 Cell Cycle Distribution

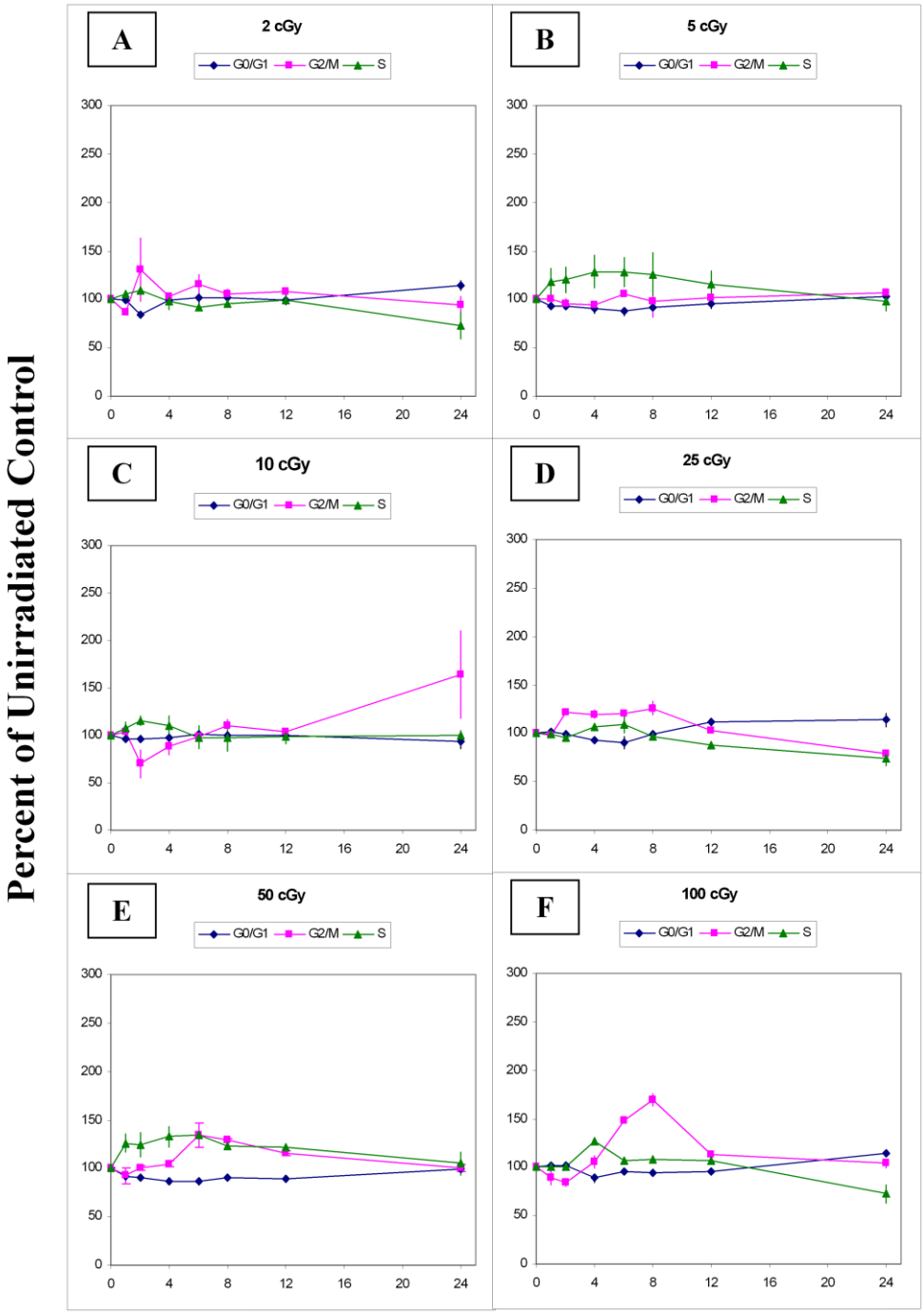

Figure 3.5. Relative distribution of human prostate cancer PC3 cells in G0/G1, S, and G2/M cell cycle phases following irradiation with 2-100 cGy. Data points represent the mean (±SEM) of three studies analyzed flow cytometrically over a 24 hour interval post irradiation. Results suggest that a marked cycle arrest is seen only following 100 cGy, occurring in the G2/M phase (panel F).

3.3 COMPARISON OF RADIATION-INDUCED CELL CYCLE DISTRIBUTIONS IN A375 AND PC3 CELLS

To facilitate comparison of the differential radiation-induced cell cycle responses between A375 human melanoma and prostate cancer PC3 cell lines, the relative distribution data for each of the cell cycle phases is presented as a function of cell type in Figures 3.6, 3.7 & 3.8. These data demonstrate that cell specific differences between the A375 and PC3 cell line exist for each cell cycle phase studied, but by far the most significant variations observed occur in the ability of the two cell lines to arrest in the G2/M phase. Indeed, comparison of the two G2/M curves displayed in Figure 3.6 suggests a highly divergent response to radiation, particularly within the very low dose range (0 – 10 cGy). For A375 cells, there exists a marked biphasic pattern in the frequency of cells accumulating in G2/M, with both very low doses (2 cGy and 5 cGy), and higher doses (50 and 100 cGy) exhibiting significant cell cycle arrest, but with intermediate doses (10 and 25 cGy) exhibiting little-to-no G2/M block. In sharp contrast to this radioresponse, no accumulation of cells in G2/M is observed in the PC3 cell line at or below 10 cGy, suggesting that exposures at such low doses do not induce a cell cycle block. Only at 25 cGy and above are fluctuations in the accumulation of cells in G2/M observed within the PC3 cell lines which may be suggestive of a cell cycle arrest, and, even then, statistically significant G2/M accumulations are seen only following 50 and 100 cGy exposures.

As with the results presented for the G2/M phase in Figure 3.6, comparisons of G0/G1 and S phase frequency distributions over a 24 hour interval following radiation (Figures 3.7 and 3.8) also demonstrate cell specific differences, but neither cell line undergoes a radiation-induced cell cycle block in either G0/G1 or S phase at any of the doses investigated in this study. Rather, the cell line specific differences for these two cell lines appear to be moderate in magnitude and often statistically insignificant. Further, when they do occur, they tend to be more pronounced in

the latter part of the time interval monitored rather than the earlier hours post irradiation where the marked G2/M accumulations occurred, and may represent variances between these two cell lines in the induction of radiation-induced cell synchrony.

Comparison of G2/M Phase Distribution Following Radiation

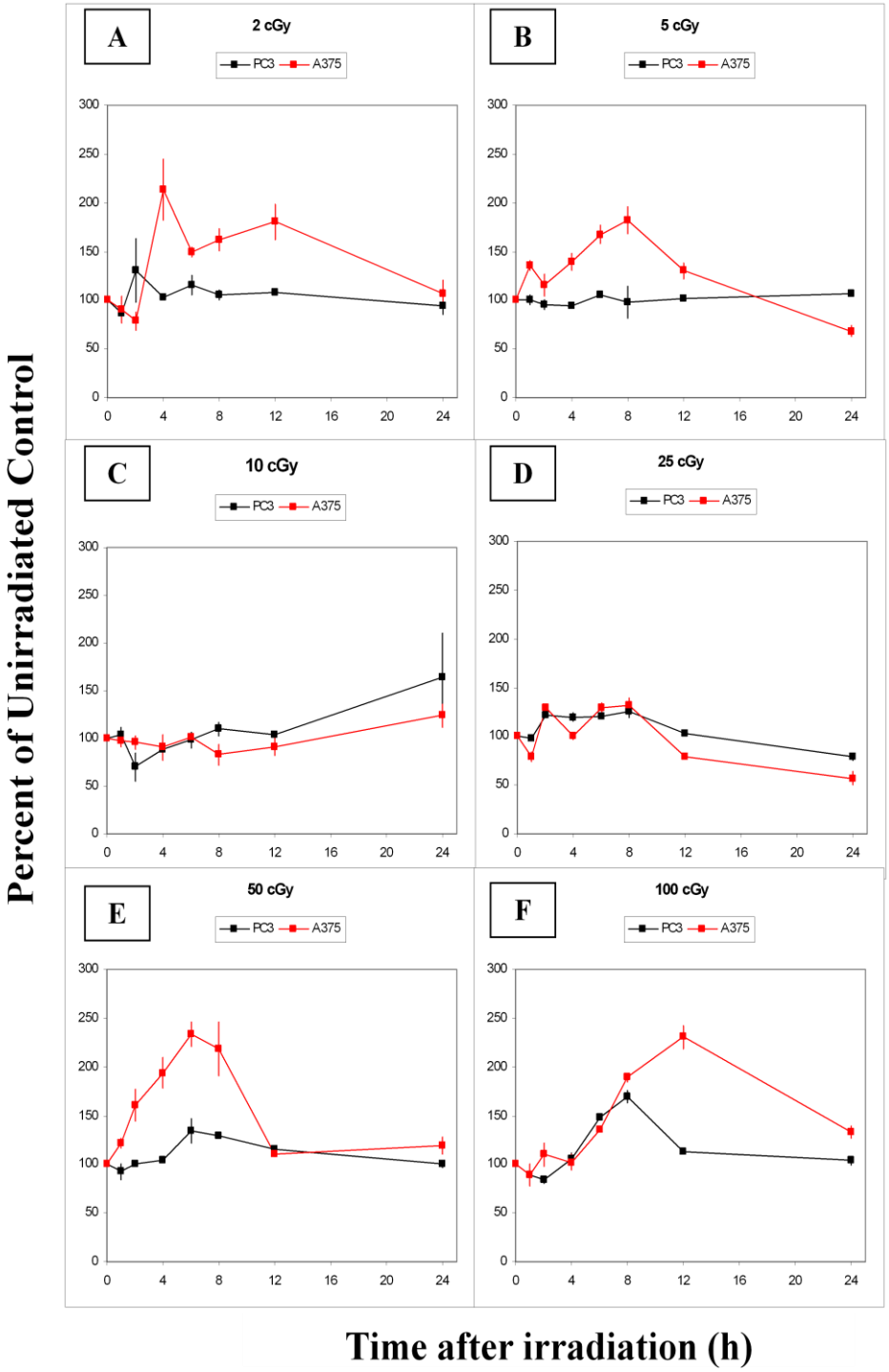

Figure 3.6. Comparison of G2/M phase frequencies in A375 and PC3 cells following irradiation as a function of cell type. Data are expressed as a percent of control, and demonstrate the marked differences in the ability of these two cell lines to arrest in the G2/M phase, especially in the very low dose range of radiation.

Comparison of G0/G1 Phase Distribution Following Radiation

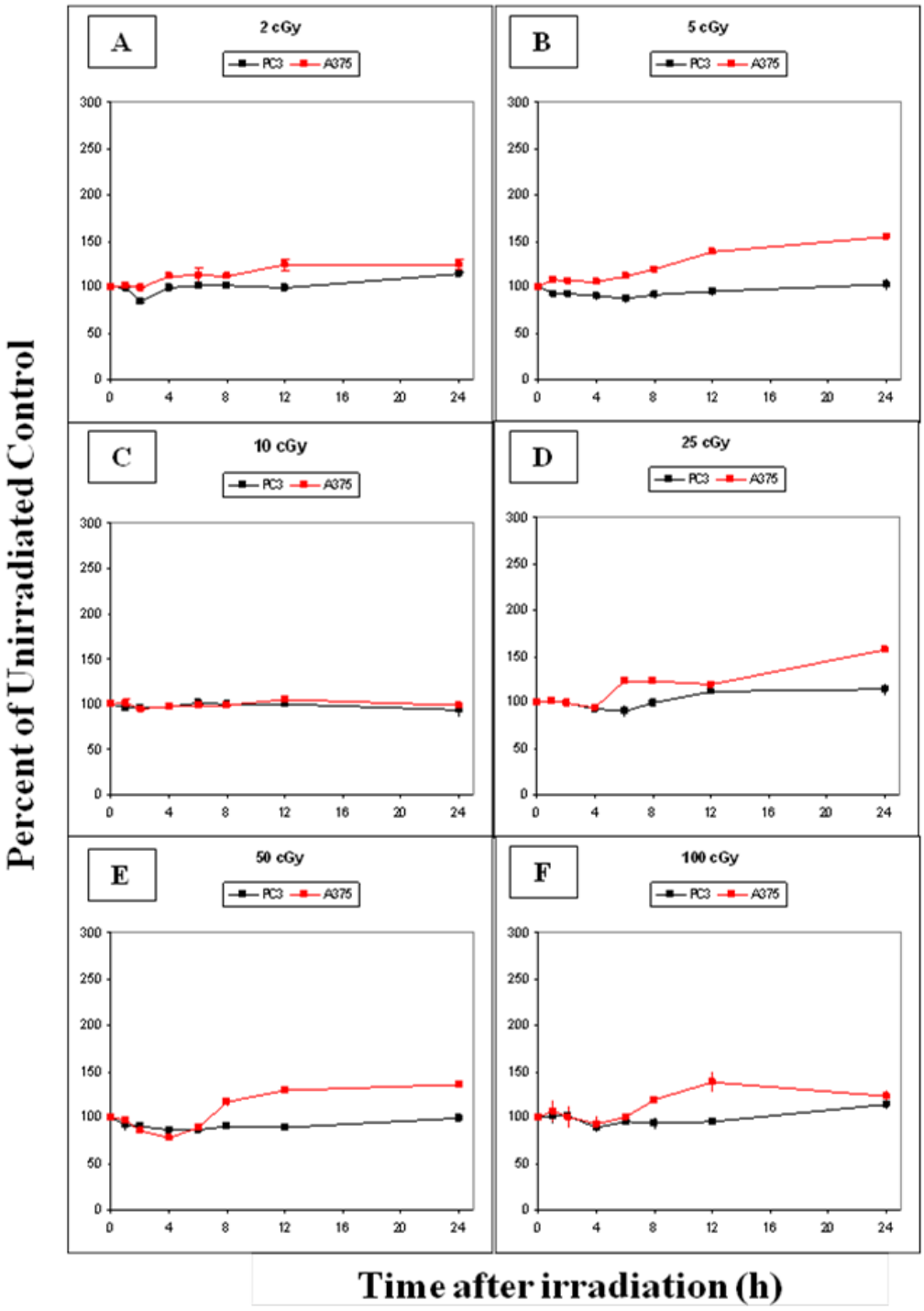

Figure 3.7. Comparison of G0/G1 phase frequency distributions following radiation as a function of cell type. Data are expressed as a percent of control, and demonstrate that cell specific differences between the A375 and PC3 cells exist, but neither cell line undergoes a G0/G1 phase cell cycle block following radiation.

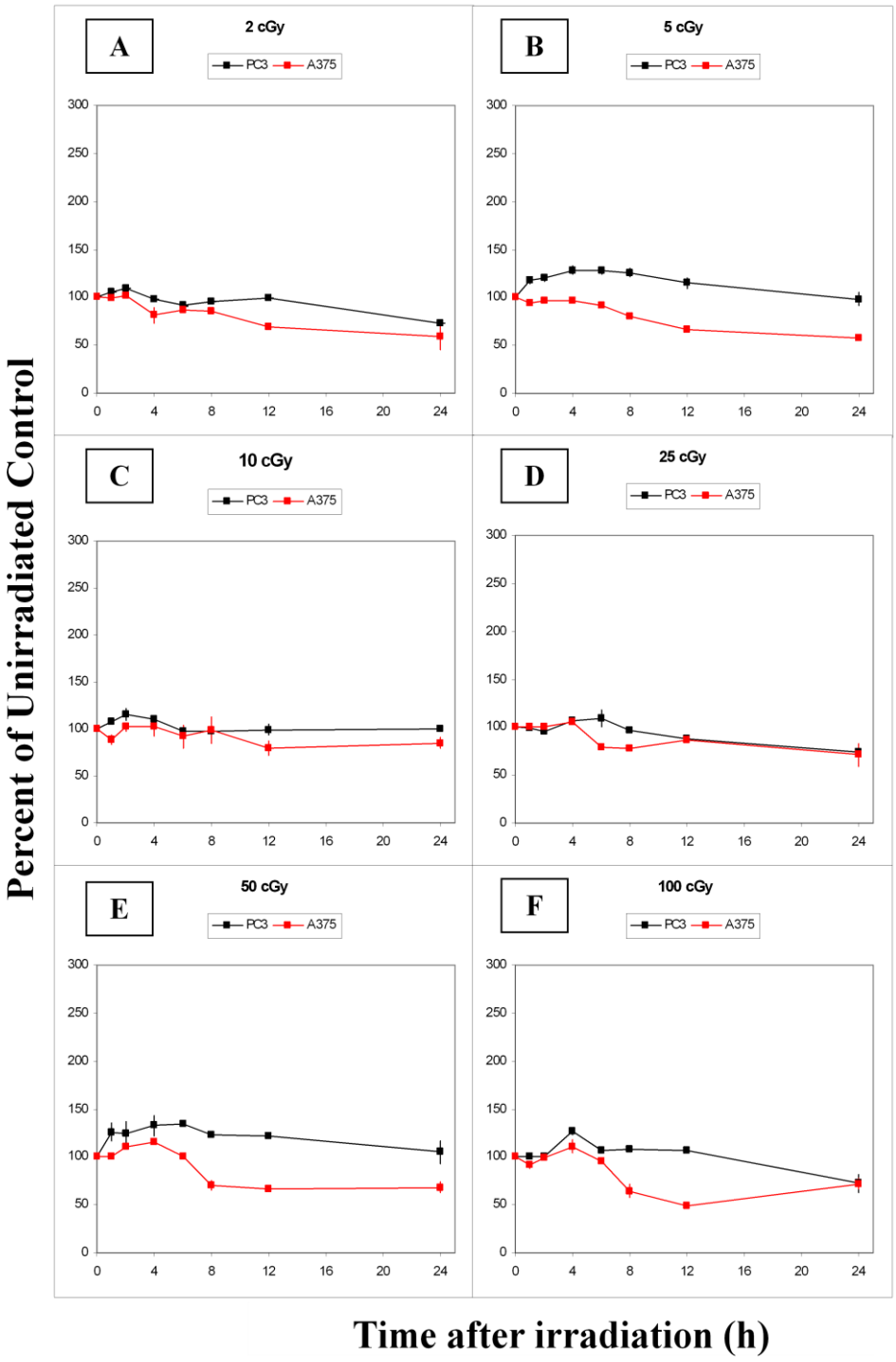

Figure 3.8. Comparison of S phase frequency distributions following radiation as a function of cell type. Data are expressed as a percent of control, and demonstrate that cell specific differences between the A375 and PC3 cells exist, but neither cell line undergoes a S phase cell cycle block following radiation.

3.4 EXPRESSION OF CYCLIN B1 LEVELS

The aim of these studies was to correlate the temporal changes in cell cycle distribution frequencies described in Sections 3.2 and 3.3 with alterations in the expression of cell cycle regulatory proteins within the cell. Because the dominant changes occurring in the flow cytometric studies of cell cycle frequency distribution were in the differential induction of the G2/M block, focus was placed upon monitoring G2/M arrest through the measurement of alterations in cyclin B1 levels within the human melanoma A375 and the prostate cancer PC3 cell lines over a 24 hour period following irradiation.

Figure 3.9 demonstrates the changes in the relative levels of cyclin B1 protein for A375 and PC3 cells exposed to 2 cGy of irradiation (top panels display the Western blot bands of protein, while the bottom panels represent the relative band intensity as analyzed by ImageJ software. As can be seen, in A375 cells, exposure to 2 cGy is correlated with a marked decrease of cyclin B1 levels at 4 and 6 hours post irradiation. Thereafter, cyclin B1 levels return to hover around control levels for the remaining time interval monitored. In contrast to the A375 cell data, PC3 cells exposed to 2 cGy demonstrate random fluctuations throughout the 24 hour interval, but no reduced levels which would be indicative of a G2/M arrest were apparent. Overall, therefore, G2/M cell cycle responses following exposure to 2 cGy, as assayed by Western blot analysis of cyclin B1 levels, produced results similar to the frequency distribution studies displayed in panel A of Figure 3.6, in that a radiation-induced G2/M block is observed in the A375 cell line, but not in the PC3 cell line. However, the duration of the cyclin B1reduction following radiation of A375 cells was much shorter than the G2/M block observed by the flow cytometric data.

Figure 3.10 demonstrates the changes in the relative levels of cyclin B1 protein for A375 and PC3 cells exposed to 5 cGy of irradiation. As in Figure 3.9, the top panels display the Western blot bands of protein, while the bottom panels represent the relative band intensity as analyzed by ImageJ software. As can be seen, in A375 cells, exposure to 5 cGy is correlated with a marked decrease of cyclin B1 levels between 2 and 6 hours post irradiation, followed by a return toward control levels between 8 and 12 hours post irradiation. Of interest, a second reduction of cyclin B1 at 24 hours post irradiation is also seen, which is most likely due to the cohort of synchronized cells present in G0/G1 at this time (Figure 3.7. Panel B), since levels of cyclin B1 are naturally quite low in the G0/G1 cell cycle phase (see Figure 1.2 in Chapter 1). In contrast to the A375 cell response, PC3 cells exposed to 5 cGy demonstrate only small fluctuations throughout the 24 hour interval, and displayed no evidence of reduced levels that would suggest the occurrence of a G2/M arrest. In summary, therefore, the G2/M cell cycle responses following exposure to 5 cGy, as assayed by Western blot analysis of cyclin B1 levels, were similar in pattern to the frequency distribution studies displayed in panel B of Figure 3.6, in that a radiation-induced G2/M block is observed in the A375 cell line, but not in the PC3 cell line. Furthermore, unlike the case for 2 cGy described above, the duration of the cyclin B1 reduction is similar to the flow cytometric data although the onset is earlier (2 hours post irradiation).

Figure 3.11 displays the changes in the relative levels of cyclin B1 protein for A375 and PC3 cells exposed to 10 cGy of irradiation. As in the previous two figures, the top panels display the Western blot bands of protein, while the bottom panels represent the relative band intensity as analyzed by ImageJ software. At this radiation dose, both the A375 and the PC3 cell lines demonstrate only small fluctuations in the levels of cyclin B1 throughout the cell cycle. No

evidence of reduced levels indicative of a G2/M block are observed. This response is in correlation with the lack of cell cycle arrest at this low dose seen in the flow cytometric studies (Figure 3.6, panels C & D).

Changes in the relative levels of cyclin B1 protein for A375 and PC3 cells exposed to 25 cGy of irradiation are presented in Figure 3.12. Similar to the 10 cGy response, following irradiation at this dose, A375 cells demonstrate only small fluctuations in the levels of cyclin B1 throughout the cell cycle, with no evidence of a G2/M block being observed. These results correlate with the flow cytometric studies on A375 cells presented previously (Figure 3.6, panel D). In contrast, while no statistically significant block in G2/M is observed in PC3 cell from the flow cytometric studies (Figure 3.6, panel D), Western blot analysis of PC3 cell response to 25 cGy irradiation displays a short-lived reduction of cyclin B1 levels at 2 hours post irradiation which may correspond to G2/M block.

Figure 3.13 demonstrates the changes in the relative levels of cyclin B1 protein for A375 and PC3 cells exposed to 50 cGy of irradiation. As can be seen, the data in both of these cell lines following irradiation indicate that a G2/M cell cycle arrest is occurring, since, in both cell lines, a greater than two-fold decrease in cyclin B1 levels at 2 and 4 hours post irradiation is observed. As following 25 cGy (Figure 3.12), for the A375 cells, this response correlates with the flow cytometric studies on A375 cells presented in Figure 3.6 (panel E), although the duration of the cyclin B1 reduction is much shorter than the G2/M block seen in the flow cytometric studies. In additon, the onset and duration of the marked G2/M block seen with Western blot analysis of PC3 cells following 50 cGy irradiation is in contrast with the G2/M cell cycle data observed from the flow cytometric studies (Figure 3.6, panel E), which, while suggesting a small G2/M accumulation may be occurring, did not show a statistically significant

pattern of G2/M arrest except at 8 hours post irradiation. Also of interest following 50 cGy is the observation that the G2/M block occurring at 2 and 4 hours post irradiation is followed in both cell lines with pronounced increase in cyclin B1 levels to above control levels by 6 hours post irradiation, and, then, a second decline in their levels over the remaining time interval monitored, so that, by 24 hours post irradiation, both the A375 and PC3 cell lines show a sharp drop in cyclin B1 levels compared to unirradiated controls. As stated above, this second reduction of cyclin B1 at 24 hours post irradiation is most likely due to the fact that, due to the phenomenon of radiation-induced synchrony, most of the cells are present in a phase of the cell cycle where the levels of cyclin B1 are naturally quite low, such as G0/G1 phase or early S phase (see Figure 1.2 in Chapter 1).

Figure 3.14 demonstrates the changes in the relative levels of cyclin B1 protein for A375 and PC3 cells exposed to 100 cGy of irradiation. As observed following a 50 cGy exposure (Figure 3.12), the data in both of these cell lines following irradiation indicate that a G2/M cell cycle arrest is occurring (although the onset at 2 hours coming sooner than the flow cytometric evidence indicating an onset of 4 hours for the G2/M arrest, and the duration of the of the cyclin B1 reduction was much shorter than the G2/M accumulation was using the flow cytometric data). The PC3 response following 100 cGy is highly similar in both magnitude and timing as seen following a 50 cGy exposure. However, in the A375 cells, differences do exist. Following 100 cGy, the G2/M block is of longer duration than that observed following 50 cGy exposure, with cyclin B1 levels being reduced through 8 hours post irradiation. Only by 12 hours post irradiation do cyclin B1 levels return to control. Furthermore, unlike the 50 cGy studies, for both cell lines, the strong G2/M block observed using Western blot analysis correlates with the the flow cytometric studies presented in panel F of Figure 3.6 that suggest a significant radiation-

induced G2/M arrest is present. Finally, as seen following a 50 cGy exposure, both the A375 and PC3 cell lines show a sharp drop in cyclin B1 levels compared to unirradiated controls by 24 hours post irradiation, which is likely due to radiation-induced synchrony of the cell populations so that most of the cells are present in a phase of the cell cycle where the levels of cyclin B1 are naturally quite low (see Figure 1.2 in Chapter 1).

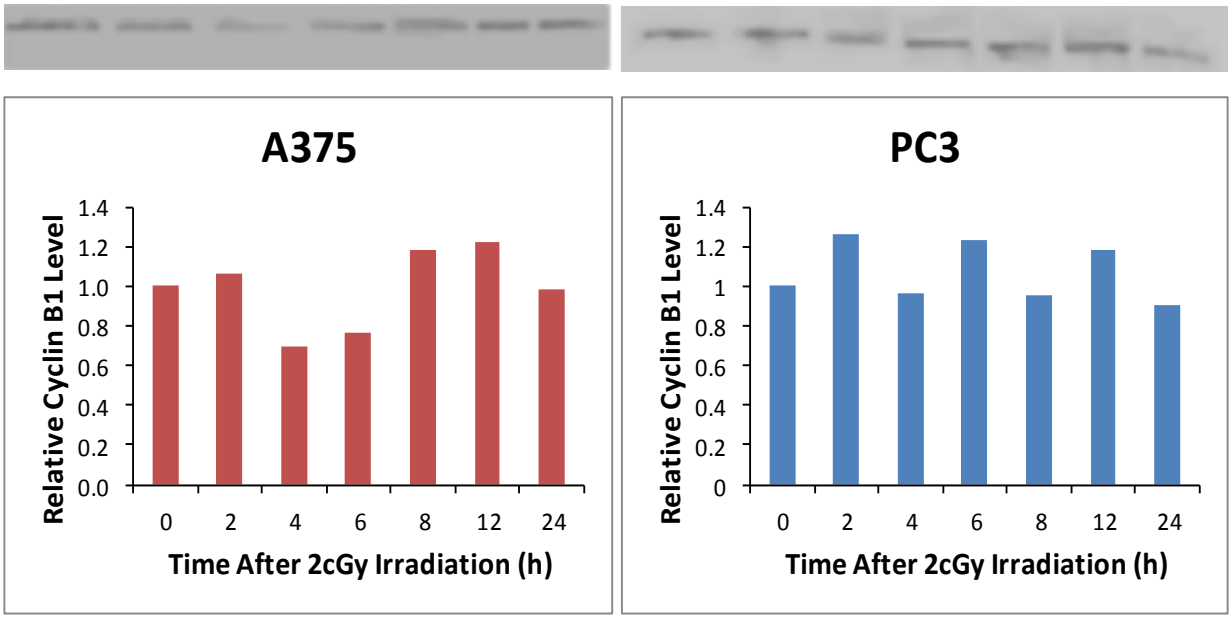

Figure 3.9. Changes in the relative levels of cyclin B1 protein over a 24-hour time interval for A375 and PC3 cells exposed to 2 cGy of irradiation. Top panels display the Western blot bands of protein, while the bottom panels represent the relative band intensity as analyzed by ImageJ software. Data demonstrate a reduction in cyclin B1 levels in A375 cells, but not in PC3 cells.

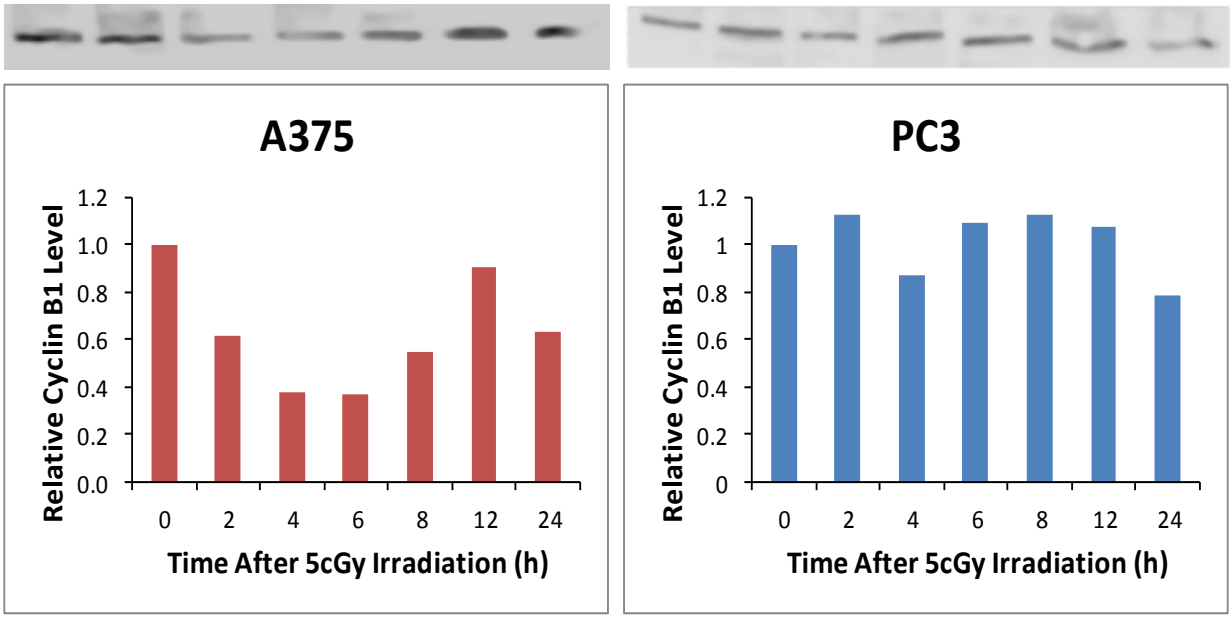

Figure 3.10. Changes in the relative levels of cyclin B1 protein over a 24-hour time interval for A375 and PC3 cells exposed to 5 cGy of irradiation. Top panels display the Western blot bands of protein, while the bottom panels represent the band intensity (relative to control) as analyzed by ImageJ software. Data demonstrate a reduction in cyclin B1 levels in A375 cells, but not in PC3 cells.

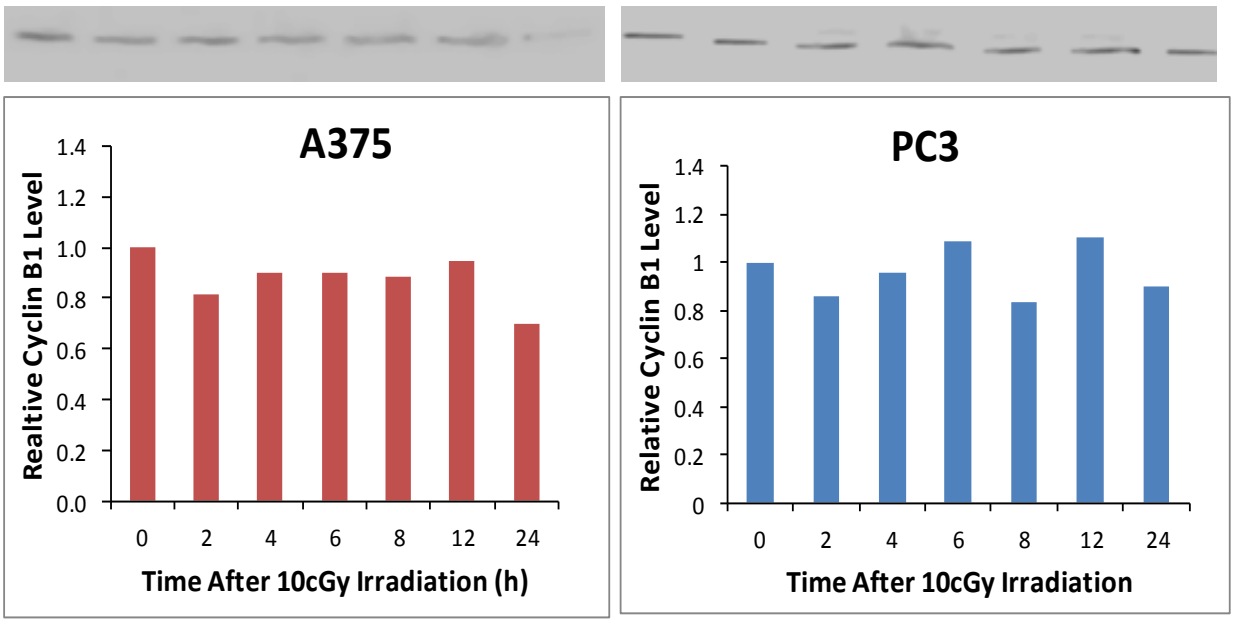

Figure 3.11. Changes in the relative levels of cyclin B1 protein over a 24-hour time interval for A375 and PC3 cells exposed to 10 cGy of irradiation. Top panels display the Western blot bands of protein, while the bottom panels represent the band intensity (relative to control) as analyzed by ImageJ software. Data display some fluctuations, but no significant reduction, in cyclin B1 levels for A375 or PC3 cells.

Cyclin B1 Levels Following 25 cGy Irradiation

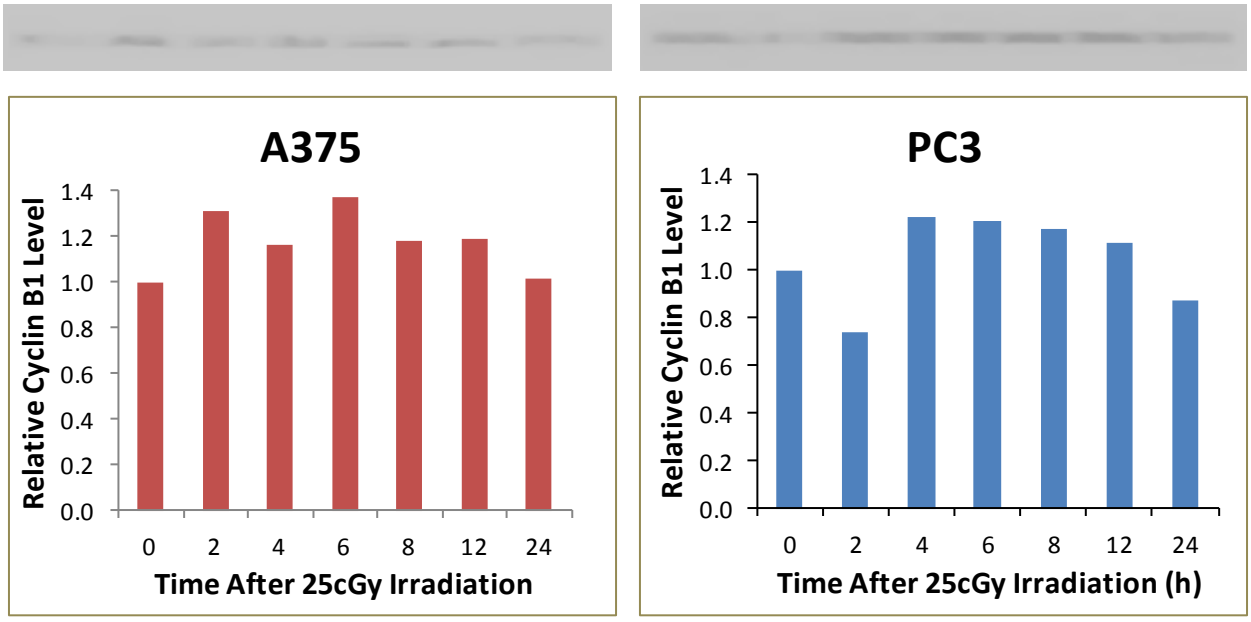

Figure 3.12. Changes in the relative levels of cyclin B1 protein over a 24-hour time interval for A375 and PC3 cells exposed to 25 cGy of irradiation. Top panels display the Western blot bands of protein, while the bottom panels represent the band intensity (relative to control) as analyzed by ImageJ software. Data display some fluctuations, but no significant reduction, in cyclin B1 levels for A375 or PC3 cells.

Cyclin B1 Levels Following 50 cGy Irradiation

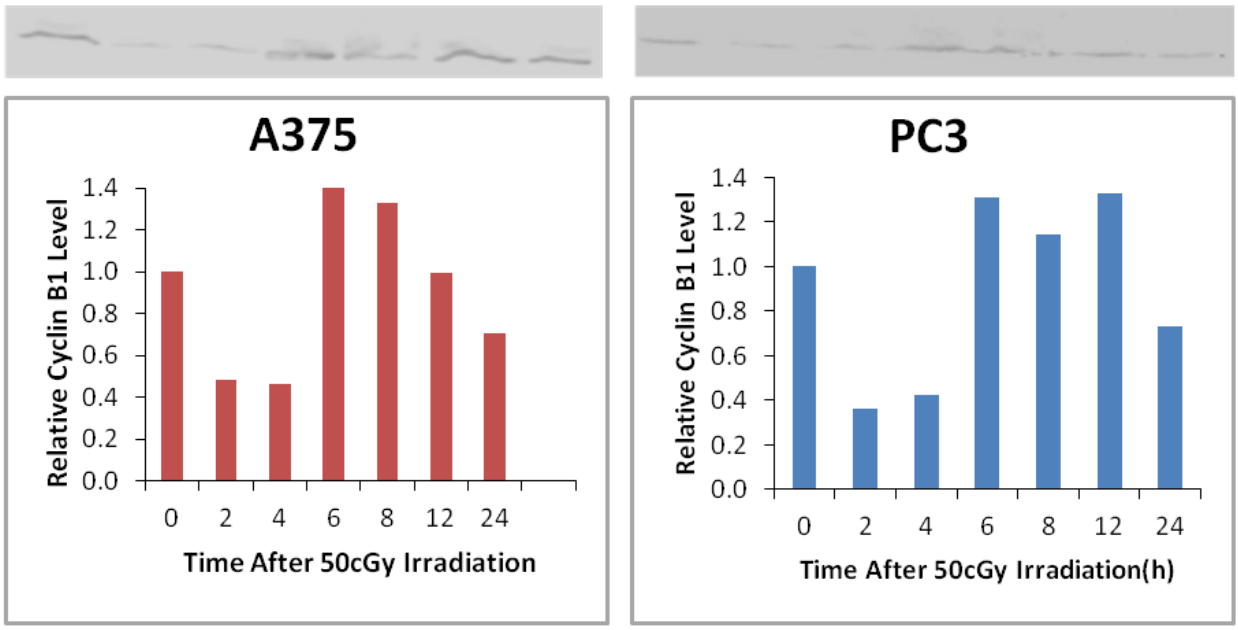

Figure 3.13. Changes in the relative levels of cyclin B1 protein over a 24-hour time interval for A375 and PC3 cells exposed to 50 cGy of irradiation. Top panels display the Western blot bands of protein, while the bottom panels represent the band intensity (relative to control) as analyzed by ImageJ software. Data demonstrate a significant reduction in cyclin B1 levels for both A375 and PC3 cells.

Cyclin B1 Levels Following 100 cGy Irradiation

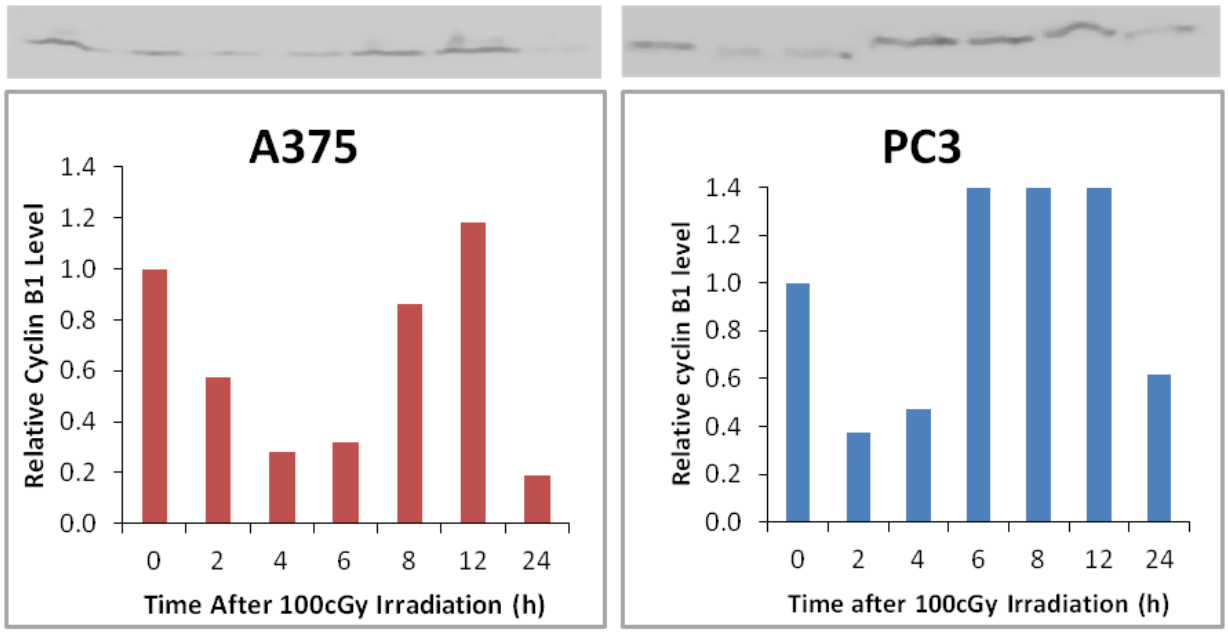

Figure 3.14. Changes in the relative levels of cyclin B1 protein over a 24-hour time interval for A375 and PC3 cells exposed to 100 cGy of irradiation. Top panels display the Western blot bands of protein, while the bottom panels represent the band intensity (relative to control) as analyzed by ImageJ software. Data demonstrate a significant reduction in cyclin B1 levels for both A375 and PC3 cells.

3.5 EXPRESSION OF ACTIVATED MAPKS AND NF-KB

Exposure to radiation has been reported to trigger upregulation of proliferative signaling cascades such as the MAPK and NF-κB pathways. Therefore, studies were undertaken to ascertain whether signaling through these proliferative pathways is being activated following exposure of A375 and PC3 cells to low doses of radiation. These studies were accomplished by monitoring the levels of phosphorylated (activated) ERK1/2, JNK1/2, p38 and NF-κB using cell-based ELISA assays that were performed 5 hours post irradiation (preliminary studies in our laboratory determined this time to be optimal). All results represent the mean ± SEM of three independent experiments on triplicate samples which have been converted to fraction of unirradiated control.

Figure 3.15 shows the protein levels of phosphorylated EKR1/2 in A375 and PC3 cells following irradiation at doses of 0 - 100 cGy. Results demonstrate a pattern of increased levels of phosphorylated ERK1/2 as a function of increasing dose for both cell lines, with statistically significant increases in phosphorylated protein levels occurring between 25 and 100 cGy both in the A375 and PC3 cell lines, suggesting an activation of this signaling cascade at these radiation doses.

As can be seen in Figure 3.16 which displays the change in expression of phosphorylated JNK1/2 in the A375 or the PC3 cell lines following exposure to radiation, levels were maximally elevated at exposure doses of 10 and 25 cGy. In both the A375 melanoma and the PC3 prostate carcinoma cell line, these increases were statistically significant at these doses.

Figure 3.17 shows the protein levels of phosphorylated p38 levels in A375 and PC3 cells following irradiation at doses of 0 - 100 cGy. In both A375 and PC3 cells, fluctuations in protein levels were observed. However, relative to unirradiated controls, there were no statistically

significant radiation-induced changes in phosphorylated p38 levels observed over the dose range investigated.

Finally, Figure 3.18 displays the relative induction of phosphorylated NF-κB obtained following exposure to low dose radiation. As can be observed, results for the A375 cells demonstrate that the levels of phosphorylated NF-κB remain similar to control following irradiation with very low doses, but from 10 – 50 cGy exposures, phosphorylation of NF-κB is significantly down-regulated relative to the unirradiated controls. This pattern is not observed in the PC3 cell line where phosphorylated protein levels fluctuate but do not demonstrate statistically significant changes except following 5 cGy where levels are down-regulated.

Phosphorylation of ERK1/2 as a Function of Radiation Dose

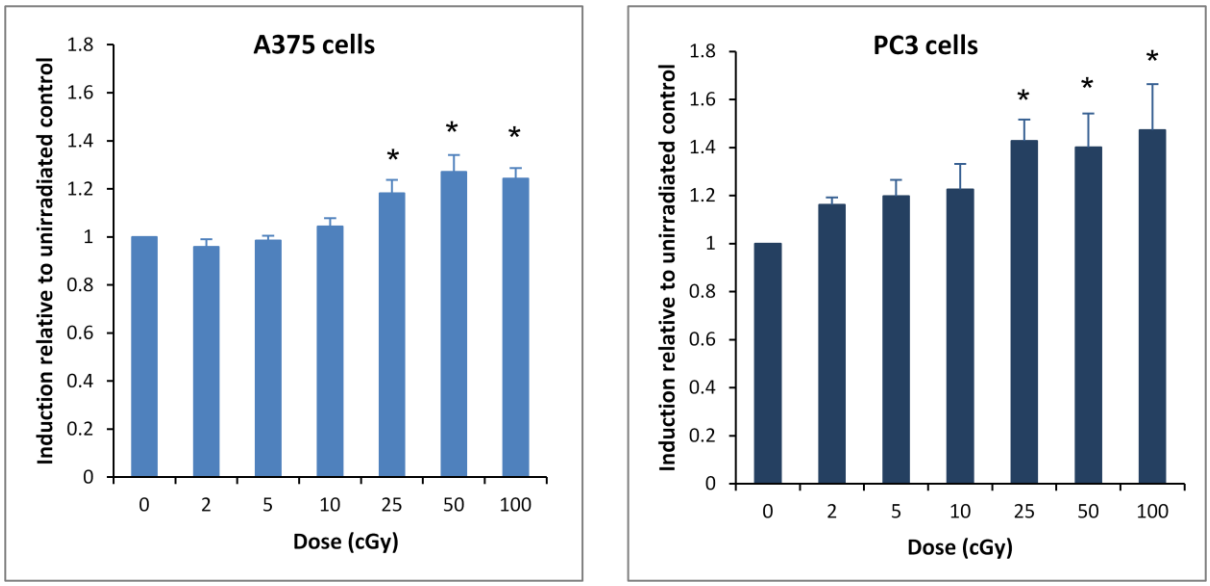

Figure 3.15 Relative induction of phosphorylated ERK1/2 obtained from a cell-based ELISA assay performed 5 hours following x-irradiation. Results represent the mean ± SEM of three independent experiments on triplicate samples which have been converted to fraction of control. Data suggest an increasing pattern of activation as a function of increasing dose. Asterisks connote data points significantly different from control.

Phosphorylation of JNK1/2 as a Function of Radiation Dose

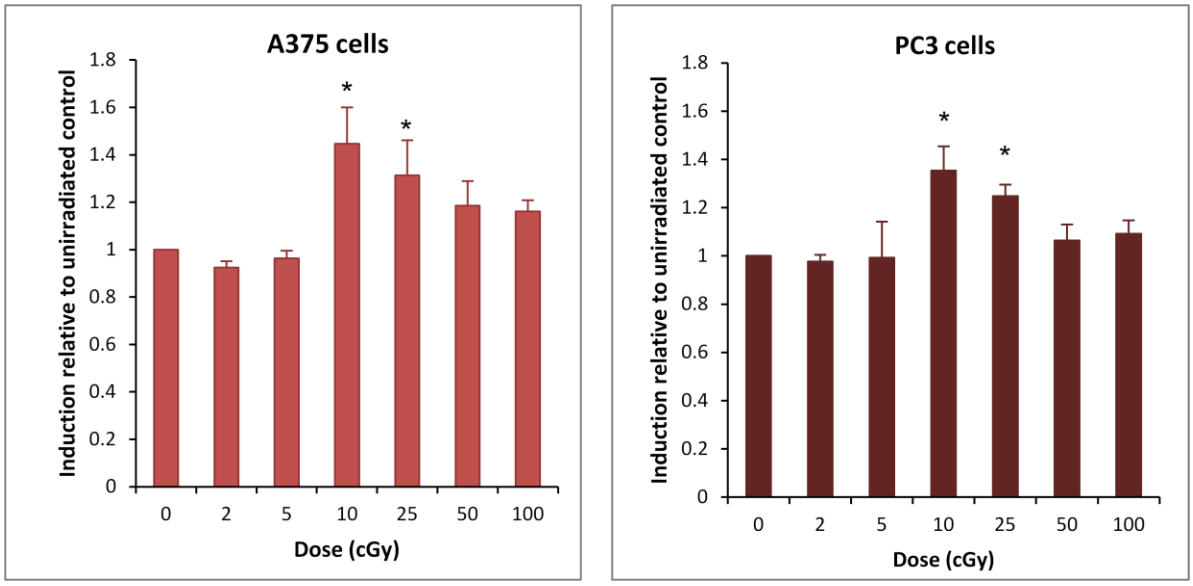

Figure 3.16 Relative induction of phosphorylated JNK1/2 obtained from a cell-based ELISA assay performed 5 hours following x-irradiation. Results represent the mean ± SEM of three independent experiments on triplicate samples which have been converted to fraction of control. Data demonstrate the presence of elevated levels following 10 and 25 cGy exposures in both cell lines. Asterisks connote data points significantly different from control.

Phosphorylation of P38 as a Function of Radiation Dose

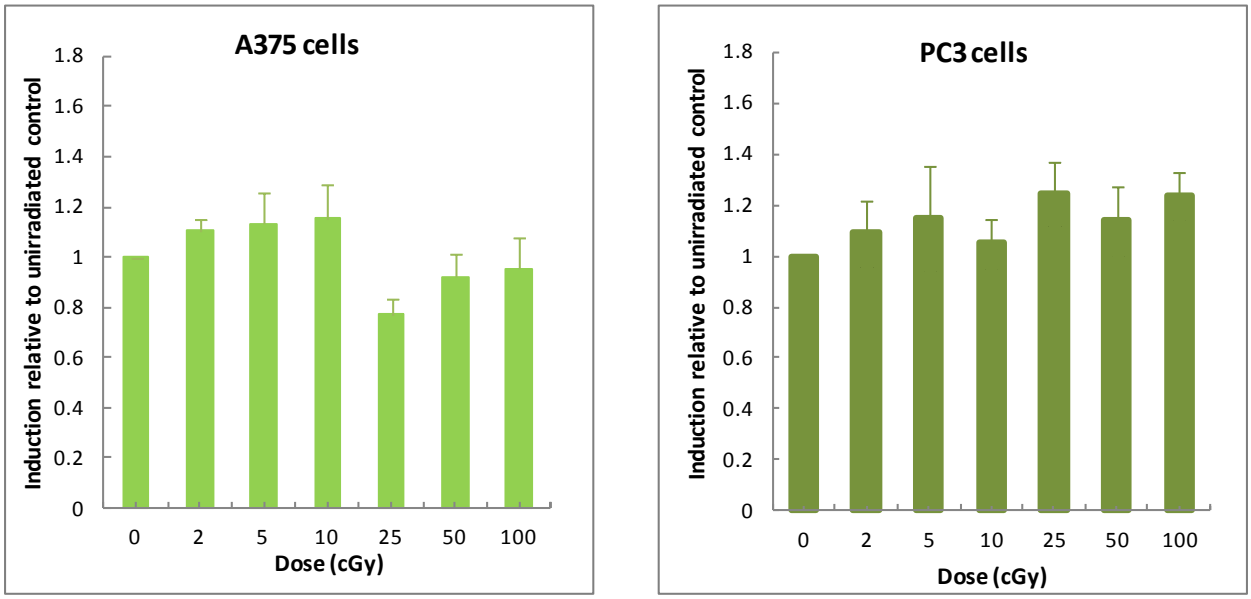

Figure 3.17 Relative induction of phosphorylated p38 obtained from a cell-based ELISA assay performed 5 hours following x-irradiation. Results represent the mean ± SEM of three independent experiments on triplicate samples which have been converted to fraction of control. Data display fluctuations in the levels of phosphorylated p38, but not significant changes are observed in either cell line.

Phosphorylation of NF-κB as a Function of Radiation Dose

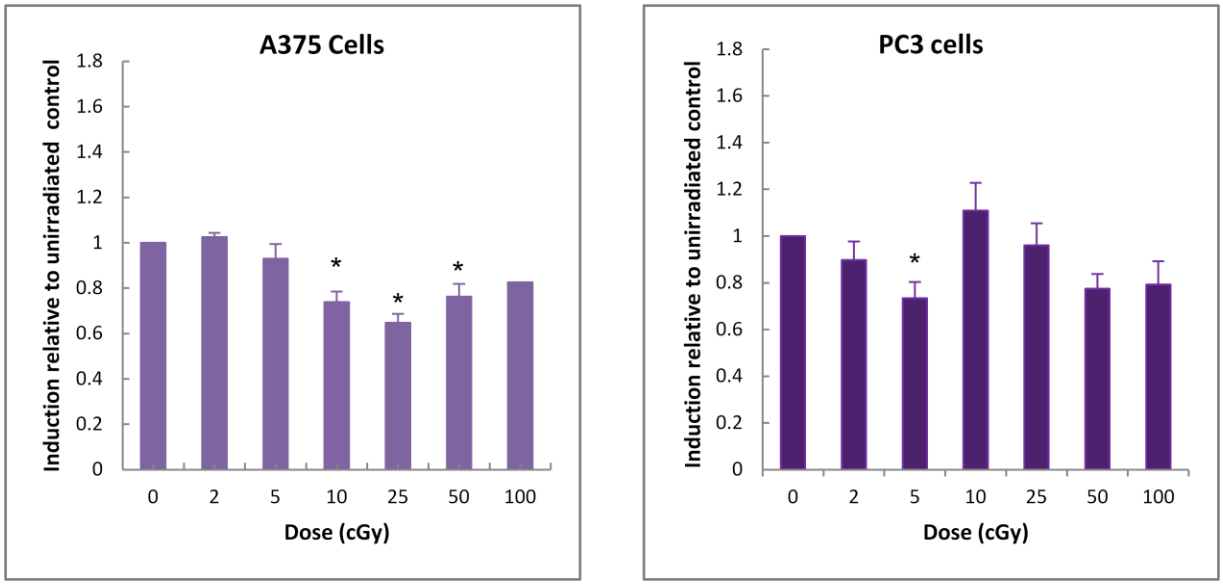

Figure 3.18 Relative induction of phosphorylated NF-κB obtained from a cell-based ELISA assay performed 5 hours following x-irradiation. Results represent the mean ± SEM of three independent experiments on triplicate samples which have been converted to fraction of control. Data demonstrate that the levels of phosphorylated NF-κB are significantly down-regulated following exposures from 10 to 50 cGy in the A375 cell line, but not in the PC3 cell line. Asterisks connote data points significantly different from control.

CHAPTER 4: DISCUSSION

4.1 SURVIVAL OF A375 AND PC3 CELLS FOLLOWING LOW DOSE RADIATION

Over the past two decades, increasing evidence has been accumulating suggesting that exposure of cells to very low dose (VLD) radiation results in a host of unpredictable responses (e.g. adaptive responses, bystander effects and inverse dose rate effects), making it clear that extrapolation of data derived from high dose studies to this very low dose region is no longer a feasible alternative. As a consequence, therefore, one goal of these studies was to characterize the response of two different cell lines, the human melanoma A375 cell line and the human prostate cancer PC3 cell line, following exposure to the low dose range of radiation. These two cell lines were selected because they represent the opposite ends of the spectrum with regard to radiation sensitivity. For example, in classical dose-response survival studies (1 Gy and greater), the A375 cells have been shown to be moderately resistant to radiation, while the PC3 cells have been shown to be relatively sensitive to radiation (135). In addition, preliminary studies within our laboratory suggested that the human melanoma A375 cell line appeared to demonstrate an interval of hyper-radioradioresistance following very low doses of radiation. This response was in sharp contrast to reported literature that argued that PC3 cells display very low dose hyper-radiosensensitivity (125). It was felt, therefore, that comparing and contrasting the radioresponse profiles of these two lines, both at the cellular level (survival) and the molecular level (cell signaling pathways), might help better elucidate the mechanisms underlying the often-times contradictory cellular responses to low dose radiation.

As stated above, the goal of this series of studies was to characterize the survival response of the human melanoma A375 cell line and the human prostate cancer PC3 cell line following exposure to the low dose range of radiation. The results of these studies demonstrated

two very different survival responses to very low dose irradiation (10 cGy and below) were present, neither of which followed classical linear quadratric theory. Specifically, the results of this investigation demonstrated that clonogenic survival is significantly increased in A375 cells when irradiated at doses between 2–5 cGy, suggesting that this cell line demonstrates low dose hyper-radioresistance. Conversely, clonogenic survival in the PC3 cells is significantly decreased at 2-5 cGy, suggesting a low dose hyper-radiosensitivity response exists. Finally, the results show that this phenomenon of increased radioresistance versus increased radiosensitivity in A375 and PC3 cells, respectively, occurrs only at the very low doses of radiation studied in this investigation (less than 10 cGy). At doses higher than 25cGy, both cell lines began to display a classical linear quadratic pattern of response to radiation.

Regarding the results of the PC3 studies, the data confirm previous reports of hyper-radiosensitivity in PC3 cells that have been demonstrated using both the conventional colony formation assays (135) and by flow cytometric methods (136). Indeed, several reports published in the last two decades have demonstrated that many mammalian cell lines exhibit hyper-radiosensitivity in the low dose range of radiation (17, 92, 96, 97, 137). For example, Wouters *et al* demonstrated that U1 melanoma, DU 145 prostate carcinoma, HT-29 colon adenocarcinoma, SiHA cervical squamous carcinoma and A549 lung adenocarcinoma cell lines exhibited low dose hyper-radiosensitivity (17). Additionally, Schettino *et al* reported low dose hyper-radiosensitivity in Chinese Hamster V79 cells (13).

The reasons for this increased sensitivity at low doses still remain to be clearly defined, although some investigators suggest that the failure to induce protective mechanisms such as cell cycle arrest may play a role. Another currently popular explanation given for the hyper-radiosensensitivity observed at very low doses is that cells need to accumulate some minimum

damage before DNA repair mechanism are turned on (56). If DNA damage is below this minimum amount, there is no upregulation of repair pathways and the damage remains within the cell, weakening it. In support of this damage threshold theory, it was observed that cells pre-treated with very low concentrations of hydrogen peroxide before irradiation did not display the hyper-radiosensensitivity seen in irradiated-only cells (127), because the DNA damage from hydrogen peroxide added on to the DNA damage from the radiation to surpass the damage threshold required for the activation of DNA repair pathways. However, not all researchers currently support the DNA damage threshold concept, arguing that most of these studies have not been based on direct measurement of DNA double strand breaks, but, rather, indirect estimates of DNA damage, such as the measurement of γ-H2AX foci, that may be prone to error (128).

In contrast to low dose hyper-radiosensitivity responses, results from the A375 experiments suggest that hyper-radioresistance is occurring following exposure to very low doses of radiation for this cell line. Furthermore, to the best of my knowledge, this is the first report documenting a low dose hyper-radioresistant response in A375 cells. However, a small fraction of other cell lines have been reported to display increased survival or hyper-radioresistance following low dose irradiation. For example, Kim *et al* demonstrated that a dose of 5 cGy stimulated proliferation in CCD 18Lu human lung fibroblasts (20), whereas Suzuki *et al* reported enhanced proliferation in normal human diploid (HE49) cells (19). As with the induction of hyper-raidosensitivity, the mechanisms responsible for observed hyper-radioresistance are still poorly understood. However, in addition to DNA damage, radiation-induced membrane-associated changes occur following irradiation of cells, which can induce the activation of major growth regulators such as epidermal growth factor receptors (EGFR), tumor

necrosis factor receptors (TNFR) and tyrosine kinase receptors (3, 61, 69, 78), and some researchers have suggested that the mechanism underlying low dose hyper-radioresistance may be due to a hyper-proliferative response brought about by the activation of these important growth factors and subsequent stimulation of proliferative pathways. For example, activation of the EGFR in the plasma membrane has been associated with stimulation of the MAPK pathways (78, 79) which, as described previously, are important mediators of enhanced cell proliferation/survival. Additionally, in Chinese hamster fibroblasts and Raji lymphoma cells irradiated at doses between 2 and 10 cGy, a pronounced hyper-proliferative response was observed (130). Furthermore, irradiation at doses between 2 and 5 cGy has been documented to cause hyper-proliferation in normal human HE49 cells (19). Finally, exposure to 50 cGy has been reported to stimulate induction of cell proliferation in mouse hematopoietic cells (21), and irradiation at 5 cGy has been shown to enhance cell proliferation via transient ERK1/2 and p38 activation in normal human lung fibroblasts (20).

In conclusion, therefore, the results of these cell survival studies add to the increasing body of evidence which suggest that the response to radiation at very low doses (0-10 cGy) is complex and cannot simply be extrapolated from the high dose range used in classical cell survival studies. Rather, these data demonstrate that response to very low dose radiation is often cell type specific and frequently contradictory.

4.2 CELL CYCLE FREQUENCY DISTRIBUTIONS OF A375 AND PC3 CELLS FOLLOWING LOW DOSE RADIATION

Collectively, the results of the flow cytometric studies monitoring the cell cycle frequency distributions of A375 and PC3 cells demonstrated the following: (1) a G2/M block is seen in both cell lines at the higher doses studied; (2) a strong G2/M block is observed in A375

cells following exposure to 2 and 5 cGy which may contribute to the hyper-radioresistance seen in this cell line within this very low dose range; (3) no evidence of G2/M arrest is observed in PC3 cells following exposure to 2 and 5 cGy where radio-hypersensitivity is documented, suggesting that the lack of a G2/M arrest may be contributing to the hyper-radiosensitivity of this cell line within this very low dose range; and (4) no significant evidence of G0/G1 or S phase arrest is seen in either cell line, but changes in G0/G1 and S accumulation by 24 hours post irradiation are present in those studies where the presence of an earlier G2/M block is seen, suggesting radiation-induced synchrony may be occurring.

As stated above, these results confirm the existence of a G2/M block occurring following irradiation with doses of 50 or 100 cGy. Since numerous studies have shown that radiation doses of about 50 cGy or higher interfere with normal progression of the cell cycle in a variety of cell lines (23, 25, 51), these results are not unexpected. Indeed, cell cycle arrest after exposure to radiation is the norm, rather than the exception, with several studies documenting the presence of arrests in all three phases of the cell cycle following irradiation, although G2/M is the most commonly reported block (25, 50, 51, 138). For example, for HeLa cells alone, separate studies have observed blocks in S phase after irradiation with 5 Gy (139), blocks in G2/M phase after irradiation with doses between 0.34 and 1.35 Gy (31), and blocks in G1, S and G2/M phases following irradiation with 3 Gy (140). Similarly, studies using Chinese hamster cells exposed to a series of doses between 1.5-6 Gy demonstrated dose dependent division delay in all three cell cycle phases (141). Furthermore, the data from these studies demonstrating that the cell cycle is arresting in G2/M is also consistent with previous studies which confirm that the most frequently induced cell cycle arrest following radiation is seen in the G2/M phase (25, 49, 50). Arrest at

this stage of the cell cycle is critical to repairing DNA before the cell enters mitosis, thereby reducing the potential for mitotic catastrophe.

Our results also indicate that the magnitude and duration of the G2/M delay in both the A375 and PC3 cells were dose dependent and far more pronounced in the A375 line than in the PC3 line. As evidenced from panels E and F of Figure 3.8, the PC3 cells irradiated with 100 cGy had a G2/M arrest that lasted from 2-12 hours and peaked at 170% of unirradiated control, while PC3 cells irradiated with 50 cGy had exhibited only small block between 4 and 12 hours which peaked at about 125% of unirradiated control values. Similarly, although the peak accumulation in A375 cells for both 50 and 100 cGy was pronounced (~ 225% of control), the duration of the block following 100 cGy was longer, lasting between 4 and 24 hours, as compared to 2 -12 hours for the 50 cGy study. These results are in agreement with numerous other studies performed at high doses that have demonstrated that the magnitude and recovery time for G2/M delays is proportional to dose administered, with higher doses exerting a longer and larger G2/M delay (142-144). For example, Walters *et al* demonstrated that Chinese hamster ovary (CHO), HeLa S-3 and murine lymphoma L-5178Y cells displayed a G2/M block that was proportional to dose (142), while Ehmann *et al* showed that for L5178YS /S leukemia mouse cells irradiated with 50, 100, 200 and 300 cGy dose dependent G2/M arrests were observed, with 50 cGy showing the least in magnitude of arrest and time of delay, while the cells irradiated with 300 cGy had a longer time delay and higher percentage of cells in G2/M (144).

A second major finding of these studies is the observation that a strong G2/M block is observed in A375 cells in the very low dose range which may contribute to the hyper-radioresistance seen at 2 and 5 cGy doses by allowing the cells time to repair before proceeding to mitosis. Surprisingly, this block is not present following 10 and 25 cGy exposures, but, as

stated above, reappears following 50 and 100 cGy exposures. What is causing this unusual pattern of G2/M arrest in A375 cells following irradiation is unclear, since cell cycle changes following low doses of radiation have not been well investigated. However, the biphasic nature of the G2/M arrest may imply the presence of two separate mechanisms in play. There are studies which suggest that very low dose radiation can modulate the expression of various genes related to cell cycle arrest in a manner quite different from that seen by higher radiation doses (145, 146). In fact, studies by Ding *et al* demonstrated that in normal skin fibroblasts (HSF42) cells, 2 cGy exposures predominantly caused expression of genes involved in DNA damage response and signal transduction, while 400 cGy exposures predominantly induced expression of genes involved in proliferation and apoptosis (147). Nevertheless, while it is reasonable to conclude that the G2/M arrest in A375 cells observed at 2 and 5 cGy may be playing a role in mediating the very low dose hyper-radioresistance seen through the facilitation of DNA repair before proceeding to mitosis, it must also be noted that most studies have postulated that the major mechanism underlying hyper-radioresistance following low dose radiation is increased proliferation mediated through activation of growth pathways such as the MAPK cascades (19, 20). Certainly more studies are warranted in this area to better understand the basis of this radioresistant phenomenon.

A third major finding of these studies was the fact that the hyper-radiosensitivity observed in PC3 cells at very low doses appears to correlate with a lack of G2/M arrest at these doses. Specifically, in this investigation, no evidence of G2/M arrest was observed in PC3 cells at the very low dose range (0-10 cGy), where hyper-radiosensitivity was seen. Failure of PC3 cells to exhibit cell cycle arrest at doses of maximal hyper-radiosensivity (2-10 cGy) is in general agreement with others (97, 148). For example, Enns and colleagues demonstrated that A549

human lung carcinoma cells that displayed hyper-radiosensitivity following 5 and 10 cGy of radiation, failed to arrest in any of the cell cycle phases at these doses (97). The precise mechanism underlying the inability of PC3 cells to arrest at these very low doses is unclear, but it is likely that the low level of DNA damage following such low doses of irradiation did not cause enough damage to trigger a G2-M arrest. As discussed earlier, a currently well-accepted theory for the failure of hyper-radiosensitive cell lines to arrest at low doses is that cells need to accumulate some minimum DNA damage before DNA repair mechanisms are triggered (56). If DNA damage is below this minimum, DNA repair pathways are not activated within the cell. In support of the minimal DNA damage theory, it was observed that cells pre-treated with very low concentration of hydrogen peroxide before irradiation lost their hyper-radiosensitivity (127), presumably because the DNA damage from hydrogen peroxide added on to the DNA damage from the radiation to surpass the damage threshold required for the activation of DNA repair pathways. Nevertheless, not all researchers currently support the DNA damage threshold concept, arguing that most DNA repair data from low dose radiation studies have been based on indirect estimates of DNA damage (measuring γ-H2AX foci) and not direct measurement of DNA double strand breaks (128). More research is needed to elucidate mechanisms of low dose hyper-radiosensitivity.

A final finding of the cycle frequency distribution studies was the lack of evidence to suggest that either cell line was arresting in G0/G1 or S phases of the cell cycle. This finding was somewhat surprising, since several investigations have documented the presence of G1 and/or S phase blocks following radiation exposure (12, 22, 27-29, 39, 41). However, since these studies used radiation doses much higher than those used in this investigation, the disparity between these reports and the results of this study may be due to differential dose effects. Of

interest, it has been noted by some investigators that G1 arrests, even when they are induced, may not play a major role in the mediation of radiation effects, and that transient delays in G1 are likely not to have a significant impact on radiation survival (149, 150). For instance, Slichenmyer et al demonstrated that, following exposure to a radiation stress, clonogenic survival for two colorectal cancer cell lines (SW480 cells which don't arrest in G1 and RKO cells which do arrest in G1) was not significantly different (149).

Although actual arrests were not observed in either cell line, changes in G0/G1 and S phase accumulation by 24 hours post irradiation were seen in those studies where the presence of an earlier G2/M block was found. As stated earlier, these observations of increased G0/G1 phase numbers and decreased S phase numbers may be due to the phenomenon of radiation-induced synchrony. Synchronization of cells after irradiation is a well-described event (151-153) in which a significant accumulation of cells in the G2/M phase is followed by release of the G2/M block and the movement of a large cohort of cells concurrently into G0/G1, where they progress through one of more cycles of cell division in tandem before reassorting into an asynchronous cell population again.

4.3 CYCLIN B1 LEVELS IN A375 AND PC3 CELLS AFTER LOW DOSE RADIATION

One aim of these studies was to investigate the effect of low doses of radiation on the expression of cell cycle regulator proteins in the effort to correlate the temporal changes in cell cycle frequency distributions with the downregulation of cyclin levels. Because the cell cycle arrests occurred only within the G2/M phase, therefore, studies were designed to monitor changes in this phase of the cell cycle by measuring cyclin B1 levels. The rationale for choosing cyclin B1 is based on the crucial role that the cyclin B1/CDK1 complex plays in triggering the

progress of cells through the G2 and M phases of the cell cycle (25, 51, 154). A decrease in cyclin B1 levels can lower the amount of cyclin B1/CDK1 complex present and, as such, can hinder entry into mitosis, leading to accumulation of cells in the G2/M phase (155-158).

Collectively, the results from these studies demonstrated the following: (1) for A375 cells, reductions in cyclin B1 levels were observed at both the very low (2 and 5 cGy) and the high (50 and 100 cGy) doses of radiation, but were not present following doses of 10 and 25 cGy, confirming the observation made in the previous section that a biphasic G2/M block is occurring; (2) for PC3 cells irradiated with doses from 2-25 cGy, cyclin B1 levels fluctuated, but displayed no significant reduction, also agreeing with the flow cytometric frequency distribution studies; (3) PC3 cells irradiated with 50 cGy, showed a marked reduction in cyclin B1 activity, but the frequency distribution data for the 50 cGy exposure demonstrated only a small G2/M accumulation; (4) PC3 cells irradiated with 100 cGy, showed a marked reduction in cyclin B1 activity which was in agreement with the frequency distribution data for the 100 cGy exposure seen in this cell line, and, finally, (5) when compared to the frequency distribution data obtained flow cytometrically, no consistent pattern in temporal onset and duration of cyclin B1 reductions could be seen. Overall, however, although not always consistent, the results of these studies showed good agreement with the flow cytometric frequency distribution studies.

Several reports have demonstrated that, for cells that display a G2 arrest, there exists a correlation between down regulation of cyclin B1 protein levels with accumulation of cells in the G2/M phase (51, 155, 159, 160). For example, Hendrikse *et al* reported a decrease in cyclin B1 levels in TK6 (a lymphoblast cell line) following 1 and 3 Gy of irradiation (161), while Muschel *et al* also reported a decrease in cyclin B1 subsequent to radiation in Hela Cells (159). In addition, Enns *et al* correlated the lack of cyclin B1 decreases following irradiation with the

hyper-radiosensitivity observed in the A549 lung adenocarcinoma cell lines after irradiation with doses of less than 20 cGy (97), and Datta *et al* demonstrated a dose dependent down regulation of cyclin B1 in U937 leukemia cell line, after being irradiated with 1, 5 and 10 Gy of irradiation (162). These data are in agreement with the above reports which suggest that a decrease in cyclin B1 levels can correlate with a G2/M block. However, our results did not demonstrate a consistent pattern in the down-regulation of cyclin B1 protein levels with respect to either the onset or the duration of G2/M arrest as measured by the flow cytometric frequency distribution data. For example, with regard to the duration of G2/M arrest, A375 cells displayed two distinct patterns of expression of cyclin B1 reduction. Specifically, A375 cells irradiated with 2 and 50 cGy displayed a short lived down-regulation of cyclin B1 protein, lasting less than six hours, while the flow cytometric data suggested a G2/M arrest of 12 or more hours in duration. On the other hand, A375 cells following 5 and 100 cGy exposures displayed a prolonged cyclin B1 reduction which was observed to last about 10 hours (2-12 hours post irradiation), a time interval more similar to what was seen in the flow cytometric data. With regard to the onset of the cyclin B1 reduction, data also varied from the flow cytometric results. For example, in A375 cells exposed to 5 and 100 cGy and PC3 cells exposed to 100 cGy, reduced levels of cyclin B1 were observed earlier than the G2/M accumulation as measured by flow cytometry, appearing at 2 hours post irradiation, while flow cytometry data demonstrated significant accumulation beginning at 4 hours post irradiation. However, following exposures of 2 cGy, the onset of cyclin B1 reduction occurred at 4 hours post irradiation in A375 cells, which was concurrent with the onset of G2/M accumulation observed in the flow cytometry studies, following a 50 cGy exposure, the rapid, and surprising, onset of G2/M arrest at one in the flow cytometry data appears earlier than the onset of cyclin B1 reduction.

It is unclear why these differing patterns of onset and duration occurred. The molecular mechanisms underlying the G2/M arrest and the reasons for the variation in the timing of cyclin B1 reductions following radiation are still relatively unknown, and seemingly contradictory reports exist in the literature. For example, some studies have shown that a decline in cyclin B1 levels is often observed before cells start accumulating into G2/M phase (161). These reports would be in agreement with our observations on A375 cells following 5 and 100 cGy and PC3 cells following 50 and 100 cGy. Studies have shown that reduced cyclin B1 levels can occur concurrent with the onset G2/M accumulation, as is seen in our studies following A375 cells irradiated with 2 and 50 cGy (161). Finally, reports have suggested that cyclin B1 levels may be be down regulated following accumulation of cells in G2/M, such as we observed in PC3 cells following 50 cGy irradiation (159). Obviously, more studies are needed to elucidate mechanisms underlying the onset and duration of G2/M arrest.

Finally, since levels of cyclin B1 are extremely low in G0/G1 and S phases (refer to Figure 1.2, Chapter 1), reduction in cyclin B1 levels may not only correlate with the presence of a G2/M block, but also can be observed in situations where a large cohort of the cells are in G0/G1 or S phases of the cell cycle, such as would be observed in a synchronized population. In this regards, the significant decreases in cyclin B1 levels seen in the A375 cells at 24 hours after 2, 5, 50 and 100 cGy of irradiation, and in the PC3 cells at 24 hours after 50 and 100 cGy of irradiation is further indication of synchronization, or, at least, partial synchronization of these two cell populations at this time. Synchronization or partial synchronization following exposure to x-rays has been observed by many radiation workers in both *in-vivo* and *in-vitro* conditions (151-153).

4.4 MAPK RESPONSE IN A375 AND PC3 CELLS AT LOW DOSES OF RADIATION

Numerous studies have shown that radiation can activate a variety of tyrosine kinase receptors, leading to activation of the family of serine-threonine kinases, known as MAP kinases (for a review see(163) and triggering of the ras-MAPK pathway (also known as the extracellular signal-regulated kinase 1 and 2 or ERK1/2 pathway), the c-jun NH_2-terminal kinase (JNK) pathway, and (3) the p38 MAPK (100, 164-166). Radiation-induced EKR1/2 has been demonstrated to be associated with signals that promote cell survival and inhibit apoptosis (79), and, hence, may be involved in cellular radioresistance such as that observed in the A375 cell studies in this investigation. In contrast, activated JNK1/2 is capable of phosphorylating the NH_2- terminal sites in c-Jun and c-Myc, leading to cell apoptotic death (61, 88), and, hence, may be involved in cellular radiosensitivity such as that observed in the PC3 cell studies. Finally, activation of the p38 MAPK pathway has been documented to have contradictory effects, promoting both cell survival and cell death (108, 109), and, therefore, may be play a role in both of the differential radiation responses observed in these studies. Given the role that the MAPK kinases may play in radiation response, therefore, it was of interest to determine if the hyper-radioresistance seen in A375 cells and/or the hyper-radiosensitivity observed in PC3 cells following exposure to 2 and 5 cGy doses could be linked to activation of one or more of these pathways. Unfortunately, in these studies, no significant changes in the activation of these pathways appeared to occur following very low dose irradiation exposures. Only a limited number of investigations have focused on the activation of these pathways following very low dose radiation, and, at odds with the results of this study, the majority of these studies suggest that low doses of radiation can stimulate proliferation or survival through activation of either ERK1/2 or p38. For example, Suzuki *et al* reported induction of hyperproliferation in HE49

normal human diploid cells *via* activation of ERK1/2 (19), and Kim *et al* demonstrated enhancement of cell proliferation following 5 cGy, *via* transient activation of ERK1/2 and p38 in CCD 18Lu normal human lung fibroblasts (20). It is unclear why the results of these studies differ from other studies, but it may involve differences in the cell lines used or the experimental assays and design. Indeed, several studies have shown that response to very low dose radiation can be highly cell type specific (reviewed in (167)).

Though MAPK changes are not linked to the differential radioreponses observed in these two cell lines following exposure to very low dose radiation, the data did show an increase in activation of ERK1/2 with increasing dose in both the PC3 and A375 cells following exposure to doses of 25 to 100 cGy. This is in agreement with other studies that have demonstrated that activation of ERK1/2 increases proportionally with increasing dose (77, 168).

4.5 NF-κB RESPONSE IN A375 AND PC3 CELLS AFTER LOW DOSE RADIATION

Similar to the MAPK pathway studies described above, the goal of these studies was to determine if changes in the activation of NF-κB in A375 and PC3 cells could be correlated with the differential radioresponse to very low dose radiation exposures observed in this investigation. However results show that there are no significant radiation-induced changes in activated NF-kB for either cell line that correlate with observed radioresponse within the very low dose range of radiation (i.e. hyper-radioresistance in A375 and hyper-radiosensitivity in PC3). Hence, it does not appear from these studies, that these differential radioresponses are associated with activation of the NF-κB pathway.

Several researchers have demonstrated that radiation can activate NF-κB (115, 123), but the pattern and magnitude of this activation has varied greatly from study to study, depending on

the cell line investigated and the experimental conditions used. For example, in U1-Mel human melanoma cells, a steady increase in activation of NF-κB was observed from 0 to 4.5 Gy, after which activation fell gradually with increasing dose (122). However, in the KG-human myeloid cell line, NF-κB was increasingly activated by ionizing radiation from 2 Gy onward, peaking at doses between 5 to 20 Gy (123). Futhermore, while studies investigating the response of NF-κB pathway to low doses of radiation are limited, Mohan *et al* reported activation of NF-κB in human EBV-transformed 244B human lymphoblastoid cells irradiated with 0.25 to 2 Gy with a maximum activation at 50 cGy (124). The results of this study differ significantly from these findings, in that no significant activation of NF-κB is present at any dose studied in the PC3 cell line except at 5 cGy where a significant decrease is seen, and, in the A375 cell line, data suggest at 10-50 cGy, activation of NF-κB is also decreased. As with the MAPK studies, the reasons underlying the differences between these findings and other reported studies may be because individual cell lines respond to low dose radiation differently or it could be due to variations in experimental design.

4.6 CONCLUSIONS

The results of these studies demonstrate two different survival responses to very low dose irradiation (hyper-radioresistance in human A375 cells vs. hyper-radiosensitivity in human PC3 cells). As such, these results add to the increasing body of evidence which postulates that the cellular response to radiation at very low doses cannot simply be extrapolated back from the responses observed in the dose range used in classical cell survival studies. Rather, response to very low dose irradiation is often contradictory and cell type specific.

Furthermore, the differences in G2/M arrest observed from both the frequency distribution and the cyclin B1 studies suggest that a differential regulation of cell cycle signaling may be involved in the contradictory survival responses observed in these two cell lines. Specifically, there is correlation between the increased radiosensitivity observed in PC3 cells at very low radiation exposure and a failure of these cells to accumulate in G2/M following irradiation, and this correlation may suggest that failure to activate the G2 checkpoint could be a potential mechanism for very low dose hyper-radiosensitivity. Conversely, the strong G2/M block observed in the A375 cells at doses of 2 and 5 cGy may contribute, at least in part, to the hyper-radioresistance seen in this cell line at this dose range.

Finally, lack of significant changes in the levels of MAPK and NF-kB pathway markers for either cell line following exposures to very low dose range radiation, suggests that the hyper-radioresistance seen in A375 cells and the hyper-radiosensitivity seen in PC3 cells at 2 and 5 cGy is not correlated with the activation of these regulatory pathways.

REFERENCES

1. Hall EJ, Wuu C-S. Radiation-induced second cancers: the impact of 3D-CRT and IMRT. *Int J Radiat Oncol Biol Phy* 2003;56:83-88.

2. Brenner DJ, Hall EJ. Computed tomography-An increasing source of radiation exposure. *New Engl J Med* 2007;357:2277-2284.

3. Schmidt-Ullrich RK Mikkelsen RB, Dent P, Todd DG, Valerie K,Kavanagh JN, Rorrer WK, Chen PB. Radiation-induced proliferation of the human A431 squamous carcinoma cells is dependent on EGFR tyrosine phosphorylation. *Oncogene* 1997;15:1191.

4. Land CE. Estimating cancer risks from low doses of ionizing radiation. *Science* 1980;209:1197-1203.

5. Howe GR, Zablotska LB, Fix JJ, Egel J, Buchanan J. Analysis of the mortality experience amongst U.S. nuclear power industry workers after chronic low-dose exposure to ionizing radiation. *Radiat Res* 2004;162:517-526.

6. Wing S, Shy CM, Wood JL, Wolf S, Cragle DL, Tankersley W, Frome EL Job factors, radiation and cancer mortality at Oak Ridge National Laboratory: Follow-up through 1984. *Am J Ind Med* 1993;23:265-279.

7. Mettler FA, Sinclair WK, Anspaugh L, Edington C, Harley JH, Ricks RC, Selby PB, Webster EW, Wyckoff HO. The 1986 and 1988 UNSCEAR (United Nations Scientific Committee on the Effects of Atomic Radiation) reports: Findings and implications. *Health Phys* 1990;58:241-250.

8. Dreyer NA, Friedlander E. Identifying the health risks from very low-dose sparsely ionizing radiation. *Am J Public Health* 1982;72:585-588.

9. Huang L, Snyder AR, Morgan WF. Radiation-induced genomic instability and its implications for radiation carcinogenesis. *Oncogene* 2003;22:5848-5854.

10. Sailor WC Bodansky D, Braun C, Fetter S, van der Zwaan B. Nuclear power: A nuclear solution to climate change? *Science* 2000;288:1177-1178.

11. Followill D, Geis P, Boyer A. Estimates of whole-body dose equivalent produced by beam intensity modulated conformal therapy. *Int J Radiat Oncol Biol Phys* 1997;38:667-672.

12. Rudoltz MS, Blank KR, Kao G, Muschel RJ, McKenna WG. Ionizing radiation and the cell cycle: A review. *Radiat Oncol Investi* 2007;4:147-158.

13. Schettino G, Folkard M, Prise KM, Vojnovic B, Held KD, Michael BD. Low-dose studies of bystander cell killing with targeted soft x rays. *Radiat Res* 2003;160:505-511.

14. Lorimore SA, Wright EG. Radiation-induced genomic instability and bystander effects: Related inflammatory-type responses to radiation-induced stress and injury? A review. *Int J of Radiat Biol* 2003;79:15-25.

15. Zhou H, Randers-Pehrson G, Waldren CA, Vannais D, Hall EJ, Hei TK. Induction of a bystander mutagenic effect of alpha particles in mammalian cells. *Proc Natl Acad Sci USA* 2000;97:2099-2104.

16. Redpath JL, Antoniono RJ. Induction of an adaptive response against spontaneous neoplastic transformation in vitro by low-dose gamma radiation. *Radiat Res* 1998;149:517-520.

17. Wouters BG, Sy AM, Skarsgard LD. Low-dose hypersensitivity and increased radioresistance in a panel of human tumor cell lines with different radiosensitivity. *Radiat Res* 1996;146:399-413.

18. Morgan WF. Non-targeted and delayed effects of exposure to ionizing radiation: II. Radiation-induced genomic instability and bystander effects in vivo, clastogenic factors and transgenerational effects. *Radiat Res* 2009;159:581-596.

19. Suzuki K, Kodama S, Watanabe M. Extremely low-dose ionizing radiation causes activation of mitogen-activated protein kinase pathway and enhances proliferation of normal human diploid cells. *Cancer Res* 2001;61:5396-5401.

20. Kim CS, Kim J-M, Nam SY, Yang KH, Jeong M, Kim HS, Lim Y-K, Kim CS, Jin Y-W, Kim J. Low-dose of ionizing radiation enhances cell proliferation via transient ERK1/2 and p38 activation in normal human lung fibroblasts. *J Radiat Res* 2007;48:407-415.

21. Wang G-J, Cai L. Induction of cell-proliferation hormesis and cell-survival adaptive response in mouse hematopoietic cells by whole-body low-dose radiation. *Toxicol. Sci.* 2000;53:369-376.

22. Qin J, Li L. Molecular anatomy of the DNA damage and replication checkpoints. *Radiat Res* 2003;159:139-148.

23. Murnane JP. Cell cycle regulation in response to DNA damage in mammalian cells: A historical perspective. *Cancer Metast Rev* 1995;14:17-29.

24. Teyssier F, Bay J-O, Dionet C,Verrelle P. Cell cycle regulation after exposure to ionizing radiation. *Bull Cancer* 1999;86:345-357.

25. Maity A, McKenna WG, Muschel RJ. The molecular basis for cell cycle delays following ionizing radiation: A review. *Radiother Oncol* 1994;31:1-13.

26. Houtgraaf JH, Versmissen J, van der Giessen WJ. A concise review of DNA damage checkpoints and repair in mammalian cells. *Cardiovasc Revasc Med* 2006;7:165-172.

27. Iliakis G, Wang YA, Guan J, Wang H. DNA damage checkpoint control in cells exposed to ionizing radiation. *Oncogene* 2003;22:5834-5847.

28. Johnson DG, Walker CL. Cyclins and cell cycle checkpoints. *Annu Rev Pharmacol* 1999;39:295.

29. Sancar A, Lindsey-Boltz LA, Unsal-Kaçmaz K, Linn S. Molecular mechanisms of mammalian DNA repair and the DNA damage checkpoints. *Annu Rev Biochem* 2004;73:39-85.

30. Hartwell LH, Kastan MB. Cell cycle control and cancer. *Science* 1994;266:1821.

31. Yamada M-a, Puck TT. Action of radiation on mammalian cells, IV. Reversible mitotic lag in the S3 HeLa cell produced by doses of x-rays. *Proc Natl Acad Sci USA* 1961;47:1181-1191.

32. Painter RB, Robertson JS. Effect of irradiation and theory of role of mitotic delay on the time course of labeling of HeLa S3 cells with tritiated thymidine. *Radiat Res* 1959;11:206-217.

33. Bakkenist CJ, Kastan MB. DNA damage activates ATM through intermolecular autophosphorylation and dimer dissociation. *Nature* 2003;421:499.

34. Pawlik TM, Keyomarsi K. Role of cell cycle in mediating sensitivity to radiotherapy. *Int J of Radiat Oncol Biol Phy* 2004;59:928-942.

35. Abraham RT. Cell cycle checkpoint signaling through the ATM and ATR kinases. *Gene Dev* 2001;15:2177-2196.

36. Lu X, Lane DP. Differential induction of transcriptionally active p53 following UV or ionizing radiation: Defects in chromosome instability syndromes? *Cell* 1993;75:765-778.

37. Kastan MB, Bartek J. Cell-cycle checkpoints and cancer. *Nature* 2004;432:316-323.

38. Banin S, Moyal L. Enhanced phosphorylation of p53 by ATM in response to DNA damage. *Science* 1998;281:1674.

39. Wang Y, Huq MS, Cheng X, Iliakis G. Regulation of DNA replication in irradiated cells by trans-acting factors. *Radiat Res* 1995;142:169-175.

40. Cleaver JE, Rose R, Mitchell DL. Replication of chromosomal and episomal DNA in X-ray-damaged human cells: A cis- or trans-acting mechanism? *Radiat Res* 1990;124:294-299.

41. Falck J, Mailand N, Syljuasen RG,Bartek J, Lukas J. The ATM-Chk2-Cdc25A checkpoint pathway guards against radioresistant DNA synthesis. *Nature* 2001;410:842-847.

42. Kastan MB. Cell cycle: Checking two steps. *Nature* 2001;410:766-767.

43. Li S, Ting NSY, Zheng L, Chen, P-L, Ziv Y, Shiloh Y, Lee, EYHP, Lee W-H. Functional link of BRCA1 and ataxia telangiectasia gene product in DNA damage response. *Nature* 2000;406:210-215.

44. Gatei M, Scott SP, Filippovitch I, Soronika N, Lavin MF, Weber B, Khanna KK. Role for ATM in DNA damage-induced phosphorylation of BRCA1. *Cancer Res* 2000;60:3299-3304.

45. Gatei M, Young D, Cerosaletti KM, Desai-Mehta A, Spring K, Kozlov S, Lavin MF, Gatti RA, Concannon P, Khanna K. ATM-dependent phosphorylation of nibrin in response to radiation exposure. *Nature Genetics* 2000;25:115.

46. Petrini JHJ. The Mre11 complex and ATM: Collaborating to navigate S phase. *Curr Opin Cell Biol* 2000;12:293-296.

47. Lee H, Larner JM, Hamlin JL. A p53-independent damage-sensing mechanism that functions as a checkpoint at the G1/S transition in Chinese hamster ovary cells. *Proc Natl Acad Sci USA* 1997;94:526.

48. Guo CY, D'Anna JA, Li R, Larner JM. The radiation-induced s-phase checkpoint is independent of CDKN1A. *Radiat Res* 1999;151:125-132.

49. McKenna WG, Iliakis G, Weiss MC, Bernhard EJ, Muschel RJ. Increased G2 delay in radiation-resistant cells obtained by transformation of primary rat embryo cells with the oncogenes H-ras and v-myc. *Radiat Res* 1991;125:283-287.

50. Su LN, Little JB. Prolonged cell cycle delay in radioresistant human cell lines transfected with activated ras oncogene and/or simian virus 40 T-antigen. *Radiat Res* 1993;133:73-79.

51. Bernhard EJ, Maity A, Muschel RJ, McKenna WG Effects of ionizing radiation on cell cycle progression. *Radiat Environ Bioph* 1995;34:79-83.

52. Xu B, Kim ST, Lim DS, Kastan MB. Two molecularly distinct G2/M checkpoints are induced by ionizing irradiation. *Mol Biol Cell* 2002;22:1049-1059.

53. Sinclair WK. Cyclic x-ray responses in mammalian cells in vitro. *Radiat Res* 1968;33:620-643.

54. Marples B. Is low-dose hyper-radiosensitivity a measure of G2-phase cell radiosensitivity? *Cancer Metast Rev* 2004;23:197-207.

55. Krueger SA, Wilson GD, Piasentin E, Joiner MC, Marples B. The effects of G2-phase enrichment and checkpoint abrogation on low-dose hyper-radiosensitivity. *Int J Radiat Oncol Biol Phy* 2010;77:1509-1517.

56. Joiner MC, Marples B, Lambin P, Short SC, Turesson I. Low-dose hypersensitivity: Current status and possible mechanisms. *Int J of Radiat Oncol Biol Phy* 2001;49:379-389.

57. Sionov RV, Haupt Y. The cellular response to p53: The decision between life and death. *Oncogene* 1999;18:6145.

58. Pouget J-P, Mather SJ. General aspects of the cellular response to low- and high-LET radiation. *Eur J Nucl Med* 2001;28:541-561.

59. Radford IR. Review: Initiation of ionizing radiation-induced apoptosis: DNA damage-mediated or does ceramide have a role? *Int J Radiat Biol* 1999;75:521-528.

60. Santana P, Peña LA, Haimovitz-Friedman A, Martin S, Green D, McLoughlin M, Cordon-Cardo C, Schuchman EH, Fuks Z. Acid sphingomyelinase-deficient human lymphoblasts and mice are defective in radiation-induced apoptosis. *Cell* 1996;86:189-199.

61. Verheij M, Bose R, Lin XH, Yao B, Jarvis WD, Grant S, Birrer MJ, Szabo E, Zon LI, Kyriakis JM, Haimovitz-Friedman A, Fuks Z, Kolesnick RN Requirement for ceramide-initiated SAPK/JNK signalling in stress-induced apoptosis. *Nature* 1996;380:75-79.

62. Zundel W, Giaccia A. Inhibition of the anti-apoptotic PI(3)K/Akt/Bad pathway by stress. *Gene Dev* 1998;12:1941-1946.

63. Dent P, Reardon DB, Park JS, Bowers G, Logsdon C, Valerie K, Schmidt-Ullrich R. Radiation-induced release of transforming growth factor alpha activates the epidermal growth factor receptor and mitogen-activated protein kinase pathway in carcinoma cells, leading to increased proliferation and protection from radiation-induced cell death. *Mol Biol Cell* 1999;10:2493-2506.

64. Xia Z, Dickens M, Raingeaud J, Davis RJ, Greenberg ME. Opposing effects of ERK and JNK-p38 MAP kinases on apoptosis. *Science* 1995;270:1326-1231.

65. Robinson MJ, Cobb MH. Mitogen-activated protein kinase pathways. *Curr Opin Cell Biol* 1997;9:180-186.

66. Schaeffer HJ, Weber MJ. Mitogen-Activated Protein Kinases: Specific Messages from Ubiquitous Messengers. *Mol. Cell. Biol.* 1999;19:2435-2444.

67. Garrington TP, Johnson GL. Organization and regulation of mitogen-activated protein kinase signaling pathways. *Curr Opin Cell Biol* 1999;11:211-218.

68. Schmidt-Ullrich RK, Dent P, Grant S, Mikkelsen RB, Valerie K. Signal Transduction and Cellular Radiation Responses. *Radiat Res* 2000;153:245-257.

69. Balaban N, Moni J, Shannon M, Dang L, Murphy E, Goldkorn T. The effect of ionizing adiation on signal transduction: antibodies to EGF receptor sensitize A431 cells to radiation. *BBA-Mol Cell Res* 1996;1314:147-156.

70. Marshall CJ. Specificity of receptor tyrosine kinase signaling: transient versus sustained extracellular signal-regulated kinase activation. *Cell* 1995;80:179-185.

71. Leach JK, Van Tuyle G, Lin PS, Schmidt-Ullrich R, Mikkelsen RB . Ionizing radiation-induced, mitochondria-dependent generation of reactive oxygen/nitrogen. *Cancer Res* 2001;61:3894-3901.

72. Sturgill TW, Ray LB. Muscle proteins related to microtubule associated protein-2 are substrates for an insulin-stimulatable kinase. *Biochem Bioph Res Co* 1986;134:565-571.

73. Dent P, Yacoub A, Contessa J, Caron R, Amorino G, Valerie K, Hagan MP, Grant S, Schmidt-Ullrich R. Stress and radiation-induced activation of multiple intracellular signaling pathways. *Radiat Res* 2003;159:283-300.

74. Dent P, Haser W, Haystead TA, Vincent LA, Roberts TM, Sturgill TW. Activation of mitogen-activated protein kinase kinase by v-Raf in NIH 3T3 cells and in vitro. *Science* 1992;257:1404.

75. Yoon S, Seger R. The extracellular signal regulated kinase: Multiple substrates regulate diverse cellular functions *Growth Factors* 2006;24:21-24.

76. Eferl R, Wagner EF. AP-1: A double-edged sword in tumorigenesis. *Nature Rev Cancer* 2003;3:859-868.

77. Schmidt-Ullrich RK, Dent P, Grant S, Mikkelsen RB, Valerie K. Signal transduction and cellular radiation responses. *Radiat Res* 2000;153:245-257.

78. Schmidt-Ullrich RK, Valerie K, Fogleman PB, Walters J. Radiation-induced autophosphorylation of epidermal growth factor receptor in human malignant mammary and squamous epithelial cells. *Radiat Res* 1996;145:81-85.

79. Carter S, Auer KL, Reardon DB, Birrer M, Fisher PB, Valerie K, Schmidt-Ullrich R, Mikkelsen R, Dent P. Inhibition of the mitogen activated protein (MAP) kinase cascade

potentiates cell killing by low dose ionizing radiation in A431 human squamous carcinoma cells. *Oncogene* 1998;16:2787.

80. Assefa Z, Valius M, Vántus T, Agostinis P, Merlevede W, Vandenheede JR.JNK/SAPK activation by platelet-derived growth factor in A431 cells requires both the phospholipase C-γ and the phosphatidylinositol 3-kinase signaling pathways of the receptor. *Biochem Bioph Res Co* 1999;261:641-645.

81. Leppä S, Bohmann D. Diverse functions of JNK signaling and c-Jun in stress response and apoptosis. *Oncogene* 1999;18:6158.

82. Ichijo H. From receptors to stress-activated MAP kinases. *Oncogene* 1999;18:6087.

83. Symons M. Signaling pathways controlled by Rho family GTP-binding proteinsin. In: Gutkind JS, editor. Networks and cell cycle control: Molecular basis of cancer and other diseases. Torowa: Humana Press, 2000: 231-246.

.

84. Yustein JT, Deshan LI, Robinson D, Kung HJ. KFC, a Ste20-like kinase with mitogenic potential and capability to activate the SAPK/JNK pathway. *Oncogene* 2000;19:710-718.

85. Davis RJ. Signal transduction by the JNK group of MAP kinases. *Cell* 2000;103:239-252.

86. Fuchs SY, Adler V, Buschmann T, Yin Z, Wu X, Jones SN, Ronai Z. JNK targets p53 ubiquitination and degradation in nonstressed cells. *Genes Dev* 1998;12:2658-2663.

87. Krishna M, Narang H. The complexity of mitogen-activated protein kinases (MAPKs) made simple. *Cell Mol Life Sci* 2008;65:3525-3544.

88. Chmura SJ, Nodzenski E, Beckett MA, Kufe DW, Quintans J, Weichselbaum RR. Loss of ceramide production confers resistance to radiation-induced apoptosis. *Cancer Res* 1997;57:1270-1275.

89. Yamamoto K, Ichijo H, Korsmeyer SJ. BCL-2 is phosphorylated and inactivated by an ASK1/Jun N-terminal protein kinase pathway normally activated at G2/M. *Mol Cell Biol* 1999;19:8469.

90. Chang L, Kamata H, Solinas G, Luo JL, Maeda S, Venuprasad K, Liu YC, Karin M. The E3 ubiquitin ligase itch couples JNK activation to TNFα-induced cell death by inducing c-FLIPL turnover. *Cell* 2006;124:601-613.

91. Wouters BG, Skarsgard LD. The response of a human tumor cell line to low radiation doses: Evidence of enhanced sensitivity. *Radiat Res* 1994;138:S76-S80.

92. Short SC, Kelly J, Mayes CR, Woodcock M, Joiner MC. Low-dose hypersensitivity after fractionated low-dose irradiation in vitro. *Int J Radiat Biol* 2001;77:655 - 664.

93. Schettino G, Folkard M, Prise KM, Vojnovic B, Bowey AG, Michael BD. Low-dose hypersensitivity in Chinese hamster V79 cells targeted with counted protons using a charged-particle microbeam. *Radiat Res* 2001;156:526-534.

94. Mothersill C, Seymour C. Low-dose radiation effects: Experimental hematology and the changing paradigm. *Exp Hematol* 2003;31:437-445.

95. Marples B, Wouters BG, Collis SJ, Chalmers AJ, Joiner MC. Low-Dose Hyper-radiosensitivity: A Consequence of Ineffective Cell Cycle Arrest of Radiation-Damaged G2-Phase Cells. *Radiat Res* 2004;161:247-255.

96. Krueger SA, Joiner MC, Weinfeld M, Piasentin E, Marples B. Role of apoptosis in low-dose hyper-radiosensitivity. *Radiat Res* 2009;167:260-267.

97. Enns L, Bogen KT, Wizniak J, Murtha AD, Weinfeld M. Low-dose radiation hypersensitivity is associated with p53-dependent apoptosis. *Mol Cancer Res* 2004;2:557-566.

98. Lee YJ, Soh JW, Dean NM, Cho CK, Kim TH, Lee SJ, Lee YS. Protein kinase Cdelta overexpression enhances radiation sensitivity via extracellular regulated protein kinase 1/2 activation, abolishing the radiation-induced G(2)-M arrest. *Cell Growth Differ* 2002;13:238-246.

99. Taher MM, Hershey CM, Oakley JD, Valerie, K. Role of the p38 and MEK-½/p42/44 MAP kinase pathways in the differential activation of human immunodeficiency virus gene expression by ultraviolet and ionizing radiation. *Photochem Photobiol* 2000;71:455-459.

100. Kim SJ, Ju JW, Oh CD, Yoon YM, Song WK, Kim JH, Yoo YJ, Bang OS, Kang SS, Chun JS. ERK-1/2 and p38 kinase oppositely regulate nitric oxide-induced apoptosis of chondrocytes in association with p53, caspase-3, and differentiation status. *J Biol Chem* 2002;277:1332.

101. Han J, Lee JD, Bibbs L, Ulevitch RJ. A MAP kinase targeted by endotoxin and hyperosmolarity in mammalian cells. *Science* 1994;265:808.

102. Freshney NW, Rawlinson L, Guesdon F, Jones E, Cowley S, Hsuan J, Saklatvala J. Interleukin-1 activates a novel protein kinase cascade that results in the phosphorylation of Hsp27. *Cell* 1994;78:1039-1049.

103. Holbrook NJ, Liu Y, Fornace Jr AJ. Signaling events controlling the molecular response to genotoxic stress. *EXS* 1996:273–288.

104. Lee SH, Eom M, Lee SJ, Kim S, Park HJ, Park D. BetaPix-enhanced p38 activation by Cdc42/Rac/PAK/MKK3/6-mediated pathway. Implication in the regulation of membrane ruffling. *J Biol Chem* 2001; 276:25066–25072

105. Schaeffer HJ, Weber MJ. Mitogen-activated protein kinases: specific messages from ubiquitous messengers. *Mol Biol Cell* 1999;19:2435.

106. Tan Y, Rouse J, Zhang A, Cariati S, Cohen P, Comb MJ. FGF and stress regulate CREB and ATF-1 via a pathway involving p38 MAP kinase and MAPKAP kinase-2. *EMBO J* 1996;15:4629.

107. Wiggin GR, Soloaga A, Foster JM, Murray-Tait V, Cohen P, Arthur JS. MSK1 and MSK2 are required for the mitogen-and stress-induced phosphorylation of CREB and ATF1 in fibroblasts. *Mol Cell Biol* 2002;22:2871.

108. Juretic N, Santibáñez JF, Hurtado C, Martínez J. ERK 1, 2 and p38 pathways are involved in the proliferative stimuli mediated by urokinase in osteoblastic SaOS-2 cell line. *J Cell Biochem* 2001;83:92-98.

109. Yosimichi G, Nakanishi T, Nishida T, Hattori T, Takano-Yamamoto T, Takigawa M. CTGF/Hcs24 induces chondrocyte differentiation through a p38 mitogen-activated protein kinase (p38MAPK), and proliferation through a p44/42 MAPK/extracellular-signal regulated kinase (ERK). *Eur J Biochem* 2001;268:6058-6065.

110. Ahmed KM, Li JJ. NF-κB-mediated adaptive resistance to ionizing radiation. *Free Radical Bio Med* 2008;44:1-13.

111. Bours V, Bonizzi G, Bentires-Alj M, Bureau F, Piette J, Lekeux P, Merville M-P. NF-κB activation in response to toxical and therapeutical agents: Role in inflammation and cancer treatment. *Toxicology* 2000;153:27-38.

112. Karin M, Cao Y, Greten FR, Li ZW. NF-κB in cancer: From innocent bystander to major culprit. *Nature Rev Cancer* 2002;2:301-310.

113. Veuger SJ, Hunter JE, Durkacz BW. Ionizing radiation-induced NF-κB activation requires PARP-1 function to confer radio-resistance. *Oncogene* 2009;28:832.

114. Baldwin AS. The NF-κB and IκB proteins: New discoveries and insights. *Annu Rev Immunol* 1996;14:649-681.

115. Magné N, Toillon RA, Bottero V, Didelot C, Houtte PV, Gérard JP, Peyron JF. NF-κB modulation and ionizing radiation: mechanisms and future directions for cancer treatment. *Cancer Lett* 2006;231:158-168.

116. Verma IM, Stevenson JK, Schwarz EM, Van Antwerp D, Miyamoto S. Rel/NF-kappa B/I kappa B family: intimate tales of association and dissociation. *Genes Dev* 1995;9:2723.

117. Lee SJ, Dimtchev A, Lavin MF, Dritschilo A, Jung M. A novel ionizing radiation-induced signaling pathway that activates the transcription factor NF-κB. *Oncogene* 1998;17:1821.

118. Piret B, Schoonbroodt S, Piette J. The ATM protein is required for sustained activation of NF-κB following DNA damage. *Oncogene* 1999;18:2261.

119. Lee SJ, Dimtchev A, Lavin MF, Dritschilo A, Jung M. A novel ionizing radiation-induced signaling pathway that activates the transcription factor NF-κB. *Oncogene* 1998;17:1821.

120. Chen C, Edelstein LC, Gelinas C. The Rel/NF-κB family directly activates expression of the apoptosis inhibitor Bcl-xL. *Mol Cell Biol* 2000;20:2687.

121. Xiao G, Harhaj EW, Sun S-C. NF-κB-inducing kinase regulates the processing of NF-κB2 p100. *Mol Cell* 2001;7:401-409.

122. Yang CR, Wilson-Van Patten C, Planchon SM, Wuerzberger-Davis SM, Davis TW, Cuthill S, Miyamoto S, Boothman DA. Coordinate modulation of Sp1, NF-kappa B, and p53 in confluent human malignant melanoma cells after ionizing radiation. *FASEB J* 2000;14:379.

123. Brach MA, Hass R, Sherman ML, Gunji H, Weichselbaum R, Kufe D. Ionizing radiation induces expression and binding activity of the nuclear factor kappa B. *J Clin Invest* 1991;88:691.

124. Prasad AV, Mohan N, Chandrasekar B, Meltz ML. Activation of nuclear factor κappa B in human lymphoblastoid cells by low-dose ionizing radiation. *Radiat Res* 1994;138:367-372.

125. Marples B, Wouters BG, Joiner MC. An association between the radiation-induced arrest of G2-phase cells and low-dose hyper-radiosensitivity: A plausible underlying mechanism? *Radiat Res* 2003;160:38-45.

126. Joiner MC, Marples B, Lambin P, Short SC, Turesson I. Low-dose hypersensitivity: Current status and possible mechanisms. *Int J Radiat Oncol Biol Phys* 2001;49:379-389.

127. Marples B, Joiner MC. The elimination of low-dose hypersensitivity in Chinese hamster V79-379A cells by pretreatment with x rays or hydrogen peroxide. *Radiat Res* 1995;141:160-169.

128. Rothkamm K, Löbrich M. Evidence for a lack of DNA double-strand break repair in human cells exposed to very low x-ray doses. *Proc Natl Acad Sci USA* 2003;100:5057-5062.

129. Marples B, Wouters BG, Collis SJ, Chalmers AJ, Joiner MC. Low-dose hyper-radiosensitivity: A consequence of ineffective cell cycle arrest of radiation-damaged G2-phase cells. *Radiat Res* 2004;161:247-255.

130. Korystov YN, Eliseeva NA, Kublik LN, Narimanov AA. The effect of low-dose irradiation on proliferation of mammalian cells in vitro. *Radiat Res* 1996;146:329-332.

131. Marples B, Krueger SA, Collis SJ, Joiner MC Low Dose hyper-radiosensitivity: A historical perspective. In: Stigbrand T, Carlsson J, Gregory PA, editors. Targeted radionuclide tumor therapy. Philadelphia: Springer, 2008: p.329-347.

132. Zhong Q, Chen CF, Li S, Chen Y, Wang CC, Xiao J, Chen PL, Sharp ZD, Lee W. Association of BRCA1 with the hRad50-hMre11-p95 complex and the DNA damage response. *Science* 1999;285:747.

133. Nagasawa H, Keng P, Harley R, Dahlberg W, Little JB. Relationship between gamma-ray-induced G2/M delay and cellular radiosensitivity. *Int J Radiat Biol* 1994;66:373-379.

134. Pizzarello DJ, Witcofski RL. Medical Radiation Biology, 3rd edition. Philadelphia: Lea and Febiger; 1982. p. 123.

135. Hermann RM, Wolff HA, Jarry H, Thelen P, Gruendker C, Rave-Fraenk M, Schmidberger H, Christiansen H. In vitro studies on the modification of low-dose hyper-radiosensitivity in prostate cancer cells by incubation with genistein and estradiol. *Radiat Oncol* 2008;3:19.

136. Wouters BG, Sy AM, Skarsgard LD. Low-dose hypersensitivity and increased radioresistance in a panel of human tumor cell lines with different radiosensitivity. *Radiat Res* 1996;146:399-413.

137. Short SC, Woodcock M, Marples B, Joiner MC. Effects of cell cycle phase on low-dose hyper-radiosensitivity. *Int J Radiat Biol* 2003;79:99.

138. Villa R, Zaffaroni N, Bearzatto A, Costa A, Sichirollo A, Silvestrini R. Effect of ionizing radiation on cell-cycle progression and cyclin B1 expression in human melanoma cells. *Int J Cancer* 1996;66:104-109.

139. Painter RB, Robertson JS. Effect of irradiation and theory of role of mitotic delay on the time course of labeling of HeLa S3 cells with tritiated thymidine. *Radiat Res* 1959;11:206-217.

140. Terasima T, Tolmach LJ. Variations in several responses of HeLa cells to x-irradiation during the division cycle. *Biophys J* 1963;3:11-33.

141. Yu C, Sinclair W. Mitotic delay and chromosamal abberations induced by X-rays in Sichronized Chinese Hamster cells invitro. *J Nat Cancer Inst* 1967;39:619-632.

142. Walters RA, Petersen DF. Radiosensitivity of mammalian cells: I. Timing and dose-dependence of radiation-induced division delay. *Biophys J* 1968;8:1475-1486.

143. Dewey WC, Highfield DP. G2 block in Chinese hamster cells induced by x-irradiation, hyperthermia, cycloheximide, or actinomycin-D. *Radiat Res* 1976;65:511-528.

144. Ehmann UK, Nagasawa H, Petersen DF, Lett JT Symptoms of x-ray damage to radiosensitive mouse leukemic cells: Asynchronous populations. *Radiat Res* 1974;60:453-472.

145. Amundson SA, Do KT, Fornace Jr AJ. Induction of stress genes by low doses of gamma rays. *Radiat Res* 1999;152:225-231.

146. Fornace AJ Jr, Amundson SA, Do KT, Meltzer P, Trent J, Bittner M. Stress-gene induction by low-dose gamma irradiation. *Mil Med* 2002;167:13-15.

147. Ding LH, Shingyoji M, Chen F, Hwang JJ, Burma S, Lee C, Cheng JF, Chen DJ. Gene expression profiles of normal human fibroblasts after exposure to ionizing radiation: A comparative study of low and high doses. *Radiat Res* 2005;164:17-26.

148. Mitchell CR, Folkard M, Joiner MC. Effects of exposure to low-dose-rate 60Co gamma rays on human tumor cells in vitro. *Radiat Res* 2002;158:311-318.

149. Slichenmyer WJ, Nelson WG, Slebos RJ, Kastan MB. Loss of a p53-associated G1 checkpoint does not decrease cell survival following DNA damage. *Cancer Res* 1993;53:4164-4168.

150. Olive PL, Banáth JP, Durand RE. Development of apoptosis and polyploidy in human lymphoblast cells as a function of position in the cycle at the time of irradiation. *Radiat Res* 1996;146:595-602.

151. Zywietz F, Jung H. Partial synchronization of three solid animal tumours by X-rays. *Eur J Cancer* 1980;16:1381-1388.

152. Linden WA, Zywietz F, Baisch H, Skiba J. Radiation-induced synchronization of the Walker carcinoma in vivo. *Eur J Cancer* 1975;11:419-423.

153. Elkind MM, Sutton H, Moses WB. Postirradiation survival kinetics of mammalian cells grown in culture. *J Cell Comp Physio* 1961;58:113-134.

154. Draetta G, Beach D. Activation of cdc2 protein kinase during mitosis in human cells: Cell cycle-dependent phosphorylation and subunit rearrangement. *Cell* 1988;54:17-26.

155. Muschel RJ, Zhang HB, Iliakis G, McKenna WG. Cyclin B expression in HeLa cells during the G2 block induced by ionizing radiation. *Cancer Res* 1991;51:5113.

156. Ward GE, Kirschner MW. Identification of cell cycle-regulated phosphorylation sites on nuclear lamin C. *Cell* 1990;61:561-577.

157. Pines J. Cyclins: Wheels within wheels. *Cell Growth Differ* 1991;2:305.

158. Nurse P. Universal control mechanism regulating onset of M-phase. *Nature* 1990;344:503-508.

159. Muschel RJ, Zhang HB, McKenna WG. Differential effect of ionizing radiation on the expression of cyclin A and cyclin B in Hela cells. *Cancer Res* 1993;53:1128-1135.

160. Theron T, Böhm L. Cyclin B1 expression in response to abrogation of the radiation-induced G2/M block in HeLa cells. *Cell Proliferat* 1998;31:49-57.

161. Hendrikse AS, Hunter AJ, Keraan M, Blekkenhorst GH Effects of low dose irradiation on TK6 and U937 cells: Induction of p53 and its role in cell-cycle delay and the adaptive response. *Int J Radiat Biol* 2000;76:11-21.

162. Datta R, Hass R, Gunji H, Weichselbaum R, Kufe D. Down-regulation of cell cycle control genes by ionizing radiation. *Cell Growth Differ* 1992;3:637-644.

163. Dent P, Yacoub A, Fisher PB, Hagan MP, Grant S. MAPK pathways in radiation responses. *Oncogene* 2003;22:5885-5896.

164. Dent P, Yacoub A, Contessa J, Caron R, Amorino G, Valerie K, Hagan MP, Grant S, Schmidt-Ullrich R. Stress and Radiation-Induced Activation of Multiple Intracellular Signaling Pathways1. *Radiat Res* 2009;159:283-300.

165. Kumar P, Miller AI, Polverini PJ. p38 MAPK mediates irradiation-induced endothelial cell apoptosis, and vascular endothelial growth factor protects endothelial cells through the phosphoinositide 3-kinase-Akt-Bcl-2 pathway. *J Biol Chem* 2004;279:43352-43360.

166. McCubrey JA, Steelman LS, Chappell WH, Abrams SL, Wong EW, Chang F, Lehmann B, Terrian DM, Milella M, Tafuri A, Stivala F, Libra M, Basecke J, Evangelisti C, Martelli AM, Franklin RA. Roles of the Raf/MEK/ERK pathway in cell growth, malignant transformation and drug resistance. *Biochim Biophys Acta.* 2007;1773:1263-1284.

167. Prise KM, Schettino G, Folkard M, Held KD. New insights on cell death from radiation exposure. *Lancet* 2005;6:520-528.

168. Narang H, Krishna M. Mitogen-activated protein kinases: Specificity of response to dose of ionizing radiation in liver. *J Radiat Res* 2004;45:213-220.